Contract No:

This document was prepared in conjunction with work accomplished under Contract No. DE-AC09-08SR22470 with the U.S. Department of Energy (DOE) Office of Environmental Management (EM).

Disclaimer:

DWPF Melter Off-Gas Flammability Assessment for Sludge Batch 9

A. S. Choi

July 2016

SRNL-STI-2016-00318, Revision 0

DISCLAIMER

Printed in the United States of America

Prepared for
U.S. Department of Energy

SRNL-STI-2016-00318
Revision 0

Keywords: *DWPF, SB9, Melter Off-Gas Flammability*

Retention: *Permanent*

DWPF Melter Off-Gas Flammability Assessment for Sludge Batch 9

A. S. Choi

July 2016

Prepared for the U.S. Department of Energy under contract number DE-AC09-08SR22470.

Savannah River National Laboratory™
OPERATED BY SAVANNAH RIVER NUCLEAR SOLUTIONS

REVIEWS AND APPROVALS

AUTHOR:

_____

A. S. Choi, Process Technology Programs/SRNL Date

TECHNICAL REVIEW:

_____

F. G. Smith, III, Environmental Modeling/SRNL, Reviewed per E7 2.60 Date

APPROVAL:

_____

F. M. Pennebaker, Manager Date
Process Technology Programs/E&CPT Research Programs/SRNL

_____

D. E. Dooley, Manager Date
E&CPT Research Programs/Environmental Stewardship/SRNL

_____

E. J. Freed, Manager Date
DWPF/Saltstone Facility Engineering/SRR

EXECUTIVE SUMMARY

The slurry feed to the Defense Waste Processing Facility (DWPF) melter contains several organic carbon species that decompose in the cold cap and produce flammable gases that could accumulate in the off-gas system and create potential flammability hazard. To mitigate such a hazard, DWPF has implemented a strategy to impose the Technical Safety Requirement (TSR) limits on all key operating variables affecting off-gas flammability and operate the melter within those limits using both hardwired/software interlocks and administrative controls. The operating variables that are currently being controlled include; (1) total organic carbon (TOC), (2) air purges for combustion and dilution, (3) melter vapor space temperature, and (4) feed rate. The safety basis limits for these operating variables are determined using two computer models, 4-stage cold cap and Melter Off-Gas (MOG) dynamics models, under the baseline upset scenario - a surge in off-gas flow due to the inherent cold cap instabilities in the slurry-fed melter.

The magnitude and duration of off-gas surges depend largely on the mode of operation. During bubbled operation, i.e., when the melt pool is agitated with the argon bubblers, off-gas tends to surge more often and in greater magnitudes than under non-bubbled mode. The current TSR limits on TOC were developed for the Sludge Batch 8 (SB8) bubbled operation for which the baseline off-gas surge is defined as follows based on the data taken during the Cold-cap Evaluation Furnace (CEF) melter run in 2010; 9 times (9X) normal condensable and 5 times (5X) normal non-condensable flows at the onset of surge and decreasing linearly to 30% of their respective peak values after 1 min. However, it was determined in 2014 that the method of controlling the feed rate under the maximum 1.5 gallons-per-minute (GPM) based on measured melter vapor space temperature was not robust enough to ensure conservatism under all feed conditions; as the total solids content of feed dropped well below the design basis 45 wt%, the measured melter vapor temperatures at near the maximum feed rate remained higher than the TSR minimum that triggers the feed interlock. Based on this finding, DWPF turned off the bubblers and has since been operating under non-bubbled mode at reduced feed rates. The reasoning was that as off-gas in general surges less frequently and in smaller magnitudes during non-bubbled operation, the potential for off-gas flammability would be lower and thus the existing TSR TOC limits would remain valid even with dilute feeds. However, the baseline 3X/3X off-gas surge for non-bubbled operation had not been validated against the facility data.

The DWPF will begin processing SB9 during the 2nd half of FY2016 and has issued a Technical Task Request (TTR) that the Savannah River National Laboratory (SRNL) personnel assess the flammability potential of SB9 and determine whether or not the existing TSR TOC limits would be applicable to SB9 under non-bubbled conditions. Therefore, the goal of this study was two-fold; (1) to validate the baseline 3X/3X off-gas surge for non-bubbled operation by comparing it against the largest melter pressure spike that has occurred in the facility since 2014 in terms of off-gas flammability potential, and (2) to determine the maximum TOC limits of SB9 as a function of nitrate for three different antifoam addition scenarios under non-bubbled conditions and compare them against the existing TSR limits. As for the TSR limits on air purges and melter vapor space temperature (i.e., Eqs. 1 to 3 in Introduction), they have remained unchanged since they were first set and constitute part of the melter operating conditions under which the TOC limits are evaluated.

To address the first goal, the DCS database was scanned for the 15-month non-bubbled operation from 11/21/2014 to 02/20/2016 and the melter pressure spike on 11/24/2014 20:14:46 with the peak pressure maxed out at +10.8" H_2O was identified as the bounding pressure spike for non-bubbled operation. The MOG dynamics model was next updated, including the addition of the feed forward control algorithm, and calibrated using the steady state data averaged over the 30-min period prior to the +10.8" H_2O pressure spike. After several iterations, when the calibrated model was run with a 24X/6X off-gas surge with a peak duration of 20 sec, it was found that the measured melter pressure and control air flow during the pressure spike were both predicted well by the model, which also predicted that the actual peak melter

pressure would have been closer to +19" H_2O. The 24X/6X off-gas surge with 20-sec peak duration was next simulated as a standalone case under the actual operating conditions at the time of pressure spike and the peak flammability of the OGCT vapor was predicted to be 13% of the LFL. The magnitudes of the baseline 3X/3X off-gas surge for non-bubbled operation were next doubled since the actual feed rate at the time of pressure spike was ½ of the safety basis limit 1.5 GPM. When the resulting 6X/6X off-gas surge with 1-min peak duration was run under the identical operating conditions, the peak flammability of the OGCT vapor was predicted to be higher at 15% of the LFL. These results showed that the current safety basis 3X/3X off-gas surge with 1-min peak duration at 1.5 GPM feed rate bounds the facility data in terms of off-gas flammability.

The 4-stage cold cap and MOG dynamics models were next run using the baseline SB9 feed composition, which was reconstituted with the flowsheet levels of coal and MCU solvent under three different antifoam addition scenarios; 728, 894 and 1,017 gallons per Chemical Processing Cell (CPC) cycle. When the baseline 3X/3X off-gas surge with 1-min peak duration was simulated with each of the three reconstituted feeds at varying nitrate levels, the results showed that the maximum TOC limits of SB9, which were calculated at the peak flammability of 60% of the LFL in the OGCT, were 1 to 11% higher than the existing TOC limits, which indicated that the flammability potential of SB9 under non-bubbled conditions is not higher than that of SB8 and thus the existing TSR TOC limits remain valid for the SB9 non-bubbled operation.

Based on the results presented in this report, it is concluded that:

1. The MOG dynamics model was successfully updated to reflect the current DCS settings and further calibrated using the latest facility data. The calibrated model predicted that the actual peak melter pressure during the apparent +10.8" H_2O pressure spike on 11/24/2014 was closer to +19" H_2O with 20-sec peak duration.

2. The current 3X/3X off-gas surge basis with 1-min peak duration at 1.5 GPM feed rate remains bounding in terms of off-gas flammability during non-bubbled operation.

3. The duration of off-gas surge has just as large an impact as its magnitude on off-gas flammability.

4. The current TSR TOC limits, which were developed for the SB8 bubbled operation, remain valid for the SB9 non-bubbled operation under all three antifoam addition scenarios considered.

5. The current TSR limits on the minimum melter vapor space temperature, minimum air purges and maximum feed rate all remain the same.

The implication of these conclusions is that no DSA change would be required for processing SB9 under non-bubbled conditions.

TABLE OF CONTENTS

LIST OF TABLES

LIST OF FIGURES

LIST OF ABBREVIATIONS

CEQ	Equivalent Conductance
CEF	Cold-cap Evaluation Furnace
DCS	Distributed Control System
DSA	Documented Safety Analysis
DWPF	Defense Waste Processing Facility
GPM	gallons per minute
HEME	High Efficiency Mist Eliminator
HEPA	High Efficiency Particulate Air
ICP	Invariant Condensed Phase
LFL	lower flammability limit
MCU	Modular Caustic-side solvent extraction Unit
MFT	Melter Feed Tank
MOG	melter off-gas
NGS	Next Generation Solvent
NIST	National Institute of Standards and Technology
OGC	Off-Gas Condenser
OGCT	Off-Gas Condensate Tank
PI	Proportional-Integral
QA	Quality Assurance
SB	sludge batch
SME	Slurry Mix Evaporator
SQAP	Software Quality Assurance Plan
SRNL	Savannah River National Laboratory
SRR	Savannah River Remediation
TOC	total organic carbon
TSR	Technical Safety Requirement
TTR	Task Technical Request
WL	waste loading

1.0 Introduction

A potential for off-gas flammability in the Defense Waste Processing Facility (DWPF) melter is mitigated by controlling the concentration of total organic carbon (TOC) in the Sludge Mix Evaporator (SME) product at below the Technical Safety Requirement (TSR) limits set as a function of nitrate under three different antifoam addition scenarios.[1] This control strategy ensures compliance with the NFPA Code 69; the concentration of flammable gases in the Off-Gas Condensate Tank (OGCT) will not exceed 60% of the lower flammability limit (LFL) in case of an off-gas surge at 1.5 GPM melter feed rate. When the melt pool is agitated with the argon bubblers (i.e., during bubbled operation), the baseline surge is defined as the condensable and non-condensable cold cap off-gas flows spiking to 9 times (9X) and 5 times (5X) their normal values, respectively, at the onset of surge and immediately decreasing linearly to 30% of their respective peak values during the next 1 minute.[2] For non-bubbled operation, the baseline surge is defined as both the condensable and non-condensable cold cap off-gas flows spiking to 3 times (3X) their respective normal values at the onset of surge and immediately decreasing linearly to 50% of their respective peak values during the next 1 minute.[2]

The TSR limits on TOC are determined using two computer models.[3,4] The cold cap model calculates the source term, i.e., the concentration of flammable gases produced during the calcine/fusion reactions in the cold cap, while the melter off-gas (MOG) dynamics model takes the source term as an input and performs the global combustion kinetics calculations in the melter vapor space. The concentration of unburned flammable gases in the melter exhaust (mainly H_2 and CO) is tracked by the model throughout the off-gas system by performing the transient mass/heat balance as well as gas dynamics calculations under the actions of various Proportional-Integral (PI) controllers and dynamic valves. The theoretical TOC limits are set when the calculated peak concentration of flammable gases in the OGCT equals 60% of the composite LFL during the surge, while maintaining the following theoretical minimum temperature and air purges at 1.5 GPM feed rate:

$$\textit{Melter vapor space temperature (TI4085D)} \geq 460\ ^{o}C \qquad (1)$$

$$\textit{Total melter air purge (FIC3221A)} \geq 900\ \textit{lb/hr} \qquad (2)$$

$$\textit{Backup film cooler air purge (FIC3221B)} \geq 233\ \textit{lb/hr} \qquad (3)$$

The current TSR TOC limits were derived for bubbled operation with Sludge Batch 8 (SB8) by applying analytical uncertainties to the theoretical limits.[1,2] However, a recent computer simulation study of non-safety off-gas component failures showed that when the ratio-bias control of the exhauster speed (FIC3691) is replaced with the feed forward control currently used in the facility, the calculated peak concentration of flammable gases in the OGCT would increase from 60 to 72% of the LFL under bubbled conditions;[5] the increase in flammability potential was attributed to a much slower, dampened response of the exhauster during a surge under the feed forward control, causing more flammable gases to accumulate in the OGCT than under the ratio-bias control. The same study also showed that the peak concentration of flammable gases in the OGCT would remain below the safety basis limit of 60% of the LFL during the baseline off-gas surge for non-bubbled operation.[5] The DWPF melter had been running with the bubblers turned off since 11/21/2014, and these findings provided the justification for continued non-bubbled operation under the existing TSR limits.

DWPF is currently scheduled to begin processing SB9 during the 4th quarter of FY2016 and DWPF Engineering has requested that the Savannah River National Laboratory (SRNL) personnel determine whether or not the current TSR TOC limits would remain applicable to SB9 under non-bubbled operating mode.[6] The Task Technical Request (TTR) outlines several tasks for SRNL, including the documentation

of inputs and assumptions used in the assessment, performing case studies using the models, and providing support to the Savannah River Remediation (SRR) personnel in documenting the results of the SB9 flammability assessment in a Type 1 calculation. This report documents the results of Task #4 and #5, as described in the TTR.[6] Specifically, the scope of this study included; (1) validation of the 3X/3X off-gas surge basis for non-bubbled operation against the facility data and (2) assessment of the SB9 flammability potential for non-bubbled operation. The results of this study showed that; (1) the current 3X/3X off-gas surge basis bounds the facility data taken during non-bubbled operation, i.e., it would lead to a higher off-gas flammability potential in the OGCT than under the largest pressure spike that has occurred since the bubblers were turned off in November 2014, and (2) the existing TSR limits set for SB8 are also applicable to SB9 under non-bubbled operating mode. This report documents the bases and results of the model calculations performed in this study along with the facility data used to validate the off-gas surge basis for non-bubbled operation.

2.0 Validation of 3X/3X Off-Gas Surge Basis

The MOG dynamics model was last validated against the facility data in 2004.[7] The validation process is normally performed in three steps. First, the Distributed Control System (DCS) database is scanned to identify and download the desired melter off-gas system operating data, usually around the time of a large pressure spike. The steady state portion of the downloaded data, i.e., data taken just before a pressure spike began, is next used to calibrate the model, i.e., adjusting the model parameters such as the flow conductance between two adjacent nodes to match measured pressure profile. Lastly, the calibrated model is run to match the measured pressure, temperature, and flow profiles during a pressure spike by adjusting the dynamic elements of the model and its inputs such as dead times and off-gas flow surge profile.

2.1 Melter Pressure Spike Data

The DCS database was scanned for the 15-month non-bubbled operation from 11/21/2014 to 02/20/2016 and a total of 226 melter pressure spikes above -2" H_2O were identified. However, most of the pressure spikes were excluded from further consideration as they either occurred during maintenance and/or off-gas surveillance activities with no feeding or lasted for less than 20 sec. The duration of a pressure spike is defined here as the time during which the melter pressure remains above -2" H_2O or an increase of >3" H_2O from the baseline -5" H_2O (relative to the Melt Cell pressure). As will be shown later in this report, the duration of pressure spike has as strong an impact as the magnitude of pressure spike itself on the downstream off-gas surge flammability. After additional scrubbing of data, it was determined that the melter pressure spike to +10.8" H_2O on 11/24/2014 20:14:46 (Figure 2-1) was the largest and thus bounding pressure spike for non-bubbled operation. The next largest pressure spike occurred on 09/22/15 18:40:32 but its magnitude (or peak pressure) was only +3.3" H_2O at a comparable duration (Figure 2-2).

Figure 2-1 shows the profiles of measured melter pressure (PIC3521), slurry feed rate (FIC3309) and forward flush rate (FIC3327) during the +10.8" H_2O pressure spike with the time zero set at 19:00:00. At the 4,473 sec mark, the melter pressure began to rise sharply from the baseline -5" H_2O but quickly plateaued at +10.8" H_2O in the next 3-4 sec, as the calibration range of transmitter PT3521 was maxed out. Thus, the actual peak melter pressure was likely much higher and such large pressure spikes in excess of ~20" H_2O could have held back the feed flow momentarily, causing the measured feed flow (FIC3309) to drop ~2 sec later. As FIC3309 continued to drop sharply in the next 2 sec or so, it went below 50% of the set point (0.75 GPM), which would have triggered a forward flush as the 3-way valve is set to travel from the feed-the-melter to forward-flush position when FIC3309 drops below 50% of the set point for as short as 0.5 sec. Figure 2-1 indeed shows that the forward-flush began at the 4,484 sec mark ~8 sec after FIC3309 dropped below 50% of its set point. At the onset of forward flush, the melter pressure control loop was in the recovery mode, as evidenced by the falling PIC3521 below 10.8" H_2O, which means that the second pressure spike that began 1-2 sec after the forward flush began was caused by the forward-flush itself, not by another surge in the cold cap off-gas flow.

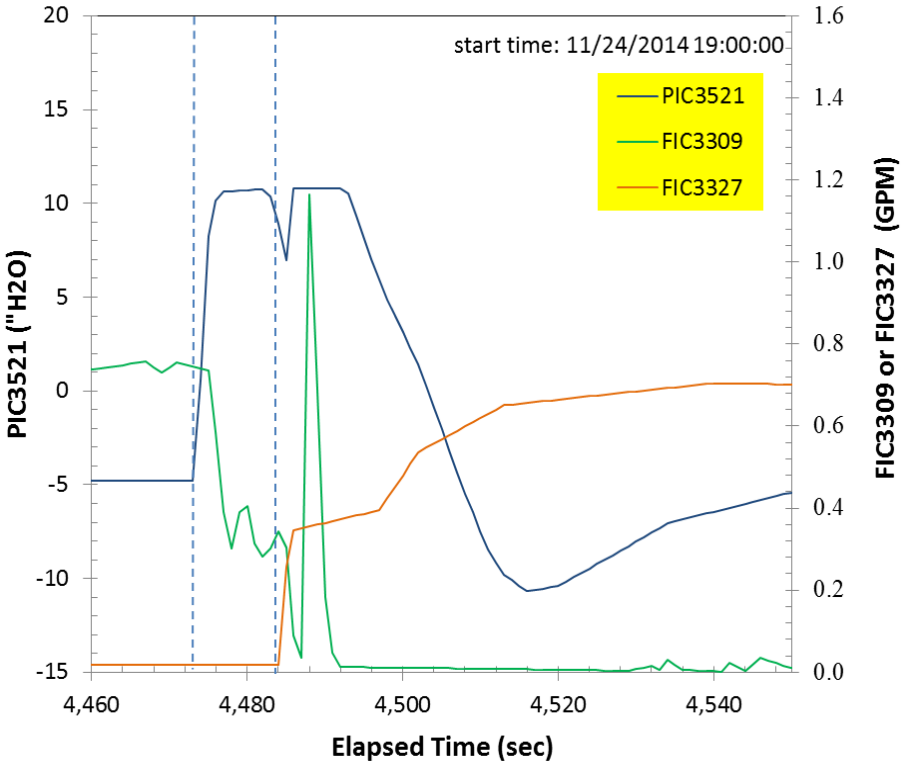

Figure 2-1. Bounding Melter Pressure Spike for Non-Bubbled Operation.

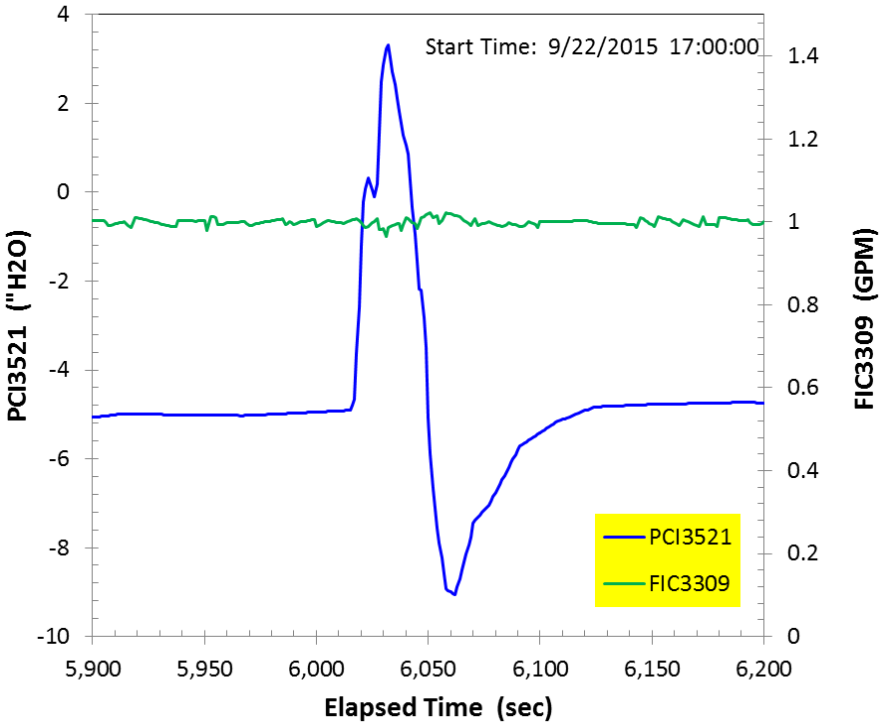

Figure 2-2. +3.3" H_2O Melter Pressure Spike During Non-Bubbled Operation.

Therefore, the focus of dynamic analysis was centered on determining the off-gas surge profile that would produce the measured PIC3521 profile from the 4,473 to 4,485 sec mark with the flat top replaced with a normal peak, as shown in Figure 2-2 for the +3.3" H_2O pressure spike.

2.2 Calibration of MOG Dynamics Model

2.2.1 Steady State Data

To determine the off-gas surge profile corresponding to the bounding pressure spike, it was necessary to calibrate the model by adjusting its parameters until predicted values matched measured steady state data, including the temperature, pressure and flow profiles throughout the system. To do so, the DCS data were averaged over a 30-min period prior to the start of surge on 11/24/2014 20:14:46, as given in the "DATA" column in Table 2-1, and used as the steady state data for the model calibration. The values given in the "MODEL" column were calculated using the calibrated model to simulate the steady state. As before, the melter vapor space gas temperature was estimated from the measured temperature (TI4085D) using the following correlation:[2]

$$T_{gas} = 0.91685\, T_{TI4085D} - 128 \qquad (4)$$

What follows next details the adjustments made to the model and its database during the calibration.

Table 2-1. Steady State Data Used for Model Calibration vs. Calibrated Model Output.

PROCESS VARIABLES	DATA	MODEL
Melter Pressure, PIC3521 ("H_2O relative to Cell)	-4.99	-4.95
Melter Vapor Space Temperature, TI4085D (^oC)	662.7	n/a
Melter Vapor Space Gas Temperature (^oC)	n/a	478.5
Air Purge to Backup Film Cooler, FIC3221B (lb/hr)	340.3	340.0
Total Melter Air Purge, FIC3221A (lb/hr)	1,069.5	1,070.0
Off-Gas Temperature at Film Cooler Exit, TIC3682 (^oC)	n/a	284.7
Melter Pressure Control Air, FIC3691 (lb/hr)	501.4	502.3
Primary Film Cooler Steam, FIC3680 (lb/hr)	278.5	278.6
ΔP across Off-Gas Header, PDI3684 ("H_2O)	0.95	0.96
OGCT Pressure, PI3485A ("H_2O relative to Cell)	-3.19	-3.12
ΔP across Steam Atomized Scrubbers (SAS), PDI3387 ("H_2O)	21.3	21.5
ΔP across Off-Gas Condenser (OGC), PDI3389 ("H_2O)	3.02	4.02*
ΔP across Condenser De-Entrainer, PDI3384 ("H_2O)	-0.14	-
ΔP across HEME, PDI3411 ("H_2O)	1.17	6.66**
ΔP across Orifice for FI3401 ("H_2O)	4.49	-
ΔP across HEPA, PDI3400 ("H_2O)	0.75	0.76
ΔP across Exhauster, PDI3582 ("H_2O)	35.44	35.55
Off-Gas Flow to HEPA, FI3401 (lb/hr)	1,662	1,690
Exhauster Speed, SIC3585 (RPM)	490.6	490.5
Melt Cell Pressure, PI5724 ("H_2O)	-1.41	-1.39
Pour Spout Pressure, PI3527 ("H_2O relative to Cell)	-0.94	-0.95
Pour Spout Pressure Control Air, FI3526 (lb/hr)	59.6	60.0

n/a = not applicable or available

* Includes ΔP across de-entrainer.

** Includes ΔP across orifice & pre-heater.

2.2.2 Determination of CEQ's

A piping and instrument diagram (P&ID) of the DWPF melter and primary off-gas system is shown in Figure 2-3 along with the two main control loops for the melter pressure (PIC3521) and exhauster speed (FIC3691). It is noted that when the measured pressure drops (ΔP's) downstream of the OGCT given in Table 2-1 are subtracted from the OGCT pressure, the resulting ΔP across the exhauster is calculated to be 28.93" H_2O compared to the measured value of 35.44" H_2O (PDI3582). The difference of 6.51" H_2O (=35.44-28.93) should then account for those ΔP's either not measured or not reported such as the ΔP's across the (FI3401) orifice, High-Efficiency Particulate Air (HEPA) filter pre-heater, and the de-entrainer filter inside the Off-Gas Condenser (OGC) (as the negative value of PDI3384 is apparently in error). According to the scaling sheet,[8] the measured orifice ΔP is converted to the off-gas flow (FI3401) using:

$$FI3401 = 784\sqrt{\Delta P} \qquad (5)$$

where FI3401 is in lb/hr and ΔP in "H_2O. When the steady state off-gas flow of 1,662 lb/hr is substituted for FI3401 in Eq. (5), the corresponding orifice ΔP is calculated to be 4.49" H_2O. When the orifice ΔP is subtracted from 6.51" H_2O, the remaining ΔP is 2.02" H_2O, which was split 50:50 between the pre-heater and the de-entrainer in this study. Thus, the given value of PDI3389 in the "MODEL" column of Table 2-1 includes ΔP's across the OGC and the de-entrainer, while that of PDI3411 includes ΔP's across the High-Efficiency Mist Eliminator (HEME), the orifice, and the pre-heater.

Once the pressure drop data were reconciled, the corresponding Equivalent Conductance (CEQ) values for each ΔP were calculated using the general flow equation:

$$W = CEQ\sqrt{\rho\,\Delta h} \qquad (6)$$

where W is the fluid flow in lb/hr, ρ the mean fluid density in lb/ft^3, Δh the driving head between two nodes in psi, and CEQ the equivalent conductance in $(lb.ft^3/psi.hr^2)^{1/2}$. The CEQ, which is a reciprocal of resistance to flow, depends only on the characteristics of flow path such as pipe diameter or number of bends but not on the driving head. For simple fluid flows in pipe, CEQ's can be readily estimated using the correlations found in the literature.[9] However, such estimation is not as straightforward in the slurry-fed DWPF melter system, as particulates continue to settle and build up on the internal surface of pipe and, as a result, the resistance (and thus ΔP) changes with time. For complex flow configurations such as those encountered in a condenser or a HEPA filter, CEQ's must be determined from measured ΔP.

Some of the key CEQ values thus determined are shown in Table 2-2. It should be noted that PDI3684 is measured from the melter (PI3521) to a pressure tap approximately half way up the vertical section of the off-gas header jumper near the control air entry point, which means that the additional pressure drop from the pressure tap to the quencher inlet, including the 180° turn at the top and the primary isolation valve (MOV3689), is not measured. The MOG dynamics model, on the other hand, attempts to calculate the pressure drop across the entire length of off-gas header connecting the two nodes; primary film cooler and quencher. To do so, the measured PDI3684 of 0.95" H_2O shown in Table 2-1 was taken as the average of the pressure drop from the melter to the primary film cooler and that from the melter to the quencher. Thus, the ΔP values given in Table 2-2 for the primary film cooler and the off-gas header do not represent measured data; instead, they were set such that their average would closely match the measured PDI3684.

Once all ΔP's were either measured or estimated, the corresponding CEQ values were calculated using Eq. (6) from known feed and air purge rates and the calculated nodal properties. However, since the entire melter and off-gas system is kept under vacuum, the measured off-gas flow (FI3401) inherently includes the cell air inleakage into the system upstream of the orifice and the methodology used to estimate the air inleakage rates to the melter, OGCT and the pour spout bellows is explained in Section 2.2.7.

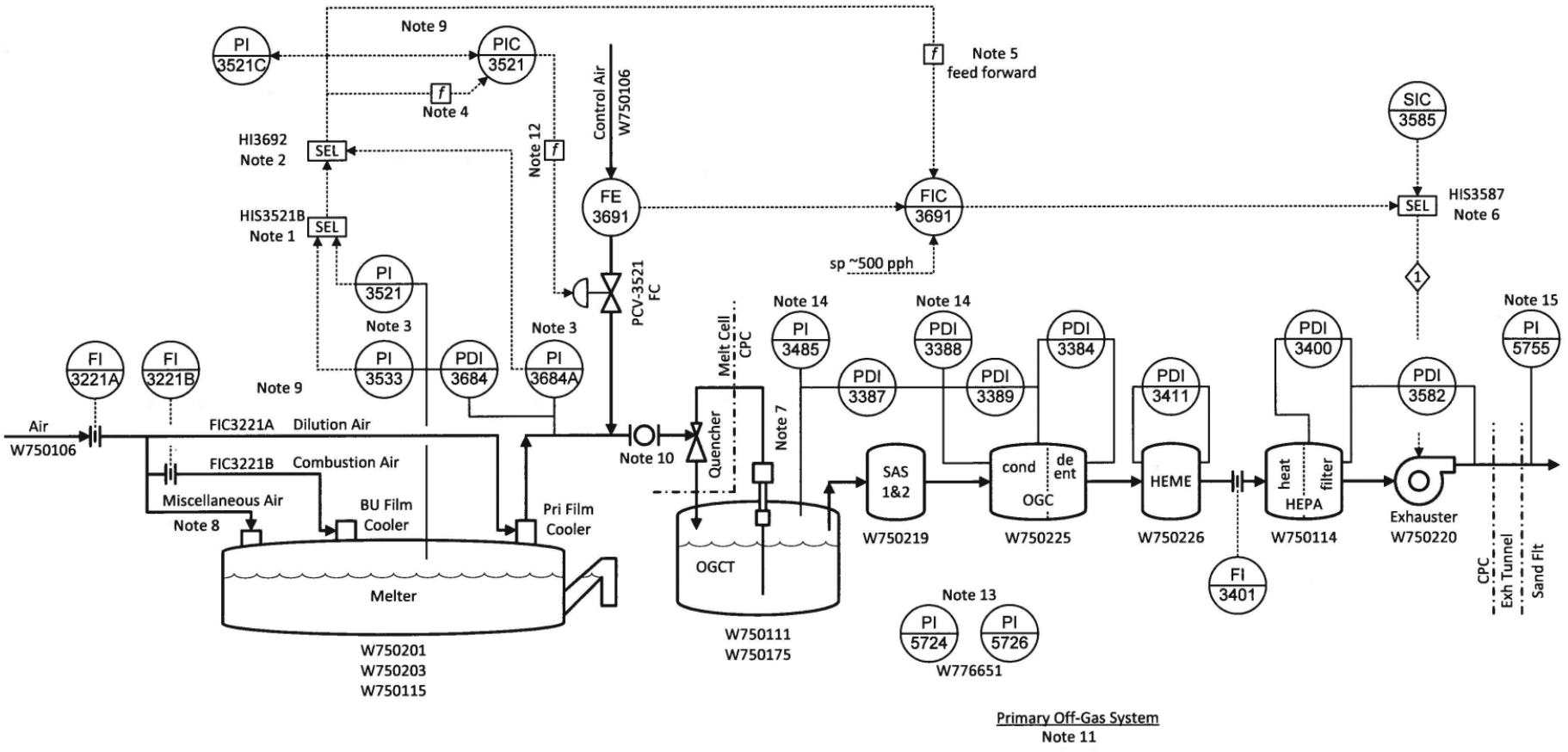

Figure 2-3. P&ID of DWPF Melter and Primary Off-Gas System (Courtesy of J. Coleman of SRR; Notes are found on the next page).

Function

Suction on the melter is generated by a combination of the quencher and exhauster. The quencher contribution is typically constant as the liquid flow though the quencher is constant. The exhauster, however, is driven by a VFD and provides variable suction. A constant air supply typically enters the melter pressure system through the Film Coolers and miscellaneous fixed inputs and a variable air supply enters through the PCV-3521 valve. All air exits through the exhauster.

PIC3521 modulates PCV-3521 to regulate melter pressure. As the valve opens, more make-up air is introduced and the pressure rises (suction is reduced). FIC3691 modulates the exhauster speed to keep the flow through PCV-3521 at ~500 pph, and thus, near the middle of its operating range.

Note that if the pressure is too low, PCV-3521 will open to increase the pressure. This will increase the FE3691 flow and cause the exhauster to slow down which will decrease the suction on the melter and, thus, further increase the melter pressure.

Notes

1 HIS3521B selects between PI3521A and PI3533A. Both transmitters come from the same pressure tap.

2 HI3692 selects between the output of HIS3521B (typical) and PI3684A (used as part of pressure protection logic).

3 Pressure is referenced to the melt cell pressure.

4 Controller gain and reset are changed when the melter pressure is farther from setpoint than specified limits.

5 Controller output is modified based on the melter pressure. There is no modification when the melter pressure is in the normal operating range.

6 HIS3587 selects which module, FIC3691 or SIC3585, controls the exhauster speed. In normal operation FIC3691 is selected.

7 Quencher pump -- HIS3343; Quencher speed -- SIC3343

8 Miscellaneous air to the melter includes purge air to the film coolers, borescope camera cooling air, and purge air to the sealpot.

9 Typical values:

FIC3691 sp	= 500 pph (operator can increase to 700 pph)
PIC3521 sp	= -5 inwc
Dilution air	= 560 pph
Combustion air	= 370 pph
Miscellaneous air	= 140 pph
FI3401	= 1750 pph (will increase as FIC3691 sp increases)

10 MOV3689 is normally open but closes on switchover to backup off-gas system.

11 See module PIC3533 for description of the backup off-gas system.

12 A software "valve cam" functionally linearizes an installed equal-percentage valve.

13 Melt cell pressure – PI5724; CPC pressure – PI5726; atm reference.

14 Pressure is referenced to CPC.

15 Pressure is referenced to atm.

Overrides

1 If a combination of melter pressure signals are high and film cooler air flows are low, then set exhauster output to 10%. (W766830)

Table 2-2. Estimated CEQ's of DWPF Melter Off-Gas System (As of 11/24/2014).

	ΔP	CEQ
	("H_2O)	$(lb.ft^3/psi.hr^2)^{1/2}$
Primary Film Cooler	0.77	30,000
Off-Gas Header	1.16	81,333
Condenser+De-Entrainer	4.01	172,000
HEME+Orifice+Pre-Heater	6.65	98,000
HEPA	0.74	900,000

2.2.3 Feed Forward Control

The feed forward control algorithm currently used in the DCS was coded into the model. Table 2-3 shows the additional percent RPM to be added to the FIC3691 output, depending on the PIC3521 input value. For example, when the melter pressure (PIC3521) spikes to +15" H_2O (or +20" H_2O from the set point), the FIC3691 output is increased by 15% of the actual exhauster speed range or:

(0.15) (RANGE(SIC3585)-ZERO(SIC3585)) = (0.15) (1,200-440) = 114 RPM.

On the other hand, when the melter pressure drops to -25" H_2O (or -20" H_2O from the set point), the FIC output is reduced by 40% or:

(-0.4) (RANGE(SIC3585)-ZERO(SIC3585)) = (-0.4) (1,200-440) = -304 RPM.

Thus, the feed forward control algorithm is more sensitive to protecting the melter from high vacuum than from high pressure. The feed forward control adders are linearly interpolated when the PIC3521 inputs fall between the threshold values.

Table 2-3. Feed Forward Control Adder to FIC3691 Output.

PIC3521	FIC3691
("H_2O)	(%)
-25	-40
-15	-20
-12	0
1	0
2	5
6	10
10	15
100	15

2.2.4 Dual Controller Settings

Two sets of GAIN and RESET values are used in the DCS for the PIC3521 loop. The normal GAIN and RESET values are 0.48 and 35.1 sec/repeat, respectively. However, when the melter pressure is 1.5" H_2O higher or 0.4" H_2O lower than the PIC3521 set point of -5" H_2O, the following SPIKE values are used: GAIN = 1.2 and RESET = 18 sec/repeat.

The FIC3691 loop was also detuned by reducing the GAIN from 0.778 to 0.15; however, the integral action of the PI controller was enhanced by reducing the RESET from 100 to 41 sec/repeat. The model has been revised to reflect these DCS settings.

2.2.5 Controller and Dynamic Valve Data

The tuning constants for the 22 PI controllers simulated in the model and their input/output values during the 30-min steady state period prior to the +10.8" H_2O pressure spike are given in Table 8-1 in Appendix A. The cross-reference between the model controllers and the corresponding DCS controllers is given in Table 8-2 in Appendix A.[10]

The characteristics of the 26 valves simulated in the model and their dynamic data during the same 30-min steady state period are given in Table 9-1 in Appendix B. The integer values shown under the "CTRL" heading in the last column corresponds to the model controller numbers found in Table 8-1. So if it is non-zero, the valve drive input (F) is received from a controller with that ID. If the value of CTRL is zero, it means that the valve is not part of any control loop and thus the valve drive input (F) is set manually. It is noted that the values of the final valve stem position (Y) are identical to their respective valve drive input values as the data represents steady state operation. The time derivative of Y (DYDT) being zero or close to zero for all valves is another indication of steady state. The location of each valve in the facility is shown in Figure 2 of the Inputs and Assumptions document[10] and the description of these valves is given in Table 9-2 in Appendix B.

2.2.6 Estimation of Calcine Gas Flows

As stated above, one of the two main goals of this study was to determine whether the off-gas surge that caused the +10.8" H_2O pressure spike would still be bounded by the baseline 3X/3X off-gas surge for non-bubbled operation in terms of off-gas flammability. For that, it is necessary to know the source term, i.e., the concentrations of H_2 and CO in the calcine gases produced from the feed. At the time of surge, the Melter Feed Tank Batch 720 (MFT720) was being fed at 0.75 GPM and the concentrations of oxidant (nitrate) and reductant (TOC) of MFT720 are compared in Table 2-4 to those of the SB8 feed for Case 26 at 894-gal antifoam addition.[2] As expected, the bounding SB8-26 feed is shown to have a higher TOC-to-nitrate ratio and thus a higher off-gas flammability potential than MFT720. For this reason, MFT720 was assumed to have the same composition as SB8-26 on a dry basis, including the nitrate and TOC, to ensure that the calculated off-gas flammability potential during the pressure spike would be conservatively high, although doing so does not affect the outcome of comparing the relative impacts on the flammability of the off-gas surge that resulted in a +10.8" H_2O pressure spike on 11/24/2014 vs. the baseline 3X/3X off-gas surge for non-bubbled operation.

Table 2-4. Comparison of Oxidant-Reductant Data for MFT720 vs. SB8-26.

	MFT720	**SB8-26**
Nitrate (mg/kg)	16,547	25,000
Formate (mg/kg)	27,599	49,254
TOC (mg/kg)	8,442	15,982
TOC/Nitrate (mole/mole)	2.64	3.30
Total Solids (wt%)	27.80	50.14
Calcined Solids (wt%)	24.20	40.21
Feed Rate (GPM)	0.75	1.50

In this study, the baseline composition of SB8-26 (and thus MFT720) was reconstituted with: (1) the Next Generation Solvent (NGS) with an additional 6 ppm TiDG due to partitioning in lieu of the current solvent used in the SB8 assessment,[2] (2) the maximum Isopar L and solvent limits of 87 ppm and 150 ppm, respectively, in the MCU effluent transfer, and (3) an additional H_2O to bring the total solids down from 50.14 to 27.8 wt%. The component feed flows of the re-constituted MFT720 are shown in Table 2-5 at the steady state feed rate of 0.75 GPM prior to the pressure spike. Based on the estimated density of 1.1724 g/ml and the calcine ratio of 0.802, the corresponding glass production rate is calculated to be 91.9 lb/hr, which is ~40% of the DWPF design basis glass production rate of 228 lb/hr. The printout of the formulas used in the charge balance and re-constitution of the baseline feed is given in Appendix C for the SB9 feed at the 894-gal antifoam addition as an example.

Table 2-5. Component Feed Flows of MFT720 @ 0.75 GPM Feed Rate.

Insoluble Solids	(lb/hr)		Soluble Solids	(lb/hr)
Fe(OH)3	13.8244		Ca(NO3)2	0.3978
Al(OH)3	8.3612		KNO3	0.1777
MnO2	2.0621		Mg(NO3)2	0.1240
Ca(OH)2	0.4692		Mn(COOH)2	0.7959
CaCO3	0		Mn(NO3)2	2.1028
CaSO4	0.1723		NaCl	0.0886
Cr(OH)3	0.0973		NaF	0
Cu(OH)2	0.1004		NaCOOH	16.2630
Mg(OH)2	0.1922		NaNO3	5.1568
Ni(OH)2	0.9993		NaNO2	0
La(OH)3	0.0372		Na2CO3	0.7683
Zn(OH)2	0.0309		Na2C2O4	0
RuO2	0.0413		Na2SO4	0.3190
RhO2	0.0087		Ni(NO3)2	0.0019
PdO	0.0007		H4SiO4	0.0090
B2O3	4.1116		HCOOH	0
Li2O	4.1960		Total Soluble	26.2049
Na2O	5.0643			
SiO2	47.0714		H2O	297.7082
TiO2	0.0947		Total Slurry	412.3928
ZrO2	0.1729			
BaSO4	0.0721		Density (g/ml)	1.1724
Coal	0.0557			
Antifoam	1.1892			
Solvent	0.0546			
Total Insoluble	88.4798			

These component feed flows were converted into the input vector for the 4-stage cold cap model run in gmole/hr, as shown in Table 2-6, using the decomposition scheme outlined in the Inputs and Assumptions document.[10] In essence, all salts except for the sulfates are pre-decomposed into oxides and gases, as they would once fed to the melter. This approach lessens the computational loads of model and helps achieve convergence faster. It is noted that the minor products of the NGS decomposition, CCl_4 and CF_4, as well as those trace-level species involving Ba, Cr, La, Rh, Ru, Ti, Zn, and Zr were excluded from the input vector, which has practically no impact as they constituted only 0.54 wt% of the dried solids and produce no flammable gases. The printout of the formulas used to develop the input vector is given in Appendix D.

Table 2-6. Input Vector for MFT720 Cold Cap Model Run @ 0.75 GPM Feed Rate.

Species	Stage 1	Stage 2	Stage 3
	(gmole/hr)	(gmole/hr)	(gmole/hr)
Solids:			
Al2O3	0	24.3098	0
B2O3	26.7887	0	0
CaO	0	3.9722	0
CuO	0.4668	0	0
Fe2O3	29.3373	0	0
K2O	0.3986	0	0
Li2O	0	63.6986	0
MgO	0	0	1.8092
MnO2	0	10.7588	0
MnO	7.8203	0	0
Na2O	68.0014	40.3507	0
NiO	4.8946	0	0
SiO2	356.7030	1.3339	0
CaSO4	0	0	0.5741
Na2SO4	0	0	1.0187
Coal	1.2144	1.0522	0.4209
Gases:			
H2O	173.4459	1.7786	0
CO	11.2072	60.2893	0
CO2	0	60.0202	0
H2	60.2893	3.5571	0
O2	2.7150	6.8964	4.1814
NO	6.2721	10.4535	4.1814
NO2	6.2721	10.4535	4.1814
HCOOH	0	0	0
CH4	7.9623	0	0

The results of the 4-stage Cold cap model run for MFT720 are shown in Table 2-7. The predicted glass compositions are split in groups or phases. The letter l after each species in the melt phase denotes "liquid." The thermodynamic properties of these melt species were taken from the National Institute of Standards and Technology (NIST) free energy database; they do not necessarily represent independent molecular or ionic species but serve to represent the local associative order.[11] Spinels readily form solid solutions with one another due to their structural similarities and thus they are allowed to form a separate phase of their own. On the other hand, each species included in the Invariant Condensed Phase (ICP) is assumed to form a separate phase by itself. As more species are included in the ICP, the total number of phases to be considered in the equilibrium calculations increases proportionally, thus making it more difficult to achieve convergence.

As expected with the bounding levels of nitrate and TOC of SB8-26, the glass produced from MFT720 was reducing with a calculated REDOX of 0.321 vs. 0.309 for the SB8-26 glass,[2] while the two main flammable gases, H_2 and CO, together make up 16.4 vol% of the calcine gases; (49.8451+18.6469) / 418.0239 = 0.164. It is also noted that 49 vol% of the calcine gases is H_2O vapor produced from the

decomposition of hydroxides and the oxidation of H_2 produced from the decomposition reactions of salts in the cold cap. The composite molecular weight and heat capacity of the calcine gases were calculated to be 24.735 g/gmole and 0.3374 Pcu/lb/°C (=Btu/lb/°F), respectively, which were input into the MOG dynamics model along with the condensable and non-condensable flow rates of 297.71 and 22.8 lb/hr, respectively.

Also shown in Table 2-7 is the minimum combustion air flow, which was calculated at 125% of the stoichiometric requirement to oxidize 3 times the normal flow of flammable gases at 1.5 GPM feed rate:

[(49.8451 + 18.6469) moles/hr H_2 +CO] (mole O_2/2 moles H_2 or CO) (mole air/0.21 mole O_2)

*(3)(0.75/1.5)(**1.25**) = 1,223 gmole/hr air*

Or = (1,223 gmole/hr air) (28.97 g/mole air) (lb/453.6 g)

= 78 lb/hr

Note that this is considerably below the theoretical minimum backup film cooler air purge (FIC3221B) of 233 lb/hr before a margin for instrument uncertainty is added.

Table 2-7. Results of MFT720 Cold Cap Model Run @ 0.75 GPM Feed Rate.

Melt:	**(gmole/hr)**		**Calcine Gases:**	**(gmole/hr)**
SiO2 l	244.9632		H2O	205.0866
Na2SiO3	109.3813		CO2	123.5242
LiBO2 l	53.4749		H2	49.8451
LiAlO2 l	48.6150		N2	20.9091
Fe3O4 l	13.5330		CO	18.6469
MgSiO3 l	1.7487		SO2	0.0036
FeO l	4.1560		NaBO2 g	0.0001
CaFe2O4	1.0157		NH3	0.0030
B2O3 l	0.0000		CH4	0.0053
Ca2SiO4	0.8985		Total	418.0239
Ca3MgSi2	0.0480		Total (lb/hr)	22.7950
Fe2SiO4	0.5760			
Li2O l	12.6448		MW (g/gmole)	24.735
K2SiO3	0.3571		Cp (Pcu/lb/°C)	0.3374
KBO2	0.0832		H2/(CO+CO2)	0.3506
Spinel:			CO/CO2	0.1510
NiFe2O4	4.8836			
Mn3O4	6.1933		Min Combustion Air @ 1.5 GPM =	1,223
CuFe2O4	0.4669			
MgFe2O4	0.0126			
ICP:			**Volatiles:**	**(gmole/hr)**
Fe2O3	0.0000		free H2O	7,496.00
NiO	0.0106		HCOOH	0
CaSO4	1.5893		Total	7,496.00
Ni3S2	0.0000		Total (lb/hr)	297.71
MnO	0.0000			
Fe^{+2}/Fe^{total} =	0.321			

2.2.7 Estimation of Air Inleakage Rates

The total air inleakage into the system was calculated as the measured off-gas flow at the orifice less the sum of air purges and calcine gas flows just estimated. Using the steady state flow data from Table 2-1,

Total Air Inleakage = FI3401 – (FIC3221A + FIC3691 + FI3526 + Calcine Gas Flows)
= 1,662 – (1,069.5 + 501.4 + 59.6 + 22.8)
= 8.7 lb/hr

This is unrealistically low as the air inleakage to the melter alone was estimated earlier to be ~50 lb/hr by performing an energy balance around the film cooler.[4,7] Unfortunately, the same methodology could not be applied in this study due to lack of off-gas temperature data at the primary film cooler exit (TIC3682). As a result, it was assumed that the melter air inleakage rate has remained the same at ~50 lb/hr to this day. Other potential sources of air inleakage include the pour spout bellows and the OGCT. Since the pour spout pressure (PI3527) was slightly negative at -0.96" H_2O (i.e., the melter was in a non-pour mode at the time of surge), a minimal air inleakage rate of ~1 lb/hr was assumed. Furthermore, the instrument accuracy of FI3401 is given as ±2% of its range from 0 to 3,036 lb/hr or ±60.7 lb/hr.[12] Thus, the air inleakage to the OGCT could be set at as high as ~18 lb/hr (=60.7+8.7-50-1). The actual air inleakage rates and the corresponding CEQ values used in the model are summarized in Table 2-8. As shown in Table 2-1, the calculated off-gas flow at the orifice, including these air inleakage rates, was 1,690 lb/hr, which is 1.7% higher than the measured FI3401 but within the range of instrument accuracy.

Table 2-8. Estimated Air Inleakage Rates and CEQ Values.

	Air Inleakage	**CEQ**
	(lb/hr)	$(lb.ft^3/psi.hr^2)^{1/2}$
Melter	50.2	4,000
OGCT	11.9	1,500
Pour Spout Bellows	1.2	500

2.3 Dynamic Simulation of +10.8" H_2O Pressure Spike

The calibrated MOG dynamics model was next run under various cold cap off-gas surge profiles until the predicted melter pressure profile matched the measured data. The total simulation time was 6 min, including the first 1-min steady state prior to the pressure spike. However, the duration of available data for the model vs. data comparison was only 12 sec long as the second pressure spike caused by the forward flush began while the system was still in the early stages of recovery from the first pressure spike, as shown in Figure 2-1, and the forward flush was not simulated in this study.

The dynamic simulation began by inputting an assumed off-gas surge profile at the 1-min mark, i.e., at the onset of pressure spike. The baseline 3X/3X off-gas surge for the non-bubbled DWPF melter proceeds as follows[10]: At time zero, the condensable and non-condensable flows that originate from the slurry feed instantly increase to 3 times (3X) their respective normal values, then immediately decrease linearly to 50% of their respective peak values during the first 1 min and further decrease linearly to their respective normal values (1X) during the next 7 min. In this study, the off-gas surge profiles were created by varying the multiplication factors for the condensable and non-condensable flows as well as the durations. The normal condensable (free H_2O in the MFT720) and non-condensable (calcine gases) flow rates are given in Table 2-7. The predicted dynamic responses of the system such as the melter pressure, control air flow, exhauster speed, etc. to a given surge profile were then compared to their respective measured data during the next 12 sec. This process was repeated by varying the multiplication factors as well as the durations until some of the key operating data were matched by the predicted values.

2.3.1 Results of Dynamic Simulation

Figure 2-4 shows the predicted melter pressure (PIC3521) and control air flow (FIC3691) profiles under the 24X/6X off-gas surge with peak duration of 20 sec vs. the DCS data. It is seen that the model predicts the measured melter pressure data very well during both the initial and the recovery phases, which gives credence to the calculated peak pressure of 19" H_2O. Incidentally, when the initial and recovery slopes of PIC3521 in Figure 2-1 (i.e., away from the plateau) are extrapolated, they would intersect at ~19" H_2O. Furthermore, the melter pressure (PIC3521) is shown to respond to the surge without any delay as the off-gas surge was initiated at the 1-min mark, as shown in Figure 2-5A. The predicted melter pressure control air profile is also shown to agree with the measured data very well, including the minimum of ~50 lb/hr.

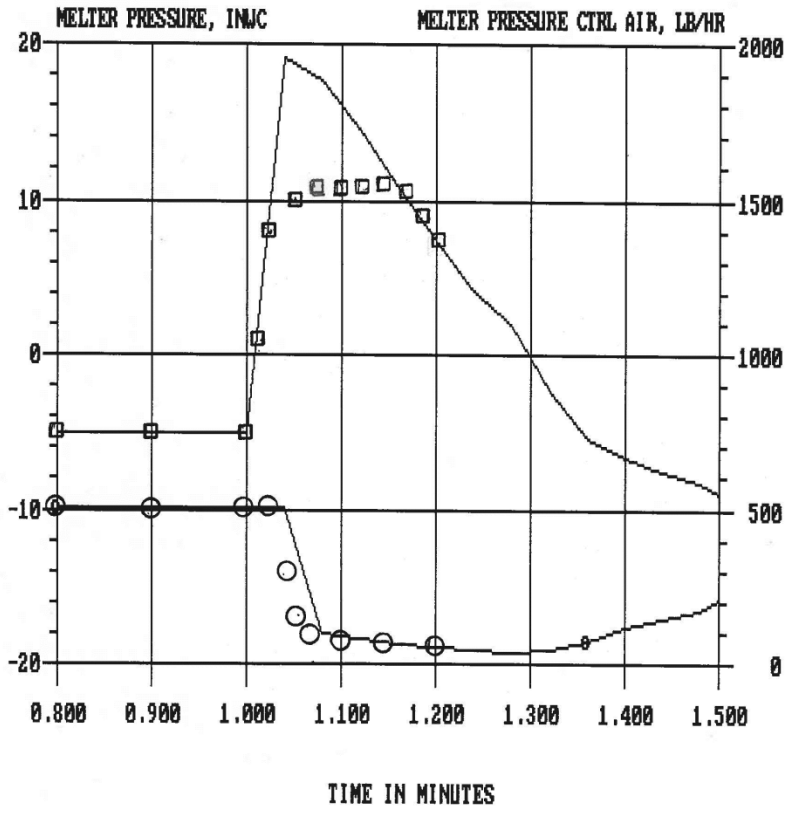

Figure 2-4. Predicted Melter Pressure and Control Air Flow During 24X/6X Surge vs. Data (□ = melter pressure; ○ = melter pressure control air).

Figure 2-5A shows the 24X/6X cold cap off-gas surge profile with a peak duration of 20 sec. Using the normal (1X) condensable and non-condensable flow rates given in Table 2-7, the peak off-gas flow rate is calculated to be (24)(297.7) + (6)(22.8) ≈ 7,280 lb/hr, and the actual peak flow shown is slightly lower. Figure 2-5B shows the predicted ΔP across the off-gas header vs. measured data (PDI3684); the latter were also maxed out at about +12" H_2O due to inadequate calibration range. Unlike the melter pressure, however, the off-gas header ΔP did not drop below the transmitter maximum at the 1.2-min mark or 12 sec into the surge, and the model correctly predicted this trend; calculated ΔP's were higher than 12" H_2O. Figure 2-5C shows that the model begins to over predict the measured ΔP across the exhauster (PDI3582) at the 1.1-min mark and, as a result, the predicted exhauster speed becomes higher than the measured data (SIC3585) by less than 20 RPM in order to pull roughly the same amount of gas over a higher ΔP (Figure 2-5D); PDI3582 actually represents pressure increase rather than pressure decrease as in all other ΔP data.

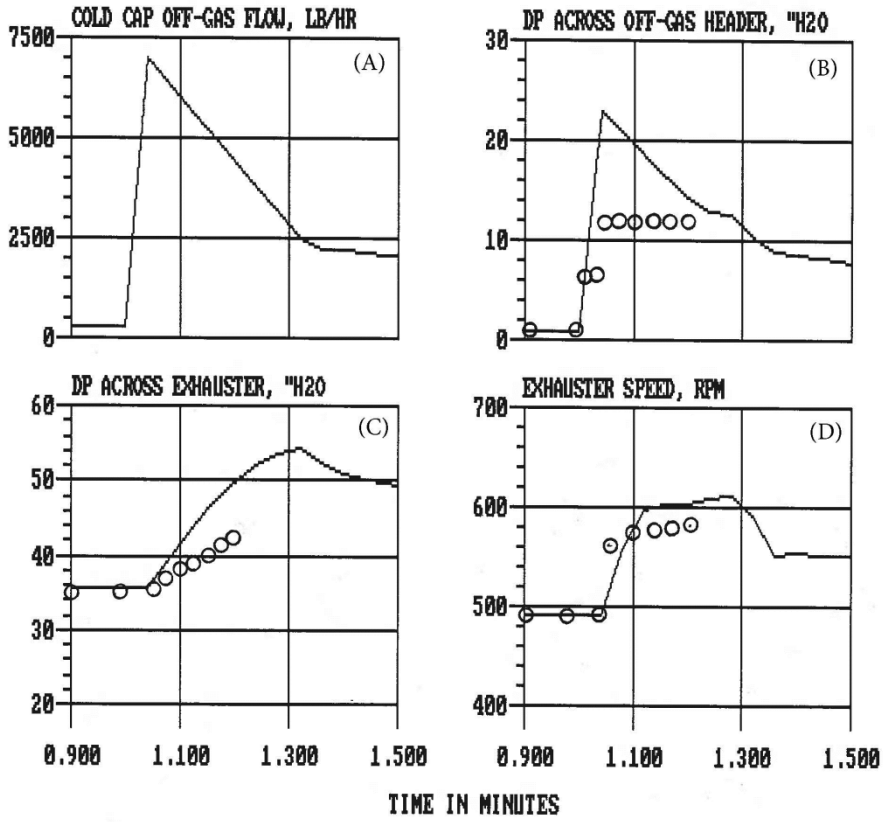

Figure 2-5. 24X/6X Off-Gas Surge and Predicted ΔP's and Exhauster Speed vs. Data (○).

The over-prediction of the exhauster ΔP is likely due to the under-prediction of the OGCT pressure, as shown in Figure 2-6. While the predicted OGCT pressure continues to drop below the initial value of -3.1" H_2O throughout the surge, the measured data shows a peak much like the melter pressure peak also shown. One potential cause for this discrepancy could be that while the model assumes 100% condensation of the condensable flow entering the quencher throughout the surge, a significant fraction of the steam flow in excess of 7,000 lb/hr at the peak of surge could have exited the quencher as a vapor, causing the OGCT pressure to rise. However, this hypothesis is not supported by the measured OGCT vapor temperature data (TI3620E), which remained constant at 29°C throughout. If 100% of excess steam indeed condenses out as assumed in the model, a large reduction in the discharge vapor volume will result, which coupled with a modest increase in the exhauster speed is expected to create vacuum downstream.

Figure 2-7 shows the predicted off-gas flow profiles through the HEME and HEPA during the surge; the latter shown by the lower curve essentially represents the exhauster suction. Prior to the surge, both flows are shown to be equal as they should under steady state. As the surge progresses, they begin to diverge due to their different CEQ values and thus ΔP's. Under steady state conditions, the non-condensable calcine gases make up less than 1% of the off-gas flow at the orifice: (22.8 lb/hr)(1-0.49)/(1,662 lb/hr) ≈ 0.007. Thus, the increase in the FI3401 data by ~400 lb/hr at the peak of surge is largely due to increased exhauster speed and the contribution by the calcine gas surge is small. Nevertheless, when the magnitude of non-condensable flow surge was set at 6X normal, the predicted off-gas flow through the HEME node is higher than the measured data by ~100 lb/hr or more at the peak of surge and does not drop below the data throughout, which suggests that the 6X non-condensable flow surge was not likely under estimated.

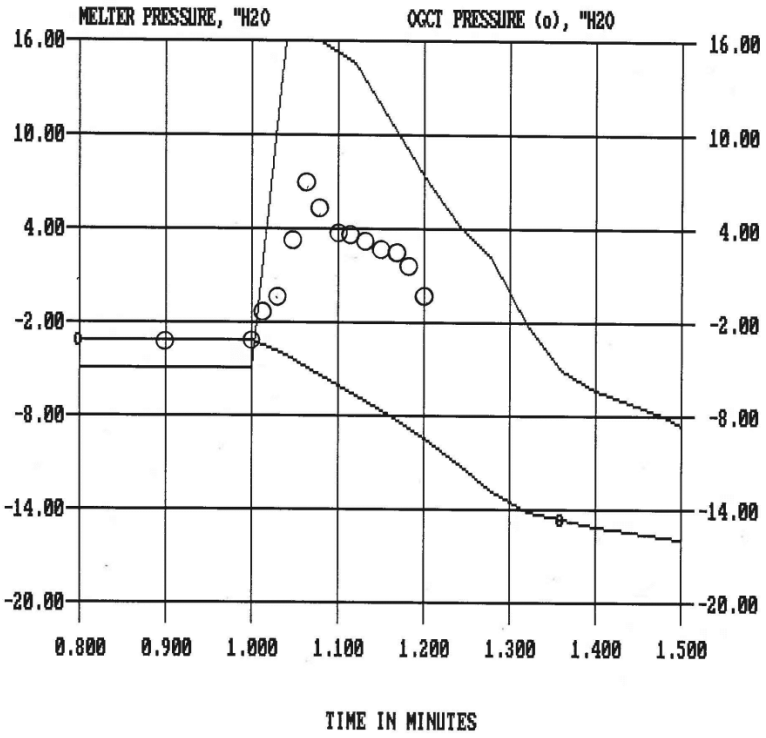

Figure 2-6. Predicted vs. Measured (○) OGCT Pressure During 24X/6X Surge.

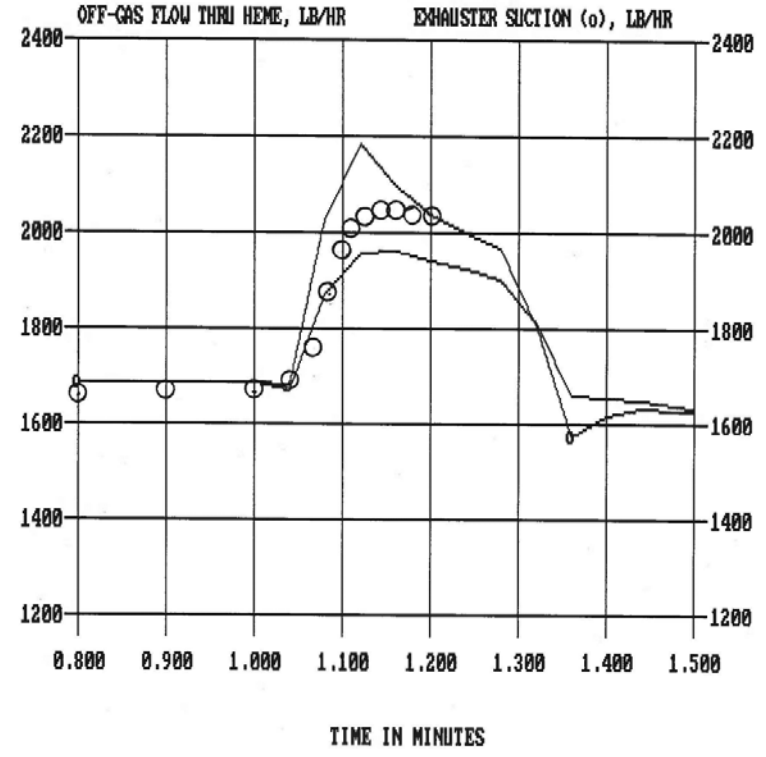

Figure 2-7. Predicted Off-Gas Flows through HEME and HEPA vs. Measured Data FI3401 (○) During 24X/6X Surge.

2.4 Comparison of Off-Gas Flammability Potentials

Once the magnitudes of condensable and non-condensable flow surges were determined for the bounding pressure spike that has occurred under non-bubbled operation, a standalone 24X/6X off-gas surge with peak duration of 20 sec was simulated using the calibrated model under the operating conditions listed in Table 2-1. As shown in Figure 2-8, the peak flammability potential of the OGCT vapor during the surge was calculated to be 13% of the LFL, which is considerably lower than 60% of the LFL despite the fact that the composition of MFT720 was adjusted to contain the bounding level of TOC. There are two main reasons for the low flammability potential. First, the total solids of MFT720 was 27.8 wt% compared to 50.1 wt% for the SB8-26, which means that at a given volumetric feed rate, the instantaneous mass feed rate of TOC in MFT720 was ~50% of that in SB8-26 and thus reduced flows of H_2 and CO. Second, the initial melter vapor space temperature of 662.7 °C at the onset of surge was considerably higher than the TSR minimum of 504 °C, including the instrument uncertainty, which resulted in higher combustion rates of H_2 and CO in the melter vapor space.

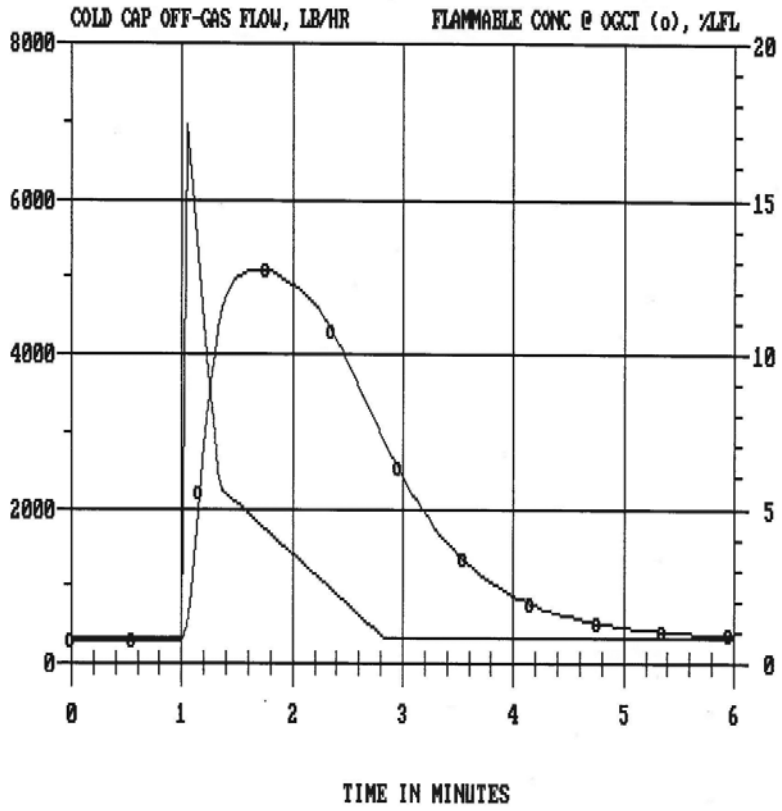

Figure 2-8. Predicted Flammability Potential of OGCT Vapor During 24X/6X Surge with 20-sec Peak Duration.

As a comparison, the baseline 3X/3X surge with 1-min peak duration for non-bubbled operation was also simulated using the same feed composition and the same operating conditions listed in Table 2-1. Since the 3X/3X surge is based on 1.5 GPM feed rate and the actual feed rate of MFT720 was 0.75 GPM, the surge magnitudes were effectively doubled to 6X/6X. As expected, the calculated cold cap off-gas flow at the peak of 6X/6X surge is shown to be 25% of that of the 24X/6X surge, i.e., 6X/24X = 0.25 or 25% (Figure 2-8 vs. Figure 2-9A). As a result, the calculated peak melter pressure is considerably lower; 0" H_2O vs. +19" H_2O for the 24X/6X surge (Figure 2-9B). However, the peak flammability potential of the OGCT vapor is slightly higher at 15% of the LFL (Figure 2-9C), which is attributed to the 3X longer duration than that of the 24X/6X. These results indicate that from the standpoint of off-gas flammability control the current 3X/3X non-bubbled surge basis at 1.5 GPM with 1-min peak duration bounds the largest pressure spike that has occurred in the facility during non-bubbled operation.

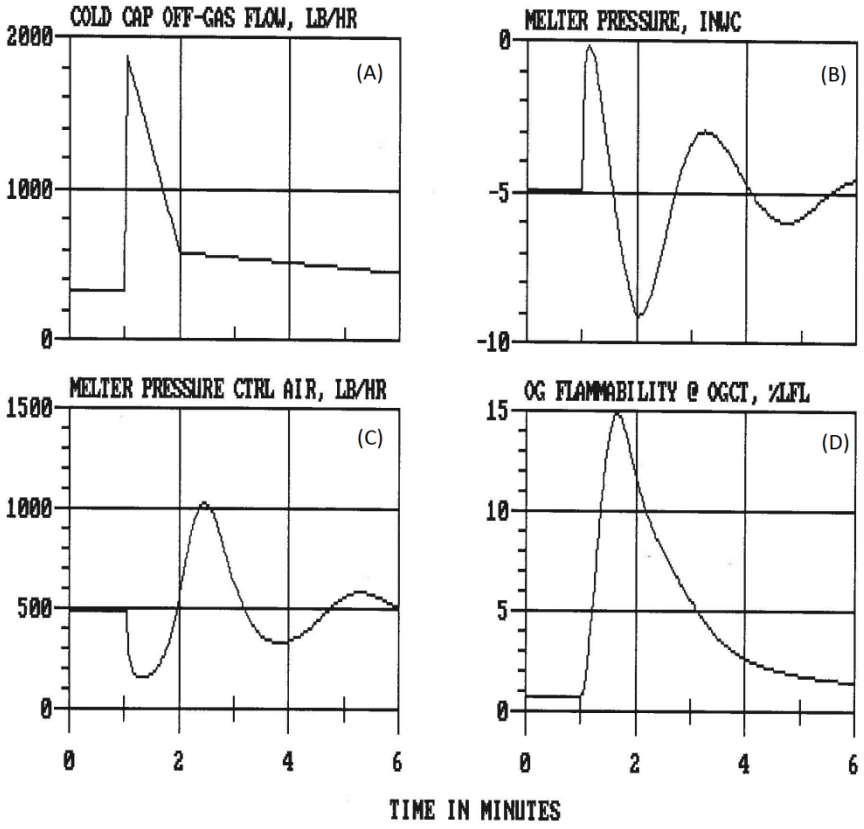

Figure 2-9. Predicted Flammability Potential of OGCT Vapor During 6X/6X Surge with 1-Min Peak Duration.

3.0 Assessment of SB9 Flammability Potential

One of the main goals of this study was to determine whether the current TSR limits on TOC set for SB8 would remain valid for SB9 under non-bubbled operation. With the MOG dynamics model fully updated and calibrated using the latest facility data, the assessment proceeded in the following steps:

1. Obtain a complete set of analytical data for the SME or SRAT product samples, including both slurry and supernate analysis, from the SB9 simulant CPC demonstration run and, if available, the Shielded Cell run with the SB9 Qualification samples.

2. Perform charge balance on the analytical data to develop a baseline SB9 melter feed composition.

3. Add to the baseline SB9 melter feed; (1) coal at 240 ppm, (2) non-volatile Modular Caustic-side solvent extraction Unit (MCU) solvent based on the maximum effluent transfer limits, and (3) antifoam based on the addition scenario of 728 gallons per CPC cycle at 20:1 dilution.[10] If desired, the volume antifoam addition may be converted to the pure antifoam mass basis.

4. Develop the input vector for the 4-stage cold cap model from the reconstituted SB9 melter feed composition, run the model and determine the calcine gas composition, including H_2 and CO.

5. Run the MOG dynamics model using the calculated H_2 and CO concentrations as the source term and calculate the bounding TOC concentration at the nitrate levels ranging from 10,000 to 70,000 ppm at 5,000 ppm increments by varying the formate level until the calculated peak concentration of flammable gases in the OGCT increases to 60% of the LFL during the 3X/3X off-gas surge.

6. Compare the calculated bounding TOC limits to the existing TOC limits set for the SB8 as a function of nitrate concentration.

7. Repeat Steps 3 through 6 for the 894 and 1,017 gal antifoam addition scenarios.

The conditions under which the MOG dynamics model was run in each case were identical to those used in the SB8 assessment,[2] including the minimum melter vapor space temperature (TI4085D) of 460 °C (Eq. 1), the minimum total melter air purge (FIC3221A) of 900 lb/hr (Eq. 2), the minimum air purge to the backup film cooler (FIC3221B) of 233 lb/hr (Eq. 3), slurry feed rate of 1.5 GPM and 3X/3X off-gas surge with 1-min peak duration.

3.1 Charge Balance

The analytical data for the SME product produced during the SB9A simulant CPC demonstration run formed the basis for developing the baseline SB9 melter feed composition.[13] The steps that were followed to reconcile the charge imbalances in the data along with the results of charge balance, including the printout of the formulas used in the spreadsheet, are documented in a separate report.[14] The charge-reconciled baseline SB9 melter feed flows at the DWPF design basis glass production rate of 228 lb/hr are shown in Table 3-1; note the composition reflects the NaOH strike made to the SME product to simulate the projected insoluble Na concentration in the Tank 51H/Tank 40H blend.[13] The total solids was high at 50.14% and, based on the estimated density of 1.437 g/ml, the volumetric feed rate was calculated to be 0.825 GPM, which is 55% of the safety basis feed rate of 1.5 GPM. The concentration (or the flow rate) of antifoam shown reflects the actual amount of antifoam added during the CPC demonstration run at 0.03 lb pure antifoam/lb Fe. The concentrations of coal and the non-volatile MCU solvent are shown to be zero, as they were not added during the simulant run. The printout of the formulas used for the charge balance and re-constitution of the baseline SB9 feed (Step 3 above) is repeated in Appendix D for the SB9 at the 894-gal antifoam addition as an example.

Table 3-1. Baseline SB9 Melter Feed Flows at 228 lb/hr Glass Production Rate.[14]

Insoluble Solids:	(lb/hr)	Soluble Solids:	(lb/hr)
Fe(OH)3	30.2084	Ca(COOH)2	0.3740
Al(OH)3	19.6114	Ca(NO3)2	0.1741
MnO2	4.5292	Mn(COOH)2	5.8068
Ca(OH)2	0	Mn(NO3)2	2.6456
Mg(OH)2	0	NaCl	0.0484
HgO	1.8272	NaF	0
Ca3(PO4)2	0	NaCOOH	27.4741
Ni(OH)2	1.6523	NaNO3	12.6741
Cr(OH)3	0	NaNO2	0
Cu(OH)2	0	NaOH	12.3590
SiO2	121.1627	Na3PO4	0
Na2O	11.6898	Ni(COOH)2	0.0039
B2O3	12.8764	Ni(NO3)2	0.0018
Li2O	8.9648	Na2CO3	0.0316
CaCO3	0	Na2C2O4	0.1713
CaSO4	0.4454	Na2SO4	0.6212
CaC2O4	1.7650	HCOOH	0
Coal	0	Total Soluble	62.3858
Antifoam	0.4681	H2O	276.0054
Solvent	0	Total Slurry	553.5922
Total Insoluble	215.2011	Total Slurry (GPM)	0.825
		Total Solids (wt%)	50.14
		Density (g/ml)	1.437

3.2 Calculation Flowchart

The determination of the maximum TOC limits at varying nitrate levels (Steps 4 and 5 described above) involves multiple calculation steps and iteration loops, as shown in Figure 3-1 for the 894-gal antifoam addition scenario. The calculation begins by fixing the total amount of antifoam added per CPC cycle at one of the following three values; 728, 894 and 1,017 gallons at 20:1 dilution. Next, the nitrate level in the reconstituted baseline feed is adjusted to 10,000 ppm by decreasing the concentrations of all nitrate salts by the same ratio. The concentrations of all formate salts are next increased or decreased uniformly, depending on the target value, by the same ratio. The 4-stage cold cap model is next run with the adjusted feed and the resulting calcine gas composition is calculated using the counter-current equilibrium reactor modeling approach.

The calculated calcine gas flows are next input into the MOG dynamics model, which then calculates the transient concentration profile of flammable gases throughout the off-gas system under the 3X/3X off-gas surge scenario. If the calculated peak concentration of H_2/CO in the OGCT vapor space is lower (higher) than 60% of the LFL, the formate level in the reconstituted feed is adjusted higher (lower) and the model runs are repeated. Once the 60% of the LFL target is met, the nitrate level in the reconstituted feed is increased by 5,000 ppm and the calculations are repeated until the nitrate level reaches 70,000 ppm. The entire calculation cycle shown in Figure 3-1 was repeated for each of the three antifoam addition cases.

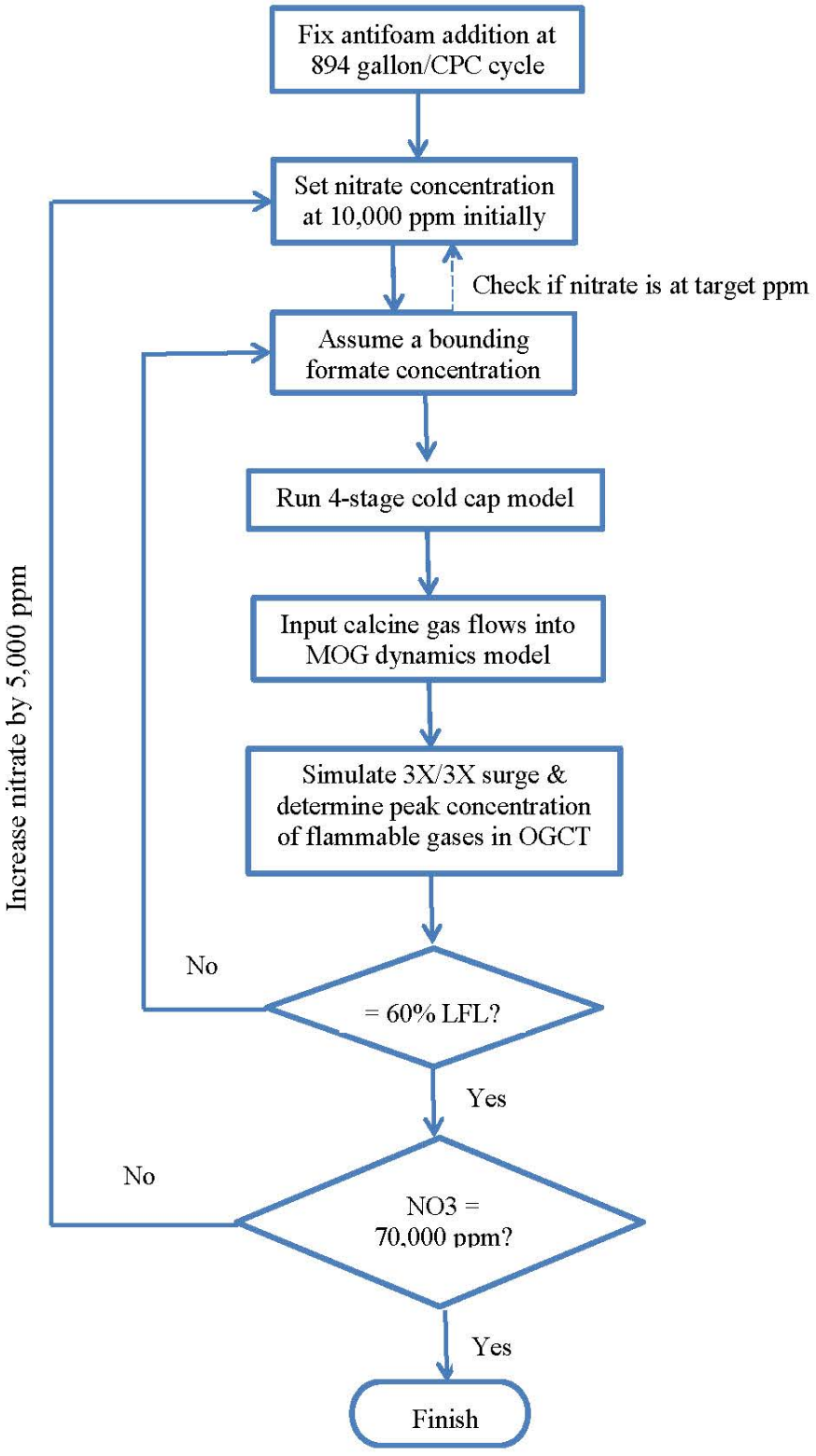

Figure 3-1. Calculation Flowchart for 894-Gallon Antifoam Addition.

3.3 Inputs and Assumptions

The inputs and assumptions used in the SB9 flammability assessment range from plant utilities (e.g., temperature, pressure and flow rates of air/steam supply) and equipment specifications (e.g., performance data for the exhauster and DCS controller tuning constants) to the fundamentals of model constructs and calculation methods (e.g., vapor-liquid equilibrium assumption). All of the key inputs and assumptions used are documented in detail in another report,[10] and thus they are not repeated here.

3.4 Results

Since the calculations were repetitive in nature from one case to the next, only the full results of the model runs for the 894-gal antifoam addition at 25,000 ppm nitrate are presented next as an example. It is also noted that the two models, 4-stage cold cap and MOG dynamics models, are collectively called the DWPF MOG flammability model.[15]

3.4.1 4-Stage Cold Cap Model Run

The bounding SB9 melter feed component flows at 1.5 GPM feed rate is shown in Table 3-2. Due to increases in nitrate (NO_3) from 20,247 to 25,000 ppm and formate (COOH) from 39,825 to 50,217 ppm (compared to the 894-gal antifoam baseline feed without the waste loading adjustment), the total solids was increased from 50.61 to 51.83 wt% and the concentration of TOC was increased from 14,235 to 16,920 ppm. These re-constituted feed flows were next converted into the cold cap model input vector shown in Table 3-3 using the decomposition scheme outlined in the Inputs and Assumptions document.[10].

Table 3-2. Re-constituted SB9 Melter Feed Flows at 1.5 GPM Feed Rate (25,000 ppm Nitrate, 894 Gallon Antifoam).

Insoluble Solids	(lb/hr)		Soluble Solids	(lb/hr)
Fe(OH)3	58.4037		Ca(COOH)2	0.9349
Al(OH)3	37.9159		Ca(NO3)2	0.4261
CaCO3	0		Mn(COOH)2	14.5134
CaSO4	0.8632		Mn(NO3)2	6.4752
CaC2O4	3.4104		NaCl	0.0935
MnO2	8.7567		NaF	0
HgO	3.5327		NaCOOH	68.6682
Ni(OH)2	3.1945		Na2CO3	0.0611
B2O3	24.8948		Na2C2O4	0.3312
Li2O	17.3326		NaNO3	31.0194
Na2O	22.6007		NaOH	23.8943
SiO2	234.2513		Na2SO4	1.2009
Coal	0.2569		Ni(COOH)2	0.0098
Antifoam	5.8111		Ni(NO3)2	0.0043
Solvent	0.0456		HCOOH	0
Total_1	421.2701		Total Soluble	147.6324
			H2O	528.7117
			Total Slurry	1097.6142
			Total Solids (wt%)	51.83
			TOC (ppm)	16,920

Table 3-3. Input Vector for 4-Stage Cold Cap Model Run @ 1.5 GPM Feed Rate (25,000 ppm Nitrate, 894 Gallon Antifoam).

Species	Stage 1	Stage 2	Stage 3
	gmole/hr	gmole/hr	gmole/hr
Al2O3	0	110.2428	0
B2O3	162.1983	0	0
CaO	0	16.5137	0
CuO	0	0	0
Fe2O3	123.9459	0	0
K2O	0	0	0
Li2O	0	263.1087	0
MgO	0	0	0
MnO2	0	45.6887	0
MnO	61.8235	0	0
Na2O	447.2661	166.7879	0
NiO	15.6706	0	0
SiO2	1,774.9736	6.5184	0
CaSO4	0	0	2.8761
Na2SO4	0	0	3.8350
coal	3.8557	4.8516	1.9406
H2O	862.3780	8.6912	0
CO	35.9260	326.5343	0
CO2	0	291.1617	0
H2	295.0852	17.3825	0
O2	12.7297	32.8046	20.0748
NO	30.1122	50.1870	20.0748
NO2	30.1122	50.1870	20.0748
CH4	36.9589	0	0

The results of 4-stage cold cap model run are shown in Table 3-4. As expected with the bounding level of TOC at 25,000 ppm nitrate, the glass was predicted to be very reducing with a calculated REDOX of 0.457; however, it was still not reducing enough to form Ni_3S_2. The concentrations of H_2 and CO were high, together making up 16.4 vol% of the total calcine gases; (244.896+91.5448)/2,059.41 = 0.164. On a dry basis, they make up 32% of non-condensable calcine gases. The composite molecular weight and heat capacity of the calcine gases were calculated to be 24.7394 g/gmole and 0.3374 Pcu/lb/°C (=Btu/lb/°F), respectively, which were input into the MOG dynamics model along with the condensable flow of 528.7 lb/hr and the non-condensable flow of 112.3 lb/hr, including the source terms, H_2 and CO.

Also shown in Table 3-4 is the minimum combustion air flow, which was calculated at 125% of the stoichiometric requirement to oxidize 3 times the normal flow of flammable gases at 1.5 GPM feed rate:

[(244.896 + 91.5448) moles/hr H_2 +CO] (mole O_2/2 moles H_2 or CO) (mole air/0.21 mole O_2)

*(3)(**1.25**) = 3,003.94 gmole/hr air*

≈ 192 lb/hr

Note that this is below the theoretical minimum backup film cooler air purge (FIC3221B) of 233 lb/hr before the margin for instrument uncertainty is added.

Table 3-4. 4-Stage Cold Cap Model Output at 1.5 GPM Feed Rate (25,000 ppm Nitrate, 894 Gallon Antifoam).

Melt:	**(gmole/hr)**		**Calcine Gases:**	**(gmole/hr)**
SiO2 l	1149.4823		H2O	1,012.9246
Na2SiO3	617.9034		CO2	609.6182
LiBO2 l	305.5288		H2	244.8960
LiAlO2 l	220.5641		N2	100.3716
Fe3O4 l	57.7992		CO	91.5448
FeO l	37.4047		SO2	0.0148
CaFe2O4	2.5919		NaBO2 g	0.0005
B2O3 l	9.4093		NH3	0.0147
Ca2SiO4	5.0510		CH4	0.0258
Fe2SiO4	9.0701		Total	2,059.4109
Li2O l	0.0012		Total (lb/hr)	112.3
Spinel:				
NiFe2O4	6.8951		MW (g/gmole)	24.7394
Mn3O4	27.4879		Cp (Pcu/lb/°C)	0.3374
CuFe2O4	0		H2/(CO+CO2)	0.3493
ICP:			CO/CO2	0.1502
Fe2O3	0			
NiO	8.7753		Min Combustion Air (lb/hr) =	192
CaSO4	6.6972			
Ni3S2	0			
MnO	25.0442		**Volatiles:**	
Cu	0		free H2O (lb/hr)	528.7
Cu2O	0		HCOOH	0
Fe^{+2}/Fe^{total} =	0.457			

3.4.2 MOG Dynamics Model Run

The results of 3X/3X surge simulation are shown in Figure 3-2 and Figure 3-3. The cold cap off-gas flow is shown to peak at ~1,900 lb/hr, which is 3X the baseline flow rate of 641 lb/hr (=528.7+112.3) (Figure 3-2A). The combined concentration of H_2 and CO in the OGCT vapor reaches 60% of the LFL ~45 sec after the surge began (Figure 3-2D). The melter vapor space gas temperature drops by ~100 °C from 294 °C initially to a minimum of ~200 °C (Figure 3-2B) so the combustion rates of H_2 and CO slow down considerably during the first 1 min. Slower combustion kinetics coupled with a 3X spike in the source term flows and the condensation of steam in the quencher causes the concentrations of H_2 and CO to peak in the OGCT vapor space.

Since the peak melter pressure is still negative (Figure 3-2C), the feed forward control adder to the FIC3691 output is zero (Table 2-3), which does not help accelerate the already-dampened response of the feed forward control, resulting in only a modest increase of 55 RPM in exhauster speed from 460 to 515 RPM (Figure 3-3D). Even at a ~100 RPM increase during the 24X/6X surge on 11/24/2014 (Figure 2-5), the OGCT pressure was still above the initial value 12 sec after surge began during the recovery phase (Figure 2-6), which indicates a positive net accumulation of off-gas, i.e., flammable gases were not being exhausted out of the OGCT fast enough. This confirms that the primary objective of feed forward control is to protect the OGCT from excessive vacuum, e.g., reaching -40" H_2O, at which point the vent valve opens and the feed is interlocked off.

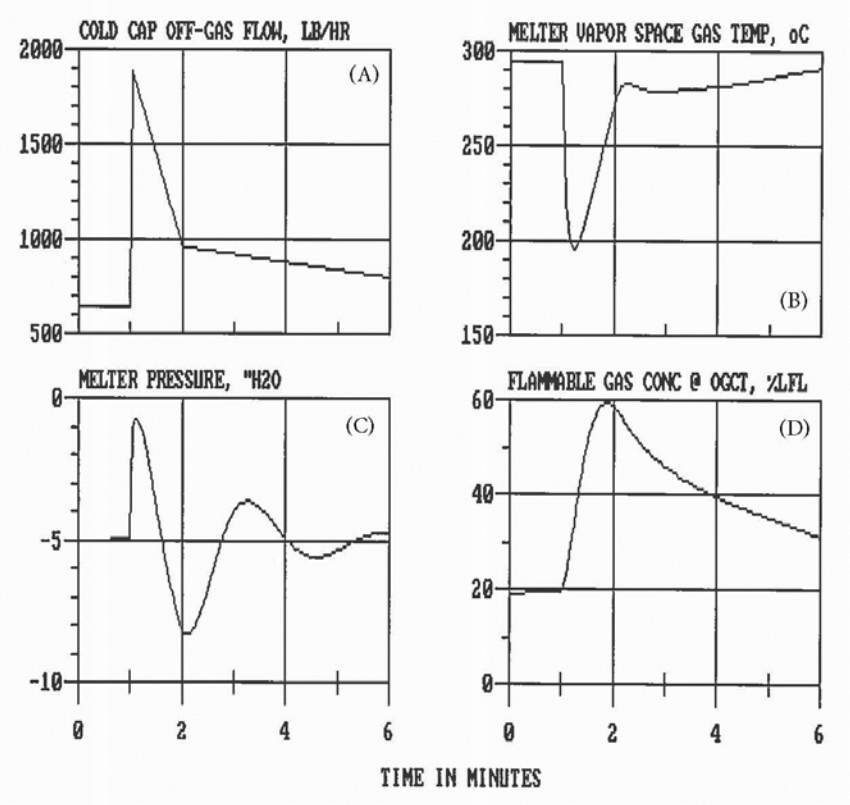

Figure 3-2. 3X/3X Surge of Bounding SB9 at 25,000 ppm Nitrate & 894-Gallon Antifoam (1).

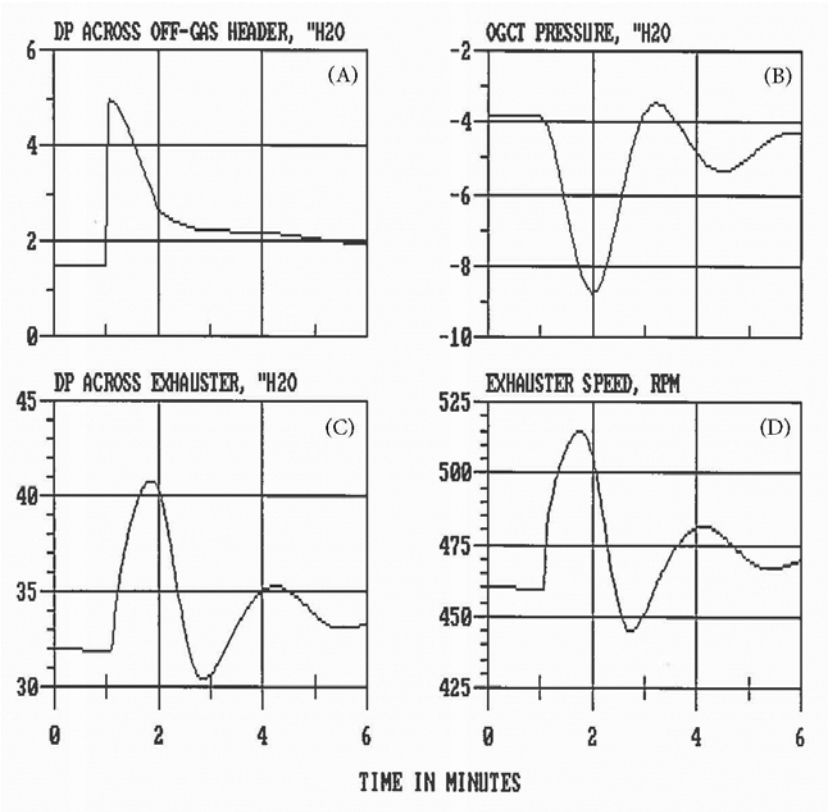

Figure 3-3. 3X/3X Surge of Bounding SB9 at 25,000 ppm Nitrate & 894-Gallon Antifoam (2).

3.4.3 Assessment of SB9 Flammability Potential

The results of the sensitivity model runs using three baseline SB9 melter feed compositions are shown in Table 3-5 and the impact of antifoam addition on the off-gas flammability potential can be clearly seen. The 128-gal antifoam case represents the SME product produced during the CPC demonstration run with the actual amount of antifoam used scaled up to the DWPF feed rate of 1.5 GPM. As expected at such low antifoam usage, the predicted flammability of the OGCT vapor peaked at only 12% of the LFL. As the antifoam addition was increased to 728 gallons along with coal and MCU solvent addition, the predicted peak flammability increased to 46% of the LFL. With further increases in antifoam, the predicted peak flammability continued to increase finally to above 60% of the LFL at the 1,017-gal antifoam addition. It is noted that besides the antifoam addition the increased flammability potentials of these baseline feeds were due in part to their waste loadings (WL) being adjusted up slightly to 36% and, to a lesser degree, the addition of coal and MCU solvent.

The results of the bounding SB9 flammability model runs at 60% of the LFL are tabulated in Table 3-6. The 894-gal antifoam addition case was run for the entire nitrate range from 10,000 to 70,000 ppm at 5,000 ppm increments, while the 728 and 1,017-gal antifoam addition cases were run at four selected nitrate concentrations. This was because the SB9 TOC limits for the 894-gal antifoam case were higher than their SB8 counterparts by 1 to 7% over the entire nitrate range (see Figure 3-4 and the percent ΔTOC data in Table 3-6), and the same trend is expected to hold for the other two antifoam addition cases, which was confirmed at 10,000, 25,000, 45,000 and 65,000 ppm nitrate, as shown in Figure 3-5 and Figure 3-6. Although the differences between the SB8 and SB9 TOC limits are not large, the percent ΔTOC's were consistently positive over the entire nitrate range, which indicates that the bounding TOC limits of SB9 would be at least equal to those of SB8 as the same model uncertainty would apply to both SB results. This means that the existing TSR TOC limits developed for the SB8 bubbled operation (under 9X/5X off-gas surge) would remain valid for the SB9 non-bubbled operation (under 3X/3X off-gas surge).

The calculated TOC-to-nitrate ratio of bounding SB8 and SB9 feeds are plotted as a function of nitrate in Figure 3-7 for the 894-gal antifoam addition case. The ratio is shown to decrease rapidly with increasing nitrate at the lower nitrate range but its rate of decrease slows down considerably at between 30,000 and 40,000 ppm nitrate depending on the antifoam addition level. It was shown earlier that the TOC-to-nitrate ratio decreases with increasing antifoam addition at a given nitrate level, indicating that the impact of antifoam addition is greater at the lower nitrate range.[2] Furthermore, although the nitrate range is set from 10,000 to 70,000 ppm, the more relevant nitrate range for the formic acid flowsheet feeds is the lower half from 10,000 to 40,000 ppm, while the upper half is the likely range for the glycolic acid flowsheet feeds. In that case, it may be possible to develop a constant TOC-to-nitrate ratio limit for the latter feeds regardless of the nitrate by taking advantage of the relative flatness of the curve at higher nitrate, which will greatly simplify the implementation and compliance of the flammability control strategy.

Figure 3-7 can also be used to point out that the TSR TOC limits should not be enforced rigidly without any exception. Suppose that we just produced a SME product using less than 894 gallons of antifoam, and its TOC-to-nitrate ratio was 0.7 at 12,500 ppm nitrate. This is an acceptable batch, since its nitrate level is within the TSR range, and the TOC-to-nitrate ratio is well under the maximum ratio of 0.98 estimated by the linear interpolation of data in Table 3-6. Now, suppose that there was a significant water inleakage due to pump trips or a ruptured pump prime H_2O line and, as a result, the nitrate level dropped to 9,500 ppm, which is outside the TSR range. Nevertheless, the TOC-to-nitrate ratio should remain the same, since dilution would lower the concentrations of not only the nitrate but the other soluble and insoluble solids, including TOC and antifoam, by the same ratio of 1.3 (=12,500/9,500). It means that the relative amounts of reductant (TOC) and oxidant (nitrate) remain the same but their instantaneous feed rates will be lower because of lower total solids and thus lower density, which in turn means that the flammability potential of the diluted feed should be lower than that of the undiluted feed at a given feed rate.

Table 3-5. Results of Sensitivity Runs for the SB9 Baseline Feeds at Varying Antifoam Additions Under 3X/3X Off-Gas Surge.

Antifoam	Nitrate	Antifoam Carbon	Coal	Oxalate Carbon	Formate Carbon	Solvent Carbon	TOC	REDOX	TS	WL	Peak Flammability	CPC Cycle Time
(gal)	(mg/kg)	(mg/kg)	(mg/kg)	(mg/kg)	(mg/kg)	(mg/kg)	(mg/kg)		(wt%)	(wt%)	(% LFL)	(hr)
128	20,253	415	0	653	10,629	0	11,697	0.122	50.14	34.5	12	116
728	21,192	2,140	237	683	11,121	51	14,233	0.461	51.20	36.0	46	123
894	21,158	2,630	237	682	11,104	51	14,704	0.468	51.27	36.0	55	123
1,017	21,133	2,993	237	681	11,091	51	15,053	0.471	51.33	36.0	62	123

Table 3-6. Results of SB9 Bounding Flammability Runs at 60% of the LFL Under 3X/3X Off-Gas Surge.

Antifoam	Nitrate	Antifoam Carbon	Coal	Oxalate Carbon	Formate Carbon	Solvent Carbon	TOC	TOC/ Nitrate	REDOX	TS	WL	ΔTOC	CPC Cycle Time
(gal)	(mg/kg)	(mg/kg)	(mg/kg)	(mg/kg)	(mg/kg)	(mg/kg)	(mg/kg)			(wt%)	(wt%)	(%)	(hr)
728	10,000	2,229	246	670	8,802	52	12,000	1.200	0.685	49.18	32.9	0.9	125
728	25,000	2,096	232	630	14,967	51	17,975	0.719	0.457	52.22	37.0	2.8	122
728	45,000	1,905	211	573	24,155	49	26,892	0.598	0.136	56.57	43.0	2.2	115
728	65,000	1,698	188	511	34,511	46	36,954	0.569	0.122	61.29	49.4	1.4	108
894	10,000	2,763	249	677	7,259	53	11,000	1.100	0.688	48.80	32.2	1.3	126
894	15,000	2,712	244	664	9,125	52	12,797	0.853	0.616	49.75	33.5	2.1	125
894	20,000	2,656	239	651	11,222	52	14,820	0.741	0.478	50.78	34.9	5.9	124
894	25,000	2,600	234	637	13,398	51	16,920	0.677	0.457	51.83	36.4	5.9	122
894	30,000	2,545	229	623	15,451	50	18,899	0.630	0.351	52.84	37.8	6.9	121
894	35,000	2,491	224	610	17,474	50	20,850	0.596	0.167	53.84	39.1	2.6	120
894	40,000	2,427	218	594	20,113	49	23,402	0.585	0.122	55.03	40.8	2.1	118
894	45,000	2,364	213	579	22,685	49	25,889	0.575	0.122	56.21	42.4	1.5	116
894	50,000	2,299	207	563	25,334	48	28,452	0.569	0.122	57.40	44.0	1.6	115
894	55,000	2,235	201	547	27,927	48	30,959	0.563	0.122	58.58	45.6	2.1	113
894	60,000	2,169	195	531	30,695	47	33,637	0.561	0.122	59.81	47.3	1.7	111
894	65,000	2,106	190	516	33,238	46	36,096	0.555	0.122	60.98	48.9	1.8	109
894	70,000	2,042	184	500	35,875	46	38,647	0.552	0.122	62.17	50.5	1.9	107
1,017	10,000	3,164	250	681	6,172	53	10,320	1.032	0.690	48.54	31.8	2.0	127
1,017	25,000	2,982	236	642	12,086	51	15,998	0.640	0.457	51.50	35.8	11.2	123
1,017	45,000	2,706	214	583	21,753	49	25,306	0.562	0.122	55.98	42.0	2.2	117
1,017	65,000	2,415	191	520	32,236	47	35,408	0.545	0.122	60.73	48.5	1.3	109

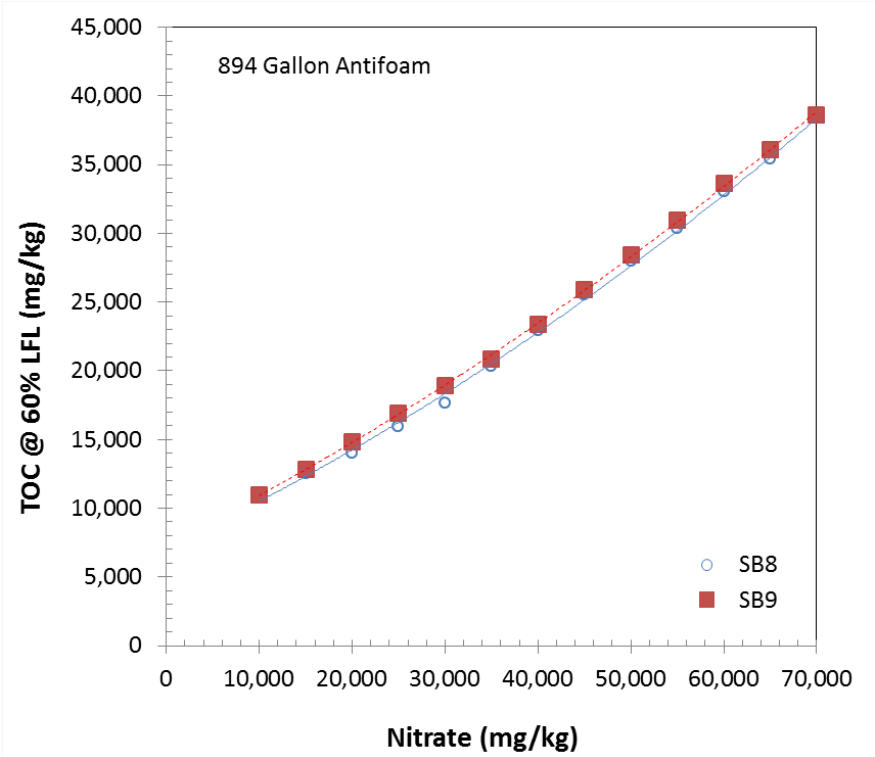

Figure 3-4. SB8 vs. SB9 Bounding TOC Limits at 894-Gallon Antifoam.

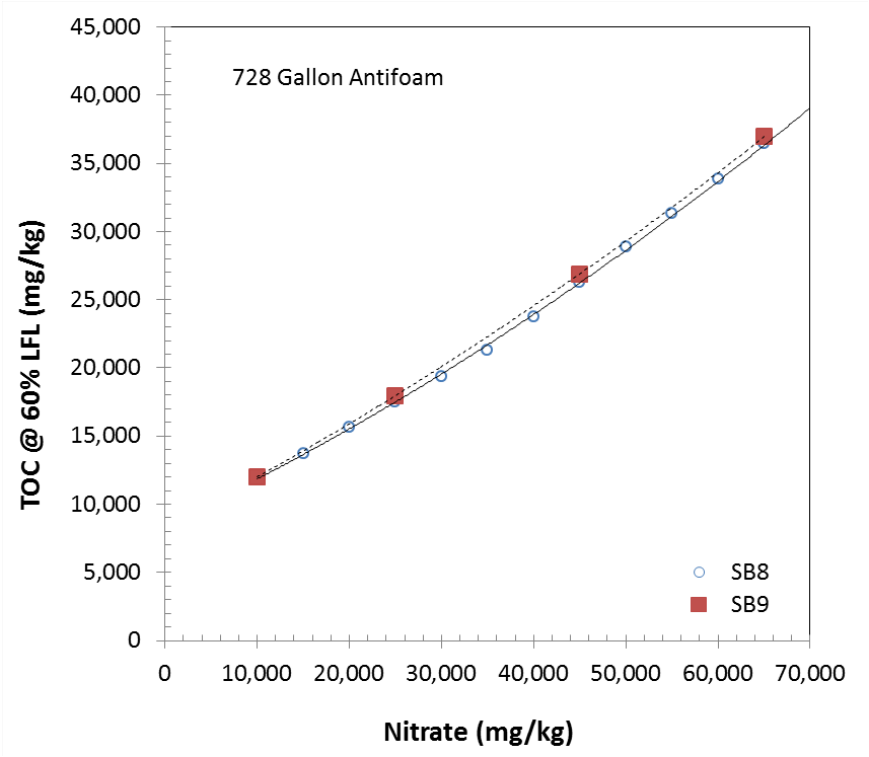

Figure 3-5. SB8 vs. SB9 Bounding TOC Limits at 728-Gallon Antifoam.

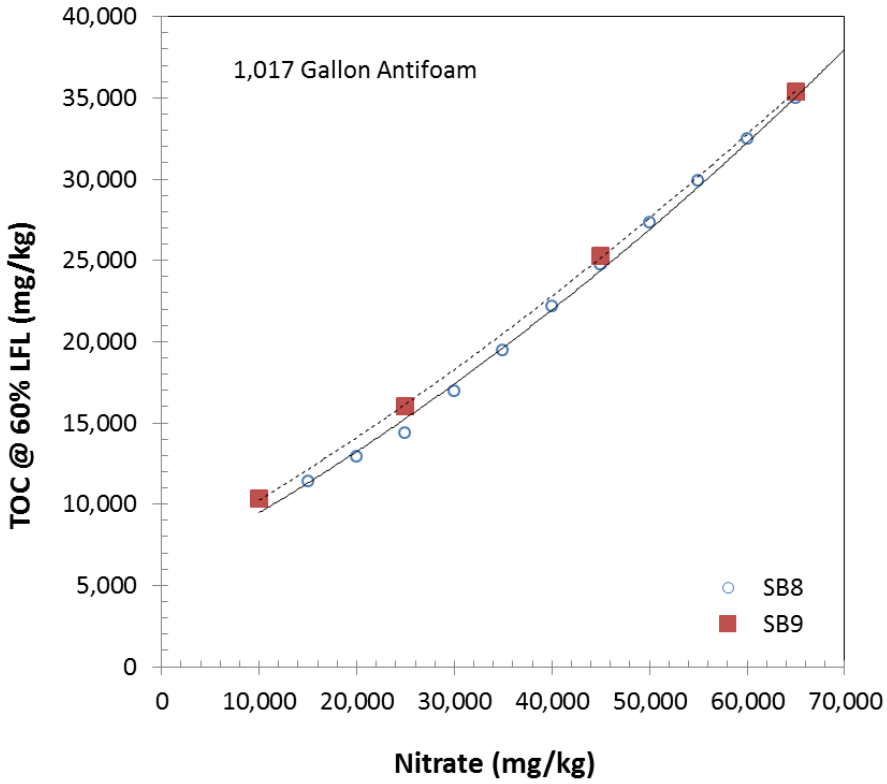

Figure 3-6. SB8 vs. SB9 Bounding TOC Limits at 1,017-Gallon Antifoam.

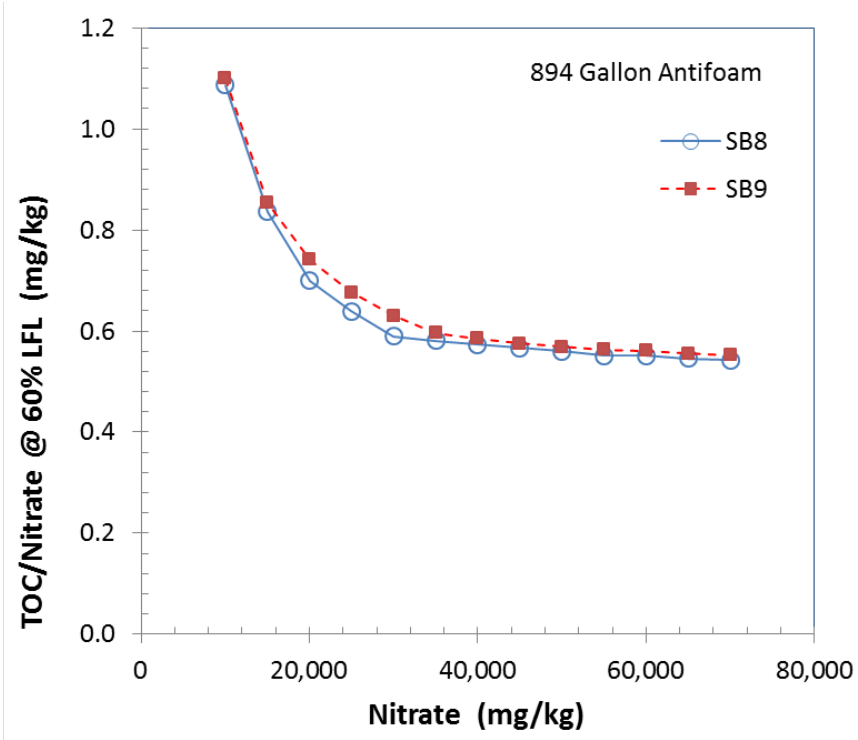

Figure 3-7. SB9 vs. SB8 Bounding TOC-to-Nitrate Ratios at 894-Gallon Antifoam Addition.

It is also noted that the SB9 feeds at the maximum TOC limits are highly concentrated, as evidenced by the total solids ranging from 49 to over 62 wt% and the WLs from 32 to over 50 wt% (Table 3-6), both of which are considerably higher than their respective nominal values of 45 and 36 wt%. It means that these bounding feeds should result in higher off-gas flammability potentials than the nominal feeds at a given TOC and nitrate. Furthermore, by assuming that the SME product constitutes the actual melter feed in the facility, additional dilution occurring to the SME transfer in the MFT was not accounted for in this study. Therefore, the assessment made in this study was based on more concentrated feeds than the actual and thus the predicted flammability potentials should be conservative.

Table 3-5 also shows the calculated CPC cycle times to support the DWPF design basis glass production rate of 228 lb/hr. As expected, the calculated cycle times for the three reconstituted baseline feeds are the same at 123 hours as nearly 100% of the antifoam decomposition products would exit the melter as gases, i.e., the glass production rate remains essentially the same regardless of the quantity of antifoam added. On the other hand, the calculated CPC cycle times for the bounding SB9 feeds are shown in Table 3-6 to decrease as the nitrate level increases for all antifoam addition cases. For example, the calculated cycle times for the 894-gal antifoam addition case decreased from 126 hours at 10,000 ppm nitrate to 107 hours at 70,000 ppm nitrate with an average of 117 hours for the entire nitrate range. This inverse relationship between the nitrate and CPC cycle time is due to the fact that the glass production rate was no longer held constant at the design basis. Instead, it was the peak off-gas flammability potential that was held constant at 60% of the LFL at each nitrate level by increasing or decreasing the formate from its baseline value, resulting in different instantaneous feed and glass production rates from one nitrate level to the next. As the total solids of each bounding SB9 feed changed, so did its density in such a way that the instantaneous volumetric feed rate increased with increasing nitrate.

The calculated CPC cycle times were used in the model to set the instantaneous feed rates of antifoam and strip effluent from the preset quantities of each stream added per CPC cycle. As a result, the shorter the cycle time, the higher the instantaneous feed rates of antifoam and solvent carbons to the melter, which is conservative from the off-gas flammability standpoint. It was determined that the calculated CPC cycle times of 123 hours for the baseline feeds and the average 117 hours for the bounding SB9 feeds are at the lower bound of the actual cycle times achieved in the facility.

4.0 Quality Assurance

The Quality Assurance (QA) requirements for this work are defined in the TTR.[6] Specifically, the work defined herein is not waste form affecting, and thus does not need to follow QA requirements of RW-0333P. This technical report supports the Type 1 calculation and thus is treated as lifetime records. This technical report and the software used to support the Type 1 calculation comply with the following:

- 1Q QAP 20-1 Software Quality Assurance
- E7, Section 5.0 Software Engineering and Control
- E7 Manual, Procedure 3.60, Technical Reports
- E7 Manual, Procedure 2.31A, LW Engineering Calculations
- E7, Procedure 2.60 technical reviews applicable to this task

Requirements for performing reviews of technical reports and the extent of review are established in Manual E7 2.60. SRNL documents the extent and type of review using the SRNL Technical Report Design Checklist contained in WSRC-IM-2002-00011, Rev. 2. The lifecycle requirements and validation techniques for the software used in this work are found in the Software Quality Assurance Plan (SQAP).[16]

5.0 Conclusions

Based on the results discussed so far, it is concluded that:

1. The MOG dynamics model was successfully updated to reflect the current DCS settings and further calibrated using the latest facility data. The calibrated model predicted that the actual peak melter pressure during the apparent +10.8" H_2O pressure spike on 11/24/2014 was closer to +19" H_2O with 20-sec peak duration.

2. The baseline 3X/3X off-gas surge with 1-min peak duration remains bounding in terms of off-gas flammability for non-bubbled operation.

3. The duration of off-gas surge has just as large an impact as its magnitude on off-gas flammability.

4. The current TSR TOC limits, which were developed for the bubbled SB8 operation, remain valid for the SB9 non-bubbled operation for all three antifoam addition scenarios considered: 728, 894 and 1,017 gallons per CPC cycle.

5. The current TSR limits on the minimum melter vapor space temperature, minimum air purges and maximum feed rate all remain the same.

The implication of these conclusions is that no DSA change would be required for processing SB9 under non-bubbled conditions.

6.0 Recommendations, Path Forward or Future Work

It is recommended that the same methodology and calculation steps used in this study to validate the non-bubbled off-gas surge basis and further assess the SB9 flammability potential be repeated in preparation for bubbled operation.

7.0 References

1. Edwards, T. B., "Integration of the Uncertainties of Anion and TOC Measurements into the Flammability Control Strategy for Sludge Batch 8 at the DWPF," ***SRNL-STI-2013-00139***, **Rev. 0**, Savannah River National Laboratory, Aiken, SC 29808, March 2013.

2. Choi, A. S., "DWPF MOG Flammability Assessment (Sludge Batch 8)," ***X-CLC-S-00164***, ***Rev. 8***, March 2013.

3. Choi, A. S., "Validation of DWPF Melter Off-Gas Combustion Model," ***WSRC-TR-2000-00100***, Westinghouse Savannah River Co., Aiken SC 29808, June 23, 2000.

4. Choi, A. S., "Validation of DWPF MOG Dynamics Model - Phase I (U)," ***WSRC-TR-96-0307***, Westinghouse Savannah River Co., Aiken SC 29808, January 7, 1997.

5. Choi, A. S., "Impact of Non-Safety Component Failures on DWPF Melter Off-Gas Flammability Safety Basis," ***SRNL-L3100-2015-00148***, ***Rev. 2***, Savannah River National Laboratory, Aiken, SC 29808, October 29, 2015.

6. Nguyen, Q., "DWPF Melter (Non-Bubbled) Off-Gas Flammability Calculation for Sludge Batch 9," ***X-TTR-S-00042***, ***Rev. 0***, Savannah River Remediation, Aiken, SC 29808, November 2015.

7. Choi, A. S., "Proposed Strategies for DWPF Melter Off-Gas Surge Control," ***WSRC-TR-2004-00156***, ***Rev. 0***, Westinghouse Savannah River Co., Aiken, SC 29808, June 2004.

8. Scaling Computation for Loop S350-ZZF-3401, ***J-DCP-S-94104***, page 2 of 19 (Reviewed by W. S. Odom), Westinghouse Savannah River Co., Aiken, SC 29808, December 1994.

9. *Flow of Fluids Through Valves, Fittings and Pipe*, Technical Paper No. 410, Crane Co. (1988).

10. Choi, A. S., "Inputs and Assumptions of the DWPF Melter Off-Gas Flammability Model," ***SRNL-L3100-2015-00217***, ***Rev. 1***, Savannah River National Laboratory, Aiken, SC 29808, June 2016.

11. Plante, E. R., Bonnell, D. W., and Hastie, J. W., "Experimental and Theoretical Determination of Oxide Glass Vapor Pressures and Activities," ***Advances in the Fusion of Glass***, **Am. Cer. Soc.**, pp 26.1-26.18 (1988).

12. Scaling Computation for Loop S350-ZZF-3401, ***J-DCP-S-94104***, page 19 of 19 (Reviewed by W. S. Odom), Westinghouse Savannah River Co., Aiken, SC 29808, December 1994.

13. Smith, T. E., "Recommendations for Melter Off-Gas Flammability Model Inputs Based on Chemical Processing Cell Simulant Runs," ***SRNL-L3100-2016-00009***, ***Rev. 0***, Savannah River National Laboratory, Aiken, SC 29808, January 28, 2016.

14. Hay, M. S., and Choi, A. S., "Charge-Balance of SB9 Simulant CPC Run Products," ***SRNL-L3100-2016-00049***, ***Rev. 0***, Savannah River National Laboratory, Aiken, SC 29808, May 12, 2016.

15. Choi, A. S., "DWPF Melter Off-Gas Flammability Model for the Nitric-Glycolic Acid Flowsheet," ***SRNL-STI-2014-00355***, ***Rev. 0***, Savannah River National Laboratory, Aiken, SC 29808, September 2014.

16. Burns, H. H., "DWPF Melter Cold Cap and Off-Gas Flammability Modeling Software Quality Assurance Plan," ***G-SQP-A-00020***, ***Rev. 0***, Savannah River National Laboratory, Aiken, SC 29808, April 2011.

8.0 Appendix A

Controller Data Summary

Table 8-1. Digital Controller Data Summary (11/24/2014 19:44:30 - 11/24/2014 20:14:33).

CONT. NO.	MODE / TYPE	COUT / ACTION	SETPT / CIN	GAIN / RSET	DERIV / SAMPLE	ZERO / RANGE	COUTLL / COUTUL	OINT / MANIN	ANTI RESET WINDUP
1	MAN	.822	350.00	1.000	.000	200.00	.000	.012	YES
	P+I	REVERSE	284.72	2.500	3.000	600.00	1.000	.822	
2	AUTO	.768	-5.00	.480	.000	-25.00	.000	.000	YES
	P+I	DIRECT	-4.95	1.709	.250	5.00	1.000	.768	
3	AUTO	.924	4.04	-1.000	.000	-20.00	.000	.000	YES
	P+I	REVERSE	4.01	1.000	1.000	5.00	1.000	.924	
4	AUTO	.354	10.00	1.000	.000	.00	.000	.000	YES
	P+I	DIRECT	10.00	2.500	3.000	20.00	1.000	.354	
5	MAN	.234	440.00	.500	.000	283.00	.010	.000	YES
	P+I	DIRECT	490.49	2.000	1.000	1200.00	1.000	.234	
6	AUTO	.267	20.00	2.000	.000	.00	.000	.000	YES
	P+I	REVERSE	19.99	5.000	3.000	100.00	1.000	.267	
7	AUTO	.120	400.00	.500	.000	.00	.010	.000	YES
	P+I	DIRECT	400.00	2.000	1.000	1200.00	1.000	.120	
8	AUTO	.050	10.00	2.000	.000	.00	.050	.004	YES
	P+I	REVERSE	8.00	2.000	3.000	50.00	1.000	.050	
9	AUTO	.544	10.00	1.000	.000	.00	.000	.000	YES
	P+I	DIRECT	10.00	2.500	3.000	20.00	1.000	.544	

Table 8-1 Cont'd

CONT. NO.	MODE TYPE	COUT ACTION	SETPT CIN	GAIN RSET	DERIV SAMPLE	ZERO RANGE	COUTLL COUTUL	OINT MANIN	ANTI RESET WINDUP
10	AUTO P+I	.234 DIRECT	500.00 502.41	.150 1.463	.000 .500	.00 1400.00	.010 1.000	.000 .234	YES
11	AUTO P+I	.050 REVERSE	10.00 8.00	2.000 2.000	.000 3.000	.00 50.00	.050 1.000	.004 .050	YES
12	AUTO P+I	.566 DIRECT	478.60 478.72	2.500 .200	.000 3.000	.00 1000.00	.000 1.000	.000 .566	YES
13	AUTO P+I	.283 DIRECT	1070.00 1070.00	.300 3.950	.000 .500	.00 1750.00	.000 1.000	.000 .283	YES
14	MAN P+I	.120 DIRECT	500.00 .00	.600 .600	.000 .500	.00 1400.00	.010 1.000	.002 .120	YES
15	AUTO P+I	.319 DIRECT	1100.00 1100.05	.500 2.000	.000 3.000	.00 2000.00	.000 1.000	.000 .319	YES
16	MAN P+I	.267 DIRECT	367.00 175.89	.500 5.000	.000 3.000	.00 500.00	.000 1.000	-.002 .267	YES
17	MAN P+I	.000 DIRECT	367.00 .00	.500 5.000	.000 3.000	.00 500.00	.000 1.000	.000 .000	YES
18	MAN P+I	.000 DIRECT	367.00 .00	.500 5.000	.000 3.000	.00 500.00	.000 1.000	.000 .000	YES
19	MAN P+I	.000 REVERSE	40.00 40.00	2.000 5.000	.000 3.000	.00 100.00	.000 1.000	.000 .000	YES

Table 8-1 Cont'd

CONT. NO.	MODE	COUT	SETPT	GAIN	DERIV	ZERO	COUTLL	OINT	ANTI RESET
	TYPE	ACTION	CIN	RSET	SAMPLE	RANGE	COUTUL	MANIN	WINDUP
20	MAN	.000	367.00	.500	.000	.00	.000	.000	YES
	P+I	DIRECT	.00	5.000	3.000	500.00	1.000	.000	
21	MAN	.000	350.00	1.000	.000	200.00	.000	.000	YES
	P+I	REVERSE	200.00	2.500	3.000	600.00	1.000	.000	
22	AUTO	.154	370.00	.300	.000	.00	.000	.000	YES
	P+I	DIRECT	370.00	3.950	.500	1150.00	1.000	.154	

Table 8-2. Cross-Reference between Model Controllers and DCS Controllers.

Model Controller No.	DCS Controller I.D.
1	TIC3682
2	PIC3521
3	PDIC3526
4	TDIC4300
5	SIC3585
6	TIC3620A
7	SIC4324
8	TIC3386
9	TDI3400
10	FIC3691
11	TIC3395
12	for model use only
13	FIC3221A
14	FIC3534
15	backup exhauster outlet flow
16	FIC3590
17	FIC4344
18	FIC4340
19	TIC3501A
20	FIC3595
21	TIC3421
22	FIC3221B

9.0 Appendix B

Dynamic Valve Data Summary

Table 9-1. Valve Data Summary (11/24/2014 19:44:30 - 11/24/2014 20:14:33).

VALVE NUMBER	CV VCON	F Y	CHAR DYNAMICS	STOPEN STCLOS	TCOPEN TCCLOS	DYDT CTRL.
1	206.00	.822	EQL PCT	5.00	1.00	.5960E-05
	105.73	.822	1ST ORD	5.00	1.00	1
2	1193.20	.768	EQL PCT	1.00	.20	-.1371E-04
	500.92	.768	1ST ORD	1.00	.20	2
3	80.00	.924	EQL PCT	1.00	.20	.4560E-04
	60.26	.924	1ST ORD	1.00	.20	3
4	206.00	.000	EQL PCT	5.00	1.00	.0000E+00
	.00	.000	1ST ORD	5.00	1.00	21
5	1440.00	.154	LINEAR	10.00	1.00	.1475E-05
	221.98	.154	1ST ORD	10.00	1.00	22
6	2480.00	.050	EQL PCT	5.00	1.00	-.3725E-06
	70.55	.050	1ST ORD	5.00	1.00	11
7	15378.00	.000	EQL PCT	5.00	1.00	.0000E+00
	.00	.000	1ST ORD	5.00	1.00	0
8	3000.00	.050	EQL PCT	5.00	1.00	-.3725E-06
	85.35	.050	1ST ORD	5.00	1.00	8
9	3000.00	1.000	EQL PCT	10.00	1.00	.0000E+00
	100.00	1.000	RAMP	10.00	1.00	0
10	3000.00	.000	EQL PCT	10.00	1.00	.0000E+00
	.00	.000	RAMP	10.00	1.00	0
11	100.00	.900	EQL PCT	5.00	1.00	.5960E-05
	100.00	.900	1ST ORD	2.00	1.00	0
12	6320.00	1.000	EQL PCT	10.00	2.00	.0000E+00
	6320.00	1.000	RAMP	10.00	2.00	0
13*	265900.00	1.000	EQL PCT	10.00	2.00	.0000E+00
	265900.00	1.000	1ST ORD	10.00	2.00	0

Table 9-1 Cont'd

VALVE NUMBER	CV VCON	F Y	CHAR DYNAMICS	STOPEN STCLOS	TCOPEN TCCLOS	DYDT CTRL.
14	1193.20	.000	EQL PCT	1.00	.20	.0000E+00
	.00	.000	1ST ORD	1.00	.20	0
15	265900.00	.980	EQL PCT	10.00	2.00	.2980E-05
	246696.30	.980	1ST ORD	10.00	2.00	0
16	1440.00	.283	LINEAR	10.00	1.00	-.2980E-05
	407.97	.283	1ST ORD	10.00	1.00	13
17	250.00	.000	LINEAR	4.00	.00	.0000E+00
	.00	.000	RAMP	4.00	.00	20
18	250.00	.000	LINEAR	4.00	.00	.0000E+00
	.00	.000	RAMP	4.00	.00	17
19	250.00	.267	LINEAR	10.00	2.00	.0000E+00
	66.75	.267	RAMP	10.00	2.00	16
20	250.00	.000	LINEAR	5.00	1.00	.0000E+00
	.00	.000	RAMP	5.00	1.00	18
21	12800.00	.000	EQL PCT	1.00	2.00	.0000E+00
	.00	.000	RAMP	1.00	2.00	0
22	15000.00	.319	EQL PCT	10.00	2.00	.0000E+00
	1167.82	.318	RAMP	10.00	2.00	15
23	12800.00	.000	EQL PCT	1.00	.00	.0000E+00
	.00	.000	RAMP	1.00	.00	0
24	100.00	.234	LINEAR	5.00	.00	.0000E+00
	.00	.234	RAMP	5.00	.00	0
25	100.00	.120	LINEAR	5.00	.00	.0000E+00
	.00	.120	RAMP	5.00	.00	0
26	12800.00	.000	EQL PCT	1.00	.00	.0000E+00
	.00	.000	RAMP	1.00	.00	0

* Valve #13, a butterfly valve in front of SAS 1, has been taken out of service.

Table 9-2. Description of Dynamic Valves Used in the Model.

Model Valve No.	Purpose:
1	primary film cooler steam
2	primary melter pressure control air
3	pour spout pressure control air
4	backup film cooler steam
5	backup film cooler air
6	chilled water to backup OGC
7	pour spout pressure control air vent to backup OGCT
8	chilled water to OGC
9	primary isolation valve (MOV3689)
10	backup isolation valve
11	pour spout pressure control air to spout jet
12	Cell air inflow to backup off-gas system
13	butterfly valve upstream of SAS #1
14	backup melter pressure control air
15	butterfly valve upstream of backup SAS #1
16	primary film cooler air
17	steam to SAS #2
18	steam to backup SAS #2
19	steam to SAS #1
20	steam to backup SAS #1
21	OGCT vent
22	backup OGCT vent
23	backup OGCT vacuum breaker
24	used to model backup exhauster speed control
25	used to model primary exhauster speed control (SIC3585)
26	OGCT vacuum breaker

10.0 Appendix C

Printout of Formulas for
Charge Balance and Re-constitution of Baseline Feeds

	A	B	C
3	**Table 1A. SRAT/SME Prod Elemental**		
4	element	AW	wt% calcine
5			solids
6			
7	Fe	55.847	='Smith SB9 SRAT-SME Data'!J23
8	Al	26.9815	='Smith SB9 SRAT-SME Data'!D23
9	Mn	54.938	='Smith SB9 SRAT-SME Data'!N23
10	Ca	40.078	='Smith SB9 SRAT-SME Data'!G23
11	U	238.03	0
12	Mg	24.305	0
13	Hg	200.59	0
14	P	30.9738	0
15	Ni	58.6934	='Smith SB9 SRAT-SME Data'!P23
16	Cr	51.9961	0
17	Cu	63.546	0
18	Ti	47.88	0
19	Si	28.0855	='Smith SB9 SRAT-SME Data'!V23
20	Na	22.9898	='Smith SB9 SRAT-SME Data'!O23
21	Th	232.0381	0
22	Zn	65.39	0
23	Pu	238.9	0
24	K	39.0983	0
25	Ru'	101.07	0
26	Rh'	102.9055	0
27	Pd'	106.42	0
28	Cd	112.411	0
29	Sr	87.62	0
30	B	10.811	='Smith SB9 SRAT-SME Data'!E23
31	Li	6.941	='Smith SB9 SRAT-SME Data'!L23
32	Cs	132.905	0
33	Ba	137.327	0
34	Sn	118.71	0
35	Pb	207.2	0
36	Tc	98.9062	0
37	La	138.9055	0
38	Zr	91.224	0
39	S	32.066	='Smith SB9 SRAT-SME Data'!U23
40	total		=SUM(C7:C39)

	E	F	G	H	I	J
71	**Table 1B. SRAT/SME Product ICP-ES Filtrate (SN) Results**					
72	element	AW	soluble	soluble	soluble	
73			(mg/L SN)	(mg/L SN)	(mole/L SN)	
74						
75	Fe	55.85	0		=G75/1000/F75	
76	Al	26.98	0		=G76/1000/F76	
77	Mn	54.94	='Smith SB9 SRAT-SME Data'!N80		=G77/1000/F77	
78	Ca	40.08	='Smith SB9 SRAT-SME Data'!G80		=G78/1000/F78	
79	U	238.03	0		=G79/1000/F79	
80	Mg	24.31	='Smith SB9 SRAT-SME Data'!M80		=G80/1000/F80	
81	Hg	200.59	0		=G81/1000/F81	
82	P	30.97	0		=G82/1000/F82	
83	Ni	58.71	='Smith SB9 SRAT-SME Data'!P80		=G83/1000/F83	
84	Cr	51.996	0		=G84/1000/F84	
85	Cu	63.546	0		=G85/1000/F85	
86	Ti	47.9	0		=IF(G86="<0.010",0,G86/1000/F86)	
87	Si	28.09	='Smith SB9 SRAT-SME Data'!V80		=G87/1000/F87	
88	Na	22.99	='Smith SB9 SRAT-SME Data'!O80		=G88/1000/F88	
89	Th	232.038	0		=G89/1000/F89	
90	Zn	65.38	0		=G90/1000/F90	
91	Pu	238.9	0		=G91/1000/F91	
92	K	39.1	='Smith SB9 SRAT-SME Data'!K80		=G92/1000/F92	
93	Ru	101.07	0		=G93/1000/F93	
94	Rh	102.91	='Smith SB9 SRAT-SME Data'!S80		=G94/1000/F94	
95	Pd	106.4	0		=G95/1000/F95	
96	Cd	112.411	0		=IF(G96="<0.010",0,G96/1000/F96)	
97	Sr	87.62	0		=G97/1000/F97	
98	B	10.81	='Smith SB9 SRAT-SME Data'!E80		=G98/1000/F98	
99	Li	6.941	='Smith SB9 SRAT-SME Data'!L80		=IF(G99="<10.0",0,G99/1000/F99)	
100	Cs	132.905	0		=G100/1000/F100	
101	Ba	137.33	0		=G101/1000/F101	
102	Ce	140.115	0		=G102/1000/F102	
103	Gd	157.25			=G103/1000/F103	
104	Pb	207.2	0		=G104/1000/F104	
105	Tc	98.9062			=G105/1000/F105	
106	Sn	118.71	='Smith SB9 SRAT-SME Data'!W80		=G106/1000/F106	
107	Zr	91.22	0		=G107/1000/F107	
108	Nd	144.242	0		=G108/1000/F108	
109	S	32.06	='Smith SB9 SRAT-SME Data'!U80		=G109/1000/F109	
110	total		=SUM(G75:G109)	=SUM(H75:H109)		

	K	L	M
71	**Table 1B. SRAT/SME Product ICP-ES Filtrate (SN) Results (Continued)**		
72	soluble	total	wt frac
73	(g/L SL)	(g/L SL)	insoluble
74			
75	=IF(G75="<0.010",0,G75/1000*S$79)	=G$48*C7*M54/100	=1-K75/L75
76	=IF(G76="<0.010",0,G76/1000*S$79)	=G$48*C8*M54/100	=1-K76/L76
77	=IF(G77="<0.010",0,G77/1000*S$79)	=G$48*C9*M54/100	=1-K77/L77
78	=IF(G78="<0.010",0,G78/1000*S$79)	=G$48*C10*M54/100*(1-C95)	=1-K78/L78
79	=IF(G79="<0.010",0,G79/1000*S$79)	=G$48*C11*M54/100	
80	=IF(G80="<0.010",0,G80/1000*S$79)	=G$48*C12*M54/100	0
81	=IF(G81="<0.010",0,G81/1000*S$79)	=G$48*C13*M54/100	
82	=IF(G82="<0.010",0,G82/1000*S$79)	=IF(C14="<0.100",K82,G$48*C14*M54/100)	=IF(L82=0,0,1-K82/L82)
83	=IF(G83="<0.010",0,G83/1000*S$79)	=G$48*C15*M54/100	=1-K83/L83
84	=IF(G84="<0.010",0,G84/1000*S$79)	=G$48*C16*M54/100	0
85	=IF(G85="<0.010",0,G85/1000*S$79)	=G$48*C17*M54/100	0
86	=IF(G86="<0.010",0,G86/1000*S$79)	=G$48*C18*M54/100	0
87	=IF(G87="<0.010",0,G87/1000*S$79)	=G$48*C19*M54/100	=1-K87/L87
88	=IF(G88="<0.010",0,IF(V97=1,T109,G88/1000*S$79))	=G$48*C20*(1+M51)*M54/100	=IF(T109>L88,0,1-K88/L88)
89	=IF(G89="<0.010",0,G89/1000*S$79)	=G$48*C21*M54/100	=IF(L89=0,1,1-K89/L89)
90	=IF(G90="<0.010",0,G90/1000*S$79)	=G$48*C22*M54/100	=IF(L90=0,0,1-K90/L90)
91	=IF(G91="<0.010",0,G91/1000*S$79)	=G$48*C23*M54/100	=IF(L91=0,1,1-K91/L91)
92	=IF(G92="<0.010",0,G92/1000*S$79)	=G$48*C24*M54/100	=IF(L92=0,1,1-K92/L92)
93	=IF(G93="<0.010",0,G93/1000*S$79)	=IF(C25="<0.100",0,G$48*C25*M54/100)	=IF(L93=0,1,1-K93/L93)
94	=IF(G94="<0.010",0,G94/1000*S$79)	=G$48*C26*M54/100	=IF(L94=0,1,1-K94/L94)
95	=IF(G95="<0.010",0,G95/1000*S$79)	=IF(C27="<0.100",0,G$48*C27*M54/100)	=IF(L95=0,1,1-K95/L95)
96	=IF(G96="<0.010",0,G96/1000*S$79)		=IF(L96=0,1,1-K96/L96)
97	=IF(G97="<0.010",0,G97/1000*S$79)	=G$48*C29*M54/100	=IF(L97=0,1,1-K97/L97)
98	=IF(G98="<0.010",0,G98/1000*S$79)	=IF(C30="<0.100",0,G$48*C30*M54/100)	=IF(L98=0,1,1-K98/L98)
99	=IF(G99="<10.0",0,G99/1000*S$79)	=IF(C31="<0.100",0,G$48*C31*M54/100)	=IF(L99=0,1,1-K99/L99)
100	=IF(G100="<0.010",0,G100/1000*S$79)	=G$48*C32*M54/100	=IF(L100=0,1,1-K100/L100)
101	=IF(G101="<0.010",0,G101/1000*S$79)	=G$48*C33*M54/100	=IF(L101=0,1,1-K101/L101)
102	=IF(G102="<0.010",0,G102/1000*S$79)	=G$48*C34*M54/100	=IF(L102=0,1,1-K102/L102)
103	=IF(G103="<0.010",0,G103/1000*S$79)	=G$48*C34*M54/100	=IF(L103=0,1,1-K103/L103)
104	=IF(G104="<0.010",0,G104/1000*S$79)	=IF(C35="NM",0,G$48*C35*M54/100)	=IF(L104=0,1,1-K104/L104)
105	=IF(G105="<0.010",0,G105/1000*S$79)	=G$48*C36*M54/100	=IF(L105=0,1,1-K105/L105)
106	=IF(G106="<0.010",0,G106/1000*S$79)	=G$48*C37*M54/100	=IF(L106=0,1,1-K106/L106)
107	=IF(G107="<0.010",0,G107/1000*S$79)	=G$48*C38*M54/100	=IF(L107=0,1,1-K107/L107)
108	=IF(G108="<0.010",0,G108/1000*S$79)	0	=IF(L108=0,1,1-K108/L108)
109	=IF(G109="<0.010",0,G109/1000*S$79)	=G$48*C39*M54/100	=IF(L109=0,1,1-K109/L109)
110	=SUM(K75:K109)		

	O	P	Q	R	S
85	**Table 1C. SRAT Product SN IC Results**				
86	IC	FW	(mg/L SN)		(mole/L SN)
87	NO3	=14.007+15.9994*3	='Smith SB9 SRAT-SME Data'IF91'(1+M53)		=IF(Q87="<100",0,Q87/1000/P87)
88	NO2	=14.007+15.9994*2	0		=IF(Q88="<100",0,Q88/1000/P88)
89	COOH '	=12.011+15.9994*2+1.0079	='Smith SB9 SRAT-SME Data'IJ91		=IF(Q89="<100",0,Q89/1000/P89)
90	C2H3O3	=12.011*2+15.9994*3+1.0079*3	0		=IF(Q90="<100",0,Q90/1000/P90)
91	C2O4	=12.011*2+15.9994*4	='Smith SB9 SRAT-SME Data'II91		=IF(Q91="<100",0,Q91/1000/P91)
92	PO4	=30.9738+15.9994*4	0		=I82
93	SO4	=32.066+15.9994*4	='Smith SB9 SRAT-SME Data'IH91		=IF(Q93="<100",0,Q93/1000/P93)
94	Cl	35.4527	='Smith SB9 SRAT-SME Data'ID91		=IF(Q94="<100",0,Q94/1000/P94)
95	F	18.9984	0		=IF(Q95="<100",0,Q95/1000/P95)
96	CO3	=12.011+15.9994*3	4492.19959938442		=IF(Q96="<100",0,Q96/1000/P96)
97	SN IC data avaiable ? (Yes = 1)				1
98	total anion =				
99	total cation =				
100	total soluble solids =				
101	measured soluble solids =				
102	soluble mass diff =				
103	total equivalent - charge =				
104	total equivalent + charge =				
105	charge imbalance =				
106					
107	adjusted total equivalent + charge =				
108	charge imbalance =				
109	adjusted Na for SN charge balance (g/L SL) =				
110	diff btw adjusted and measured Na (g/L SL) =				
111	Na2O for SN charge balance (g/L calcine solids) =				
112	diff btw adj'd SN and mea'd/adj'd SL Na (g/L SL) =				

	T	U	V
85	**Table 1C. SRAT Product SN IC Results (Continued)**		
86	(g/L SL)	(mole/L SN)	(g/L SL)
87	=S87*S$79*P87	=IF(U103=1,S87,S87*(1+U$105))	=U87*S$79*P87
88	=S88*S$79*P88	=S88	=U88*S$79*P88
89	=S89*S$79*P89	=IF(U103=2,S89,S89*(1+U$105))	=U89*S$79*P89
90	=S90*S$79*P90	=IF(U103=2,S90,S90*(1+U$105))	=U90*S$79*P90
91	=S91*S$79*P91	=IF(U103=2,S91,S91*(1+U$105))	=U91*S$79*P91
92	=S92*S$79*P92	=S92	=U92*S$79*P92
93	=S93*S$79*P93	=S93	=U93*S$79*P93
94	=S94*S$79*P94	=S94	=U94*S$79*P94
95	=S95*S$79*P95	=S95	=U95*S$79*P95
96	=S96*S$79*P96	=IF(U103=2,S96,S96*(1+U$105))	=U96*S$79*P96
97	Adjust Na ? (if yes, = 1)		1
98	=IF(S97=1,SUM(T87:T96),"n/a")		=IF(S97=1,SUM(V87:V96),"n/a")
99	=K110-K109	If = 1, adj C	=K110-K109
100	=IF(S97=1,SUM(T98:T99),"n/a")	2, match NO3	=IF(S97=1,SUM(V98:V99),"n/a")
101	=G47	3, adj both	=G47
102	=IF(S97=1,(T100-T101)/T101,"n/a")	which anion =	=IF(S97=1,(V100-V101)/V101,"n/a")
103	=IF(S97=1,S87+S88+S89+S90+S91*2+S92*3+S93*2+S94+S95+S96*2,"n/a")	1	=IF(S97=1,U87+U88+U89+U90+U91*2+U92*3+U93+U95+U96*2,"n/a")
104	=I75*3+I76*3+I77*2+I78*2+I80*2+I83*2+I84*3+I85*2+I86*2+I87*4+I88+I90*2+I92+I93*2+I94*2+I95*2+I97*2+I101*2+I104*2+I106*4+I107*4+I108*3	anion adj =	=I75*3+I76*3+I77*2+I78*2+I80*2+I83*2+I84*3+I85+I87*4+I88+I90*2+I92+I93*2+I94*2+I95*2+I97*2+I04*2+I106*4+I107*4+I108*3
105	=IF(S97=1,(T103-T104)/T104,"n/a")	0	=IF(S97=1,(V103-T104)/T104,"n/a")
106		**OR**	
107	=I75*3+I76*3+I77*2+I78*2+I80*2+I83*2+I84*3+I85*2+I86*2+I87*4+G88*(1+U108)/1000/F88+I90*2+I92+I93*2+I94*2+I95*2+I97*2+I101*2+I104*2+I106*4+I107*4+I108*3	SN Na adj =	
108	=(T103-T107)/T103	0.085115	
109	=G88*(1+U108)/1000*S79		
110	=(T109-G$48*C20/100)/(G$48*C20/100)		
111	=T109/G48*100/B20/2*F20		
112	=(T109-G$48*C20/100*(1+M51)*M54)/(G$48*C20/100*(1+M51)*M54)		

	E	F	G
3	**Table 2. SRAT/SME calcine data**		
4	calcine		
5	solids	MW	g / 100g
6			
7	Fe2O3	=B7*2+15.9994*3	=C7/B7/2*F7*M54
8	Al2O3	=B8*2+15.9994*3	=C8/B8/2*F8*M54
9	MnO	=B9+15.9994	=C9/B9*F9*M54
10	CaO	=B10+15.9994	=C10/B10*F10*M54*(1-C95)
11	U3O8	=B11*3+15.9994*8	=C11/B11/3*F11*M54
12	MgO	=B12+15.9994	=C12/B12*F12*M54
13	HgO	=B13+15.9994	0
14	P2O5	=B14*2+15.9994*5	=IF(C14>0,C14/B14/2*F14*M54,IF(C101>0,C101*G7/F7*2*B7/P92/2*F14))
15	NiO	=B15+15.9994	=C15/B15*F15*M54
16	Cr2O3	=B16*2+15.9994*3	=C16/B16/2*F16*M54
17	CuO	=B17+15.9994	=C17/B17*F17*M54
18	TiO2	=B18+15.9994*2	=C18/B18*F18*M54
19	SiO2	=B19+15.9994*2	=C19/B19*F19*M54
20	Na2O	=B20*2+15.9994	=C20/B20/2*F20*M54*(1+M51)
21	ThO2	=B21+15.9994*2	=C21/B21*F21*M54
22	ZnO	=B22+15.9994	=C22/B22*F22*M54
23	PuO2	=B23+15.9994*2	=C23/B23*F23*M54
24	K2O	=B24*2+15.9994	=C24/B24/2*F24*M54
25	RuO2	=B25+15.9994*2	=C25/B25*F25*M54
26	RhO2	=B26+15.9994*2	=C26/B26*F26*M54
27	PdO	=B27+15.9994	=IF(C27="<0.100",0,C27/B27/2*F27*M54)
28	CdO	=B28+15.9994	=IF(C28="<0.010",0,C28/B28/2*F28*M54)
29	SrO	=B29+15.9994	=C29/B29*F29*M54
30	B2O3	=B30*2+15.9994*3	=IF(C30="<0.100",0,C30/B30/2*F30*M54)
31	Li2O	=B31*2+15.9994	=IF(C31="<0.100",0,C31/B31/2*F31*M54)
32	Cs2O	=B32*2+15.9994	=C32/B32*F32*M54
33	BaO	=B33+15.9994	=C33/B33*F33*M54
34	SnO	=B34+15.9994	=C34/B34/2*F34*M54
35	PbO	=B35+15.9994	=C35/B35*F35*M54
36	TcO2	=B36+15.9994*2	=C36/B36*F36*M54
37	La2O3	=B37*2+15.9994*3	=C37/B37/2*F37*M54
38	ZrO2	=B38+15.9994*2	=C38/B38*F38*M54
39	SO3	=B39+15.9994*3	=C39/B39*F39/(1-M50)*M54
40	Total		=SUM(G7:G39)

	K	L	M
3	**Table 3A. SRAT/SME Insolubles**		
4	insoluble	MW	g/L slurry
5	solids		
6			
7	Fe(OH)3	=B7+(15.9994+1.0079)*3	=G7*$G$49*I7/F7*2*L7
8	Al(OH)3	=B8+(15.9994+1.0079)*3	=G8*$G$49*I8*(1-G59/100)/F8*2*L8
9	MnO2	=B9+15.9994*2	=G9*$G$49*I9/F9*L9
10	Ca(OH)2	=B10+(15.9994+1.0079)*2	=(G10*$G$49*I10/F10-M14/L14*3-M39/L39-M40/L40-M41/L41)*L10
11	Na2U2O7	=B20*2+B11*2+15.9994*7	=G11*$G$49*I11/F11*3/2*L11
12	Mg(OH)2	=B12+(15.9994+1.0079)*2	=G12*$G$49*I12/F12*L12
13	HgO	=F13	=M7/L7*B7*'Report Tables'!E42/B13*L13
14	Ca3(PO4)2	=B10*3+(B14+15.9994*4)*2	=G14*$G$49*I14/F14*L14
15	Ni(OH)2	=B15+(15.9994+1.0079)*2	=G15*$G$49*I15/F15*L15
16	Cr(OH)3	=B16+(15.9994+1.0079)*3	=G16*$G$49*I16/F16*2*L16
17	Cu(OH)2	=B17+(15.9994+1.0079)*2	=G17*$G$49*I17/F17*L17
18	TiO2	=B18+15.9994*2	=G18*$G$49*I18/F18*L18
19	SiO2	=B19+15.9994*2	=G19*$G$49*I19/F19*L19
20	Na2O	=B20*2+15.9994	=(G20*$G$49*I20/F20-M11/L11)*L20
21	ThO2	=B21+15.9994*2	=G21*$G$49*I21/F21*L21
22	Zn(OH)2	=B22+(15.9994+1.0079)*2	=G22*$G$49*I22/F22*L22
23	PuO2	=B23+15.9994*2	=G23*$G$49*I23/F23*L23
24	K2O	=B24*2+15.9994	=G24*$G$49*I24/F24*L24
25	RuO2	=B25+15.9994*2	=G25*$G$49*I25/F25*L25
26	RhO2	=B26+15.9994*2	=G26*$G$49*I26/F26*L26
27	PdO	=B27+15.9994	=G27*$G$49*I27/F27*L27
28	Cd(OH)2	=B28+(1.0079+15.9994)*2	=G28*$G$49*I28/F28*L28
29	Sr(OH)2	=B29+(15.9994+1.0079)*2	=G29*$G$49*I29/F29*L29
30	B2O3	=B30*2+15.9994*3	=G30*$G$49*I30/F30*L30
31	Li2O	=B31*2+15.9994	=G31*$G$49*I31/F31*L31
32	Cs2O	=B32*2+15.9994	=G32*$G$49*I32/F32*L32
33	BaSO4	=B33+B39+15.9994*4	=G33*$G$49*I33/F33*L33
34	Sn(OH)2	=B34+(15.9994+1.0079)*2	=G34*$G$49*I34/F34*L34
35	PbSO4	=B35+B39+15.9994*4	=G35*$G$49*I35/F35*L35
36	TcO2	=B36+15.9994*2	=G36*$G$49*I36/F36*L36
37	La(OH)3	=B37+(15.9994+1.0079)*3	=G37*$G$49*I37/F37*2*L37
38	ZrO2	=B38+15.9994*2	=G38*$G$49*I38/F38*L38
39	CaCO3	=B10+12.011+15.9994*3	0
40	CaSO4	=B10+B39+15.9994*4	=G10*$G$49*I10*V53/F10*L40
41	CaC2O4	=B10+12.011*2+15.9994*4	=G10*$G$49*I10/F10*V52*L41
42	Na2C2O4	=B20*2+12.011*2+15.9994*4	0
43	AlOOH	=B8+15.9994+15.9994+1.0079	=G8*$G$49*I8*(G59/100)/F8*2*L43
44	antifoam	=G136	=IF(Q142=1,M7/L7*B7*'Report Tables'!H210,IF(Q142=0,0*G43*1000,M7/L7*B7*G125*(1-G130/G128)*(1-G131)))
45	Total		=SUM(M7:M44)
46	target		=G46
47	Δ (%)		=(M45-M46)/M46*100
48	Δ w/o antifoam (%)		=(M45-M44-M46)/M46*100

	O	P	Q
3	**Table 3B. SRAT/SME Solubles**		
4	soluble	MW	g/L slurry
5	solids		
6			
7	Ca(COOH)2	=B10+P89*2	=G10*$G$49*(1-I10)/F10*V56*P7*G65
8	Ca(C2H3O3)2	=B10+P90*2	=G10*$G$49*(1-I10)/F10*U56*P8*G66
9	Ca(NO3)2	=B10+P87*2	=G10*$G$49*(1-I10)/F10*T56*P9*G67
10	Fe(COOH)3	=B7+P89*3	=G7*$G$49*(1-I7)/F7*2*V61*P10*G65
11	Fe(C2H3O3)3	=B7+P90*3	=G7*$G$49*(1-I7)/F7*2*U61*P11*G66
12	Fe(NO3)3	=B7+P87*3	=G7*$G$49*(1-I7)/F7*2*T61*P12*G67
13	Al(COOH)3	=B8+P89*3	=G8*$G$49*(1-I8)/F8*2*V62*P13*G65
14	Al(C2H3O3)3	=B8+P90*3	=G8*$G$49*(1-I8)/F8*2*U62*P14*G66
15	Al(NO3)3	=B8+P87*3	=G8*$G$49*(1-I8)/F8*2*T62*P15*G67
16	CsCOOH	=B32+P89	=G32*$G$49*(1-I32)/F32*2*V64*P16*G65
17	CsC2H3O3	=B32+P90	=G32*$G$49*(1-I32)/F32*2*U64*P17*G66
18	CsNO3	=B32+P87	=G32*$G$49*(1-I32)/F32*2*T64*P18*G67
19	Cu(COOH)2	=B17+P89*2	=G17*$G$49*(1-I17)/F17*V57*P19*G65
20	Cu(C2H3O3)2	=B17+P90*2	=G17*$G$49*(1-I17)/F17*U57*P20*G66
21	Cu(NO3)2	=B17+P87*2	=G17*$G$49*(1-I17)/F17*T57*P21*G67
22	KCOOH	=B24+P89	=G24*$G$49*(1-I24)/F24*2*V63*P22*G65
23	KC2H3O3	=B24+P90	=G24*$G$49*(1-I24)/F24*2*U63*P23*G66
24	KNO3	=B24+P87	=G24*$G$49*(1-I24)/F24*2*T63*P24*G67
25	Mg(COOH)2	=B12+P89*2	=G12*$G$49*(1-I12)/F12*V59*P25*G65
26	Mg(C2H3O3)2	=B12+P90*2	=G12*$G$49*(1-I12)/F12*U59*P26*G66
27	Mg(NO3)2	=B12+P87*2	=G12*$G$49*(1-I12)/F12*T59*P27*G67
28	Mn(COOH)2	=B9+P89*2	=G9*$G$49*(1-I9)/F9*V58*P28*G65
29	Mn(C2H3O3)2	=B9+P90*2	=G9*$G$49*(1-I9)/F9*U58*P29*G66
30	Mn(NO3)2	=B9+P87*2	=G9*$G$49*(1-I9)/F9*T58*P30*G67
31	NH4COOH	=14.007+1.0079*4+P89	
32	NH4NO3	=14.007+1.0079*4+P87	
33	NaCl	=B20+35.4527	=G20*$G$49*U17/100/F20*2*P33
34	NaF	=B20+18.9984	=G20*$G$49*U16/100/F20*2*P34
35	NaCOOH	=B20+P89	=G20*$G$49*U11/100/F20*2*P35*G65
36	NaC2H3O3	=B20+P90	=G20*$G$49*U12/100/F20*2*P36*G66
37	NaNO3	=B20+P87	=G20*$G$49*U7/100/F20*2*P37*G67
38	NaNO2	=B20+P88	=G20*$G$49*U8/100/F20*2*P38*G67
39	Na3PO4	=B20*3+P92	=G20*$G$49*U13/100/F20*2/3*P39
40	Ni(COOH)2	=B15+P89*2	=G15*$G$49*(1-I15)/F15*V60*P40*G65
41	Ni(C2H3O3)2	=B15+P90*2	=G15*$G$49*(1-I15)/F15*U60*P41*G66
42	Ni(NO3)2	=B15+P87*2	=G15*$G$49*(1-I15)/F15*T60*P42*G67
43	Pb(NO3)2	=B35+P87*2	=G35*$G$49*(1-I35)/F35*P43*G67
44	Pd(NO3)2	=B27+P87*2	=G27*$G$49*(1-I27)/F27*P44*G67
45	Sr(COOH)2	=B29+P89*2	=G29*$G$49*(1-I29)/F29*V68*P45*G65
46	Sr(C2H3O3)2	=B29+P90*2	=G29*$G$49*(1-I29)/F29*U68*P46*G66
47	Sr(NO3)2	=B29+P87*2	=G29*$G$49*(1-I29)/F29*P47*T68*G67
48	UO2(COOH)2	=B11+15.9994*2+P89*2	=G11*G49*(1-I11)/F11*3*V67*P48*G65
49	UO2(C2H3O3)2	=B11+15.9994*2+P90*2	=G11*G49*(1-I11)/F11*3*U67*P49*G66
50	UO2(NO3)2	=B11+15.9994*2+P87*2	=G11*$G$49*(1-I11)/F11*3*T67*P50*G67

	O	P	Q
50	**Table 3B. SRAT/SME Solubles (Continued)**		
51	La(COOH)3	=B37+P89*3	=G37*G49*(1-I37)/F37*2*V66*P51*G65
52	La(C2H3O3)3	=B37+P90*3	=G37*G49*(1-I37)/F37*2*U66*P52*G66
53	La(NO3)3	=B37+P87*3	=G37*$G$49*(1-I37)/F37*2*T66*P53*G67
54	Zn(COOH)2	=B22+P89*2	=G22*$G$49*(1-I22)/F22*V65*P54*G65
55	Zn(C2H3O3)2	=B22+P90*2	=G22*$G$49*(1-I22)/F22*U65*P55*G66
56	Zn(NO3)2	=B22+P87*2	=G22*$G$49*(1-I22)/F22*T65*P56*G67
57	Na2CO3	=B20*2+P96	=IF(ABS(U9)<0.002,0,G20*$G$49/F20*2*U9/100/2*P57)
58	Na2C2O4	=B20*2+P91	=T28/P91*P58
59	Na2SO4	=B20*2+P93	=G20*$G$49*U14/100/F20*P59
60	H4SiO4	=1.0079*4+B19+15.9994*4	=G19*$G$49*(1-I19)/F19*P60
61	Total		=SUM(Q7:Q60)
62	target		=G47
63	Δ (%)		=(Q61-Q62)/Q62*100
64	HCOOH	=1.0079+P89	=(AE84*P89-AE92)/P89*P64
65	C2H4O3	=P90+1.0079	=(AE72*P90-AE80)/P90*P65
66	calc'd H2O	=1.0079*2+15.9994	=G43*1000-M45-Q61
67	calc'd total solids (g/L)		=M45+Q61
68	total solid (wt%) =		=(M45+Q61)/(Q66+Q67)
69	diff from density-TS data		=(Q67-G45)/G45

	S	T	U
3	**Table 4. Total Na Distribution**		
4	assumed Na		
5	distribution		(mole %)
6			
7	NO3		15.8120585465746
8	NO2		0
9	CO3		=100-SUM(U7:U8)-SUM(U10:U18)
10	Oxide		=M20/L20*2/(G20*G49/F20*2)*100
11	COOH		42.8384173641063
12	C2H3O3		0
13	PO4		0
14	SO4		0.927415780904888
15	C2O4		=(Q58/P58+M42/L42)/(G20*G49/F20)*100
16	F		0
17	Cl		0.0877927744005453
18	U2O7		=M11/L11*2/(G20*G49/F20*2)*100
19	total		=SUM(U7:U18)

	S	T	U	V
21	**Table 5. Comparison with IC Data**			
22	IC	target	actual	delta
23		(g/L)	(g/L)	(%)
24	NO3	=IF(V36<7,AE104,'Smith SB9 SRAT-SME Data'!F46*(1+M53)/1000*G43)	=P87*(Q9/P9*2+Q12/P12*3+Q15/P15*3+Q18/P18+Q21/P21*2+Q24/P24+Q27/P27*2+Q30/P30*2+Q32/P32+Q37/P37+Q42/P42*2+Q43/P43*2+Q44/P44*2+Q47/P47*2+Q50/P50*2+Q53/P53*3+Q56/P56*2)	=(U24-T24)/T24*100
25	NO2	=IF('Smith SB9 SRAT-SME Data'!E46="<500",0,'Smith SB9 SRAT-SME Data'!E46/1000*G43)	=P88*Q38/P38	=IF(T25=0,"",(U25-T25)/T25*100)
26	COOH	=IF(V36<7,AE92,'Smith SB9 SRAT-SME Data'!J46*(1+M52)/1000*G43)	=P89*(Q7/P7*2+Q10/P10*3+Q13/P13*3+Q16/P16+Q19/P19*2+Q22/P22+Q25/P25*2+Q28/P28*2+Q31/P31+Q35/P35+Q40/P40*2+Q45/P45*2+Q48/P48*2+Q51/P51*3+Q54/P54*2)	=(U26-T26)/T26*100
27	C2H3O3	0	=P90*(Q8/P8*2+Q11/P11*3+Q14/P14*3+Q17/P17+Q20/P20*2+Q23/P23+Q26/P26*2+Q29/P29*2+Q36/P36+Q41/P41*2+Q46/P46*2+Q49/P49*2+Q52/P52*3+Q55/P55*2)	0
28	C2O4	=IF(T84=1,'Smith SB9 SRAT-SME Data'!I46*(1+M52)*G68/1000*G43,T91)	=P91*Q58/P58	=IF(T28=0,"",(U28-T28)/T28*100)
29	PO4	=IF(G61=1,G14/F14*2*P92*G49,'Smith SB9 SRAT-SME Data'!K46/1000*G43)	=Q39/P39*(P39-B20*3)	=IF(T29=U29,0,(U29-T29)/T29*100)
30	SO4	=IF(M60=1,'Smith SB9 SRAT-SME Data'!H46/1000*G43,IF(M60=2,M58,M59))	=Q59/P59*(P59-B20*2)	=IF(T30=0,"",(U30-T30)/T30*100)
31	Cl	='Smith SB9 SRAT-SME Data'!D46/1000*G43	=Q33/P33*35.453	=IF(T31=0,"",(U31-T31)/T31*100)
32	F	=IF('Smith SB9 SRAT-SME Data'!C46="<500",0,'Smith SB9 SRAT-SME Data'!C46/1000*G43)	=Q34/P34*19	=IF(T32=0,"",(U32-T32)/T32*100)
33	CO3	='Report Tables'!H199/1000*G43	=Q57/P57*(P57-B20*2)	=IF(T33=0,"",(U33-T33)/T33*100)
34	CO3 (ppm)	=T33/(G43*1000)/60*12*1000000	=U33/(G43*1000)/60*12*1000000	
35	**Table 6. Bases and Assumptions:**			
36	1. pH of SRAT or SME product			='Smith SB9 SRAT-SME Data'!H63
37	2. Given data is for SME ? Yes =1			1
38	3. Coal addition (lb/L slurry) =			1.10106004622004
39	4. acid addition (% stoichiometry) =			120
40	5. Total solids in SRAT/SME Prod =			='Smith SB9 SRAT-SME Data'!F56
41	Insoluble solids in SRAT/SME (wt%) =			='Smith SB9 SRAT-SME Data'!I56
42	Calcine solids in SRAT/SME (wt%) =			='Smith SB9 SRAT-SME Data'!K56
43	6. Glass production rate (lb/hr) =			217.691348096407
44	7. Glass entrainment (wt%) =			0
45	8. Target waste loading (wt%) =			=AP81
46	9. req'd waste oxide feed rate (lb/hr) =			=V43/(1-V44/100)*V45/100
47	10. Req'd frit rate (lb/hr) =			=IF(V37=1,0,V43/(1-V44/100)-V46)
48	11. Remediate NGA feed? (if =1, yes)			0
49	12. If = 1, add NaOH for SB9 sim remed			1

	A	B	C	D	E	F	G
42	**Table 7. Additional SRAT Product data:**						
43	slurry density (g/ml) =						='Smith SB9 SRAT-SME Data'!I63
44	supernate density (g/ml) =						='Smith SB9 SRAT-SME Data'!J63
45	total solids (g/L slurry) =						=G43*1000*V40
46	insoluble solids (g/L slurry) =						=IF(V41="n/a","n/a",G43*1000*V41)
47	soluble solids (g/L slurry) =						=IF(V41="n/a","n/a",G43*1000*(V40-V41))
48	calcine solids (g/L slurry) =						=G43*1000*V42
49	multiplification factor to convert to L slurry basis =						=G48/G40
50	measured calcine ratio of SRAT or SME product =						=G48/G45
51	calculated calcine ratio of SRAT or SME product =						=G48/(Q61+M45-M13-M44)

	I	J	K	L	M
49	**Table 8. Charge Balance Adjustments:**				
50	assumed % loss S during calcination =				0
51	% adj'ment for slurry ICP Na =				0.12
52	% adj'ment for slurry IC carbon data =				0
53	% adj'ment for slurry IC NO3 data =				0
54	Multiplification factor of ICP data =				1
55	**Table 9. Sulfate Balance:**				
56	total SO4 from SL ICP (g/L slurry) =				=G39*G49/F39*P93
57	soluble SO4 from SL IC (g/L slurry) =				='Smith SB9 SRAT-SME Data'!H46/1000*G43
58	soluble SO4 from SN ICP (g/L slurry) =				=K109/F109*P93
59	soluble SO4 from SN IC (g/L slurry) =				=T93
60	which soluble data to use ?				
61	target insoluble SO4 (g/L slurry) =				=IF(M60=1,M56-M57,IF(M60=2,M56-M58,IF(M60="",M57-M59,M56-M59)))
62	actual insoluble SO4 (g/L slurry) =				=(M33/L33+M35/L35+M40/L40)*P93
63	diff insoluble SO4 (%) =				=(M62-M61)/M61*100
64	**Table 10. Oxalate Balance:**				
65	oxalate added to simulant (g/L SL) =				='Smith SB9 SRAT-SME Data'!C99*M7/L7*B7
66	measured soluble oxalate (g/L SL) =				=T28
67	calc'd insoluble oxalate (g/L SL) =				=M65-T91
68	C2O4 as CaC2O4 (g/L SL) =				=M41/L41*P91
69	Diff btw insoluble and C2O4 as Ca (%)				=IF(M67<0,"n/a",(M67-M68)/M67)

	S	T	U	V
51	**Table 11. Assumed Ca Partitioning**			
52	fraction insoluble Ca as CaC2O4 =			=1-V53
53	fraction insoluble Ca as SO4 =			0.192349095256777
54	**Table 12. Partitioning of soluble metals:**			
55		frac NO3	frac glycolate	frac form
56	Ca	='Smith SB9 SRAT-SME Data'!F46/P87/('Smith SB9 SRAT-SME Data'!F46/P87+'Smith SB9 SRAT-SME Data'!J46/P89)	0	=1-T56-U56
57	Cu	=T$56	=U$56	=1-T57-U57
58	Mn	=T$56	=U$56	=1-T58-U58
59	Mg	=T$56	=U$56	=1-T59-U59
60	Ni	=T$56	=U$56	=1-T60-U60
61	Fe	=T$56	=U$56	=1-T61-U61
62	Al	=T$56	=U$56	=1-T62-U62
63	K	=T$56	=U$56	=1-T63-U63
64	Cs	=T$56	=U$56	=1-T64-U64
65	Zn	=T$56	=U$56	=1-T65-U65
66	La	=T$56	=U$56	=1-T66-U66
67	U	=T$56	=U$56	=1-T67-U67
68	Sr	=T$56	=U$56	=1-T68-U68

	A	B	C	D	E	F	G
64	**Table 13. Vary nitrate & TOC for case study:**						
65	multiplification factor for formate =						1
66	multiplification factor for glycolate =						0
67	multiplification factor for nitrate =						1
68	multiplification factor for C2O4 =						1

	Y	Z	AA	AB	AC	AD	AE
71	**Table 14A. Estimation of free glycolic acid at acidic pH**						
72	total [C2H3O3-] from IC (M) =						0
73	pKa for C2H4O3 dissociation at 25 deg C =						3.83
74	dissociated C2H4O3 (M) =						=AE72/(1+10^(AE73-V36))
75	undissociated C2H4O3 (M) =						=10^(AE73-V36)*AE74
76	calculated [H+] (M) =						=IF(AE74=0,0,10^(-AE73)*AE75/AE74)
77	calculated pH =						=IF(AE76=0,"n/a",-LOG(AE76))
78	total [HOCH2COO-] due to free glycolic acid (M) =						=IF(AE100>0,AE75,AE75+AE76)
79	dissociated [HOCH2COO-] (g/L) =						0
80	adjusted dissociated [HOCH2COO-] (g/L) =						=IF(AE75<0.001,AE72*P90,AE79*T82)
81	fraction undissociated glycolic acid =						=(AE72*P90-AE80)/AE72/P90
82							
83	**Table 14B. Estimation of free formic acid at acidic pH**						
84	total [COOH-] from IC (M) =						='Smith SB9 SRAT-SME Data'!J46*(1+M52)/1000*G43/P89
85	pKa for HCOOH dissociation at 25 deg C =						3.75
86	dissociated HCOOH (M) =						=AE84/(1+10^(AE85-V36))
87	undissociated HCOOH (M) =						=10^(AE85-V36)*AE86
88	calculated [H+] (M) =						=10^(-AE85)*AE87/AE86
89	calculated pH =						=-LOG(AE88)
90	total [COOH-] due to free formic acid (M) =						=IF(AE100>0,AE87,AE87+AE88)
91	dissociated [COOH-] (g/L) =						='Smith SB9 SRAT-SME Data'!J46*(1+M52)/1000*G43-AE90*P89
92	adjusted dissociated [COOH-] (g/L) =						=IF(AE87<0.001,AE84*P89,AE91*T82)
93	fraction undissociated formic acid =						=(AE84*45.02-AE92)/AE84/45.02
94							
95	**Table 14C. Estimation of free nitric acid at acidic pH**						
96	total [NO3-] from IC (M) =						='Smith SB9 SRAT-SME Data'!F46*(1+M53)/1000*G43/P87
97	approx. pKa for HNO3 dissociation at 25 deg C =						-2
98	dissociated HNO3 (M) =						=AE96/(1+10^(AE97-V36))
99	undissociated HNO3 (M) =						=10^(AE97-V36)*AE98
100	calculated [H+] (M) =						=10^(-AE97)*AE99/AE98
101	calculated pH =						=-LOG(AE100)
102	total [NO3-] due to free nitric acid (M) =						=AE99+AE100
103	dissociated [NO3-] (g/L) =						='Smith SB9 SRAT-SME Data'!F46*(1+M53)/1000*G43-AE102*P87
104	final dissociated [NO3-] (g/L) =						=IF(AE99<0.001,AE96*P87,AE103)

	A	B	C	D	E	F	G
116	**Table 15. Antifoam addition to SRAT or SME (if V37 = 1):**						
117	Basis (gal slurry) =						1
118	mass of Fe (kg) =						=G117*3.7854*G43*V42*C7/100
119	nominal SRAT transfer volume (gal) =						=IF(V37=1,Q173,AVERAGE(Q163:Q164))
120	antifoam added to SRAT (gal/gal transfer) =						=IF(V37=1,(G128+G129)*G151/Q119,G128*G151/G119)
121	antifoam concentration (wt%) =						=1/20*100
122	antifoam density @ 100% conc (g/ml) =						0.997
123	density of antifoam solution (g/ml) =						=G122*G121/100+1*(1-G121/100)
124	mass of antifoam added to SRAT (kg/gal fresh sludge) =						=G120*3.7854*G123*G121/100
125	antifoam-to-Fe mass ratio =						=G124/G118
126							
127	**Table 16. DWPF Baseline Antifoam Addition:**						Original IIT747
128	to SRAT during SME_563 (gal/6,500 gal SRAT batch) =						='C:\DWPF\Alt reductant flowsheet\2014 CEF test\model eval glycolic FS\[SB6-CEF-FN analytical IC.xlsx]SME 557-563'!U14+'C:\DWPF\Alt reductant flowsheet\2014 CEF test\model eval glycolic FS\[SB6-CEF-FN analytical IC.xlsx]SME 557-563'!V14
129	to SME (SME-563) (gal/4,500 gal SRAT product exc heel) =						='C:\DWPF\Alt reductant flowsheet\2014 CEF test\model eval glycolic FS\[SB6-CEF-FN analytical IC.xlsx]SME 557-563'!W14
130	antifoam added during SRAT caustic boiling (gal) =						0
131	depolymerized antifoam (% SRAT non-caustic addition) =						0
132	depolymerized antifoam (% SME addition) =						0
133	MW of antifoam part A (90%) =						=(8+2*8)*12.0107+(24+4*8)*1.0079+3*28.0855+(2+1*8)*15.9994
134	MW of antifoam part B (10%) =						=(8+2*12)*12.0107+(24+4*12)*1.0079+3*28.0855+(2+1*12)*15.99
135	wt fraction of part A =						0.9
136	composition MW =						=G133*G135+G134*(1-G135)
137	wt% carbon =						=((8+2*8)*G135+(8+2*12)*(1-G135))*12.0107/G136
138	wt% hydrogen =						=((24+4*8)*G135+(24+4*12)*(1-G135))*1.0079/G136
139	wt% silicon =						=3*B19/G136
140	wt% oxygen =						=((2+1*8)*G135+(2+1*12)*(1-G135))*15.9994/G136
141	moles of polyether group per mole of composite MW =						=(G136-((3+2+3)*12.0107+(9+6+9)*1.0079+3*28.0855+2*15.9994))/(1*15.9994+2*12.0107+4*1.0079)
142	moles of Si in per composite MW =						=3
143	moles of C in per composite MW =						=8+2*G141
144	moles of H in per composite MW =						=8*3+4*G141
145	moles of O in per composite MW =						=2+1*G141
146	confirm compositie MW =						=G143*12.0107+G144*1.0079+G142*28.0855+G145*15.9994
147	wt% trimethylsiloxane group =						=(G142*B19+G143*8/(8+G141*2)*12.0107+G144*(9+6+9)/((9+6+9)+4*G141)*1.0079+G145*2/(2+G141)*15.9994)/G146
148	wt% polydimethyl ether group =						=1-G147
149	confirm wt% polydimethyl ether group =						=(2*12.0107+15.9994+4*1.0079)*G141/G146
150	multiples of antifoam added during SME 563 to set						
151	conversion factor from SME563 to target antifoam volume =						1.07322929171669
152	target 20:1 antifoam addition per CPC cycle (gal) =						=(G128+G129)*G151

	A	B	C	D	E	F	G	H	I
154	**Table 17. MCU-NGS Solvent revised per SRNL-STI-2013-00035 with 6 ppm TiDG**								
155									ORNL data
156	MaxCalix								or Targets
157		MW =					955.31		-
158		CAS No. =					1227059-50-8		
159		Density =					1.054		
160		MF =					C62H82O8		
161	check	MW =					=62*12.0107+82*1.0079+8*15.9994		
162	Cs-7SB								
163		MW =					338.34		338.35
164		CAS No. =					308362-88-1		
165		Density =					1.1735		
166		MF =					C16H22F4O3		
167	check	MW =					=16*12.0107+22*1.0079+4*18.9984+3*1		
168	TiDG								
169		MW =					516.34		-
170		CAS No. =					n/a		
171		Density =					0.809		
172		MF =					C31H66ClN3		
173	check	MW =					=31*12.0107+66*1.0079+1*35.4527+3*14.007		
174	Isopar L								
175		MW =					170		
176		CAS No. =					64742-48-9		
177		Density =					0.730523680649527		0.763
178		MF =					CnH2n+2		
179		n =					12		
180	check	MW =					=G179*12.0107+(2*G179+2)*1.0079		
181	Distributions from AD analysis (wt%):								
182		Isopar L					0.739		
183		Cs-7SB					0.202		
184		MaxCalix					0.057		
185		TiDG					0.002		
186		total					=SUM(G182:G185)		
187		Composite density =					=G159*G184+G165*G183+G171*G185+G177*G182		0.8386
188	Estimated Conc:								
189		Basis (L solution) =					1		
190		Isopar L							
191		Cs-7SB (M) =					=G187*1000*G183/G163		0.5
192		MaxCalix (M) =					=G187*1000*G184/G157		0.05
193		TiDG (M) =					=G187*1000*G185/G169		0.003
194	Adjusted distributions w/ 6 ppm TiDG entrainment (wt%):								
195		Isopar L					0.7032		
196		Cs-7SB					0.1922		
197		MaxCalix					0.0542		
198		TiDG					0.0504		
199		total					=SUM(G195:G198)		
200		Composite density =					=G159*G197+G165*G196+G171*G198+G177*G195		
201		# of moles in 1 g solvent =					=G195/G180+G196/G163+G197/G157+G198/G169		

	A	B	C	D	E	F	G	H	I
201	**Table 17. MCU-NGS Solvent revised per SRNL-STI-2013-00035 with 6 ppm TiDG (Continued)**								
202	Adjusted distributions w/ 6 ppm TiDG entrainment (mol%):								
203		Isopar L					=G195/G180/G201		
204		Cs-7SB					=G196/G163/G201		
205		MaxCalix					=G197/G157/G201		
206		TiDG					=G198/G169/G201		
207		total					=SUM(G203:G206)		
208	Estimated Conc:								
209		Basis (L solution) =					1		
210		Isopar L							
211		Cs-7SB (M) =					=G200*1000*G196/G163		
212		MaxCalix (M) =					=G200*1000*G197/G157		
213		TiDG (M) =					=G200*1000*G198/G169		
214	Composite:								
215		MW =					=G203*G180+G204*G163+G205*G157+G206*G169		
216		Density =					=G195*G177+G196*G165+G197*G159+G198*G171		
217		assumed # of carbon in mole of Isopar					15		
218		mole of element per mole composite							
219			C				=G203*G179+G204*16+G205*62+G206*31		
220			H				=G203*(2*G179+2)+G204*22+G205*82+G206*66		
221			O				=G203*0+G204*3+G205*8+G206*0		
222			N				=G203*0+G204*0+G205*0+G206*3		
223			F				=G203*0+G204*4+G205*0+G206*0		
224			Cl				=G203*0+G204*0+G205*0+G206*1		
225		check	MW				=G219*12.0107+G220*1.0079+G221*15.9994+G222*14.0067+G223*18.9984+G224*35.4527		
226	ref volume of strip effluent to SEFT (gal/transfer) =						15000		
227	density of strip effluent (g/ml) =						1.002		
228	max conc of solvent in strip effluent (ppm) =						150		
229	mass of solvent (lb/transfer) =						=G226*3.7854*G227*1000/453.6*G228/1000000		
230	instantaneous solvent feed rate (lb/hr) =						=IF(Q183=0,G229/Q178,G229/Q185)		
231	**MCU input into SME product:**								
232	non-volatile solvent excluding Isopar L (lb/hr) =						=G230*(G199-G195)		
233	Adjusted distributions w/o Isopar L (wt%):								
234		Isopar L					0		
235		Cs-7SB					=G196/(G$199-G$195)		
236		MaxCalix					=G197/(G$199-G$195)		
237		TiDG					=G198/(G$199-G$195)		
238		total					=SUM(G234:G237)		
239		total moles in 1 g non-volatile =					=G235/G163+G236/G157+G237/G173		

	A	B	C	D	E	F	G	H	I
239	**Table 17. MCU-NGS Solvent revised per SRNL-STI-2013-00035 with 6 ppm TiDG (Continued)**								
240	Adjusted distributions w/o Isopar L (mol%):								
241		Cs-7SB					=G235/G163/G239		
242		MaxCalix					=G236/G157/G239		
243		TiDG					=G237/G173/G239		
244		total					=SUM(G241:G243)		
245		MW =					=G241*G163+G242*G157+G243*G169		
246		mole of element per mole nonvolatile							
247			C				=G241*16+G242*62+G243*31		
248			H				=G241*22+G242*82+G243*66		
249			O				=G241*3+G242*8+G243*0		
250			N				=G241*0+G242*0+G243*3		
251			F				=G241*4+G242*0+G243*0		
252			Cl				=G241*0+G242*0+G243*1		
253		check	MW				=G247*12.0107+G248*1.0079+G249*16+G250*14.0067+G251*18.9984+G252*35.4527		
254		mass fractions							
255			C				=G247*12.0107/G245		
256			H				=G248*1.0079/G245		
257			O				=G249*16/G245		
258			N				=G250*14.0067/G245		
259			F				=G251*18.9984/G245		
260			Cl				=G252*35.4527/G245		
261			total				=SUM(G255:G260)		
262	Decomposition of nonvolatile strip effluent:								L3100-15-217
263			CH4 (mole/mole nonvolatile)				=G248/4		8.165
264			CO				=G249		2.988
265			CF4				=G251/4		0.7863
266			CCl4				=G252/4		0.0338
267			C				=G247-G263-G264-G265-G266		9.669
268			N2				=G250/2		0.2027
269		check element balance							
270			C (mole/mole nonvolatile)				=G263+G264+G265+G266+G267		
271			H				=G263*4		
272			O				=G264		
273			N				=G268*2		
274			F				=G265*4		
275			Cl				=G266*4		

	K	L	M	N	O	P	Q
154	**Table 18. SME Transfer and Cycle Time:**						
155	Oxalix acid added during one ARP cycle (gal) =						500
156	oxalic acid conc (M) =						0.5
157	ref oxalate in each PRFT transfer (lb) =						=Q155*3.7854*Q156*88/453.6
158	min oxalate in each PRFT transfer (lb) =						0
159	max SRAT prod volume following conc (gal) =						7409
160	min SRAT prod volume following conc (gal) =						5847
161	max SRAT heel following transfer to SME (gal) =						1663
162	min SRAT heel following transfer to SME (gal) =						1247
163	max SRAT prod transfer to SME (gal) =						=Q159-Q162
164	min SRAT prod transfer to SME (gal) =						=Q160-Q161
165	max SME prod volume following conc (gal) =						7664
166	min SME prod volume following conc (gal) =						6228
167	SME 563 end volume (gal) =						7161
168	max SME heel following transfer to MFT (gal) =						1503
169	min SME heel following transfer to MFT (gal) =						1410
170	SME 563 heel (gal) =						1483
171	max SME product transfer to MFF (gal/CPC cycle) =						=Q165-Q169
172	min SME product transfer to MFF (gal/CPC cycle) =						=Q166-Q168
173	SME 563 transfer (gal) =						=Q167-Q170
174	max Na2C2O4 in SME prod for ref ARP addn (lb/gal) =						=Q157/88*134/Q172
175	min Na2C2O4 in SME prod for ref ARP addn (lb/gal) =						=Q157/88*134/Q171
176	Na2C2O4 addition for zero PRFT transfer (lb/gal) =						=Q158
177	Req'd SME transfer rate @ 228 lb/ht glass & 100% att (gpm) =						='ccinput_SB9-894B'!D7
178	CPC cycle time for SME563 @ 228 lb/hr glass & 100% att (hr) =						=Q173/Q177/60
179	instantaneous max salt Na2C2O4 in SME563 transfer (lb/hr) =						=Q174*Q173/Q178
180	inst max salt Na2C2O4 in SME563 (X SME563 transfer) =						=Q179/AK53
181	instantaneous min salt Na2C2O4 in SME563 transfer (lb/hr) =						
182	**Added for SB9:**						
183	which SME transfer volume to use (if = 0, use 5,678 gal) =						0
184	nominal SME transfer volume (gal) =						=IF(Q183=0,Q173,4600)
185	CPC cycle time to meet 228 lb/hr glass & 100% att (hr) =						=IF(Q183=0,Q173/Q177/60,Q184/Q177/60)

	X	Y	Z	AA	AB
3	**Table 19. SRAT Product Flow @ 100% attainment**				
4	insoluble			soluble	
5	solids	lb/hr		solids	lb/hr
6					
7	Fe(OH)3	=IF($V$37=1,M7*$V$43/$G$48,M7*$V$46/$G$48)		Ca(COOH)2	=IF($V$37=1,Q7*$V$43/$G$48,Q7*$V$46/$G$48)
8	Al(OH)3	=IF($V$37=1,M8*$V$43/$G$48,M8*$V$46/$G$48)		Ca(C2H3O3)2	=IF($V$37=1,Q8*$V$43/$G$48,Q8*$V$46/$G$48)
9	MnO2	=IF($V$37=1,M9*$V$43/$G$48,M9*$V$46/$G$48)		Ca(NO3)2	=IF($V$37=1,Q9*$V$43/$G$48,Q9*$V$46/$G$48)
10	Ca(OH)2	=IF($V$37=1,M10*$V$43/$G$48,M10*$V$46/$G$48)		Fe(COOH)3	=IF($V$37=1,Q10*$V$43/$G$48,Q10*$V$46/$G$48)
11	Na2U2O7	=IF($V$37=1,M11*$V$43/$G$48,M11*$V$46/$G$48)		Fe(C2H3O3)3	=IF($V$37=1,Q11*$V$43/$G$48,Q11*$V$46/$G$48)
12	Mg(OH)2	=IF($V$37=1,M12*$V$43/$G$48,M12*$V$46/$G$48)		Fe(NO3)3	=IF($V$37=1,Q12*$V$43/$G$48,Q12*$V$46/$G$48)
13	HgO	=IF($V$37=1,M13*$V$43/$G$48,M13*$V$46/$G$48)		Al(COOH)3	=IF($V$37=1,Q13*$V$43/$G$48,Q13*$V$46/$G$48)
14	Ca3(PO4)2	=IF($V$37=1,M14*$V$43/$G$48,M14*$V$46/$G$48)		Al(C2H3O3)3	=IF($V$37=1,Q14*$V$43/$G$48,Q14*$V$46/$G$48)
15	Ni(OH)2	=IF($V$37=1,M15*$V$43/$G$48,M15*$V$46/$G$48)		Al(NO3)3	=IF($V$37=1,Q15*$V$43/$G$48,Q15*$V$46/$G$48)
16	Cr(OH)3	=IF($V$37=1,M16*$V$43/$G$48,M16*$V$46/$G$48)		CsCOOH	=IF($V$37=1,Q16*$V$43/$G$48,Q16*$V$46/$G$48)
17	Cu(OH)2	=IF($V$37=1,M17*$V$43/$G$48,M17*$V$46/$G$48)		CsC2H3O3	=IF($V$37=1,Q17*$V$43/$G$48,Q17*$V$46/$G$48)
18	TiO2	=IF($V$37=1,M18*$V$43/$G$48,M18*$V$46/$G$48)		CsNO3	=IF($V$37=1,Q18*$V$43/$G$48,Q18*$V$46/$G$48)
19	SiO2	=IF($V$37=1,M19*$V$43/$G$48,M19*$V$46/$G$48)		Cu(COOH)2	=IF($V$37=1,Q19*$V$43/$G$48,Q19*$V$46/$G$48)
20	Na2O	=IF($V$37=1,M20*$V$43/$G$48,M20*$V$46/$G$48)		Cu(C2H3O3)2	=IF($V$37=1,Q20*$V$43/$G$48,Q20*$V$46/$G$48)
21	ThO2	=IF($V$37=1,M21*$V$43/$G$48,M21*$V$46/$G$48)		Cu(NO3)2	=IF($V$37=1,Q21*$V$43/$G$48,Q21*$V$46/$G$48)
22	Zn(OH)2	=IF($V$37=1,M22*$V$43/$G$48,M22*$V$46/$G$48)		KCOOH	=IF($V$37=1,Q22*$V$43/$G$48,Q22*$V$46/$G$48)
23	PuO2	=IF($V$37=1,M23*$V$43/$G$48,M23*$V$46/$G$48)		KC2H3O3	=IF($V$37=1,Q23*$V$43/$G$48,Q23*$V$46/$G$48)
24	K2O	=IF($V$37=1,M24*$V$43/$G$48,M24*$V$46/$G$48)		KNO3	=IF($V$37=1,Q24*$V$43/$G$48,Q24*$V$46/$G$48)
25	RuO2	=IF($V$37=1,M25*$V$43/$G$48,M25*$V$46/$G$48)		Mg(COOH)2	=IF($V$37=1,Q25*$V$43/$G$48,Q25*$V$46/$G$48)
26	RhO2	=IF($V$37=1,M26*$V$43/$G$48,M26*$V$46/$G$48)		Mg(C2H3O3)2	=IF($V$37=1,Q26*$V$43/$G$48,Q26*$V$46/$G$48)
27	PdO	=IF($V$37=1,M27*$V$43/$G$48,M27*$V$46/$G$48)		Mg(NO3)2	=IF($V$37=1,Q27*$V$43/$G$48,Q27*$V$46/$G$48)
28	Cd(OH)2	=IF($V$37=1,M28*$V$43/$G$48,M28*$V$46/$G$48)		Mn(COOH)2	=IF($V$37=1,Q28*$V$43/$G$48,Q28*$V$46/$G$48)
29	Sr(OH)2	=IF($V$37=1,M29*$V$43/$G$48,M29*$V$46/$G$48)		Mn(C2H3O3)2	=IF($V$37=1,Q29*$V$43/$G$48,Q29*$V$46/$G$48)
30	B2O3	=IF($V$37=1,M30*$V$43/$G$48,M30*$V$46/$G$48)		Mn(NO3)2	=IF($V$37=1,Q30*$V$43/$G$48,Q30*$V$46/$G$48)
31	Li2O	=IF($V$37=1,M31*$V$43/$G$48,M31*$V$46/$G$48)		NH4COOH	=IF($V$37=1,Q31*$V$43/$G$48,Q31*$V$46/$G$48)
32	Cs2O	=IF($V$37=1,M32*$V$43/$G$48,M32*$V$46/$G$48)		NH4NO3	=IF($V$37=1,Q32*$V$43/$G$48,Q32*$V$46/$G$48)
33	BaSO4	=IF($V$37=1,M33*$V$43/$G$48,M33*$V$46/$G$48)		NaCl	=IF($V$37=1,Q33*$V$43/$G$48,Q33*$V$46/$G$48)
34	Sn(OH)2	=IF($V$37=1,M34*$V$43/$G$48,M34*$V$46/$G$48)		NaF	=IF($V$37=1,Q34*$V$43/$G$48,Q34*$V$46/$G$48)
35	PbSO4	=IF($V$37=1,M35*$V$43/$G$48,M35*$V$46/$G$48)		NaCOOH	=IF($V$37=1,Q35*$V$43/$G$48,Q35*$V$46/$G$48)
36	TcO2	=IF($V$37=1,M36*$V$43/$G$48,M36*$V$46/$G$48)		NaC2H3O3	=IF($V$37=1,Q36*$V$43/$G$48,Q36*$V$46/$G$48)
37	La(OH)3	=IF($V$37=1,M37*$V$43/$G$48,M37*$V$46/$G$48)		NaNO3	=IF($V$37=1,Q37*$V$43/$G$48,Q37*$V$46/$G$48)

	X	Y	Z	AA	AB
37	**Table 19. SRAT Product Flow @ 100% attainment (Continued)**				
38	ZrO2	=IF($V$37=1,M38*$V$43/$G$48,M38*$V$46/$G$48)		NaNO2	=IF($V$37=1,Q38*$V$43/$G$48,Q38*$V$46/$G$48)
39	CaCO3	=IF($V$37=1,M39*$V$43/$G$48,M39*$V$46/$G$48)		NaOH	
40	CaSO4	=IF($V$37=1,M40*$V$43/$G$48,M40*$V$46/$G$48)		Na3PO4	=IF($V$37=1,Q39*$V$43/$G$48,Q39*$V$46/$G$48)
41	CaC2O4	=IF($V$37=1,M41*$V$43/$G$48,M41*$V$46/$G$48)		Ni(COOH)2	=IF($V$37=1,Q40*$V$43/$G$48,Q40*$V$46/$G$48)
42	Na2C2O4	=IF($V$37=1,M42*$V$43/$G$48,M42*$V$46/$G$48)		Ni(C2H3O3)2	=IF($V$37=1,Q41*$V$43/$G$48,Q41*$V$46/$G$48)
43	AlOOH	=IF($V$37=1,M43*$V$43/$G$48,M43*$V$46/$G$48)		Ni(NO3)2	=IF($V$37=1,Q42*$V$43/$G$48,Q42*$V$46/$G$48)
44	antifoam	=IF($V$37=1,M44*$V$43/$G$48,M44*$V$46/$G$48)		Pb(NO3)2	=IF($V$37=1,Q43*$V$43/$G$48,Q43*$V$46/$G$48)
45	tot insoluble	=SUM(Y7:Y44)		Pd(NO3)2	=IF($V$37=1,Q44*$V$43/$G$48,Q44*$V$46/$G$48)
46				Sr(COOH)2	=IF($V$37=1,Q45*$V$43/$G$48,Q45*$V$46/$G$48)
47				Sr(C2H3O3)2	=IF($V$37=1,Q46*$V$43/$G$48,Q46*$V$46/$G$48)
48				Sr(NO3)2	=IF($V$37=1,Q47*$V$43/$G$48,Q47*$V$46/$G$48)
49				UO2(COOH)2	=IF($V$37=1,Q48*$V$43/$G$48,Q48*$V$46/$G$48)
50				UO2(C2H3O3)2	=IF($V$37=1,Q49*$V$43/$G$48,Q49*$V$46/$G$48)
51				UO2(NO3)2	=IF($V$37=1,Q50*$V$43/$G$48,Q50*$V$46/$G$48)
52				La(COOH)3	=IF($V$37=1,Q51*$V$43/$G$48,Q51*$V$46/$G$48)
53				La(C2H2O3O3	=IF($V$37=1,Q52*$V$43/$G$48,Q52*$V$46/$G$48)
54				La(NO3)3	=IF($V$37=1,Q53*$V$43/$G$48,Q53*$V$46/$G$48)
55				Zn(COOH)2	=IF($V$37=1,Q54*$V$43/$G$48,Q54*$V$46/$G$48)
56				Zn(C2H3O3)2	=IF($V$37=1,Q55*$V$43/$G$48,Q55*$V$46/$G$48)
57				Zn(NO3)2	=IF($V$37=1,Q56*$V$43/$G$48,Q56*$V$46/$G$48)
58				Na2CO3	=IF($V$37=1,Q57*$V$43/$G$48,Q57*$V$46/$G$48)
59				Na2C2O4	=IF($V$37=1,Q58*$V$43/$G$48,Q58*$V$46/$G$48)
60				Na2SO4	=IF($V$37=1,Q59*$V$43/$G$48,Q59*$V$46/$G$48)
61				H4SiO4	=IF($V$37=1,Q60*$V$43/$G$48,Q60*$V$46/$G$48)
62				HCOOH	=IF($V$37=1,Q64*$V$43/$G$48,Q64*$V$46/$G$48)
63				C2H4O3	=IF($V$37=1,Q65*$V$43/$G$48,Q65*$V$46/$G$48)
64				total soluble	=SUM(AB7:AB63)
65				H2O	=IF($V$37=1,Q66*$V$43/$G$48,Q66*$V$46/$G$48)
66				total slurry	=Y45+AB64+AB65
67				total solid (wt%)	=(Y45+AB64-AB62)/AB66

	AD	AE	AF
3	**Table 20. Add Frit, HCOOH & coal.**		
4	Frit 803	wt%	lb/hr
5		(target)	(calc'd)
6	B2O3	8	=IF($AE$12<100,$V$47*AE6/$AE$12,IF($AE$12>100,$V$47*AE6/$AE$12,$V$47*AE6/100))
7	Li2O	6	=IF($AE$12<100,$V$47*AE7/$AE$12,IF($AE$12>100,$V$47*AE7/$AE$12,$V$47*AE7/100))
8	MgO	=0	=IF($AE$12<100,$V$47*AE8/$AE$12,IF($AE$12>100,$V$47*AE8/$AE$12,$V$47*AE8/100))
9	Na2O	8	=IF($AE$12<100,$V$47*AE9/$AE$12,IF($AE$12>100,$V$47*AE9/$AE$12,$V$47*AE9/100))
10	NaCOOH	0	=IF($AE$12<100,$V$47*AE10/$AE$12,IF($AE$12>100,$V$47*AE10/$AE$12,$V$47*AE10/100))
11	SiO2	=100-SUM(AE6:AE10)	=IF($AE$12<100,$V$47*AE11/$AE$12,IF($AE$12>100,$V$47*AE11/$AE$12,$V$47*AE11/100))
12	total	=SUM(AE6:AE11)	=SUM(AF6:AF11)
13			
14	HCOOH		=0*0.9/383*AF12
15	coal		=V38*V46/G48
16	strip effluent		0

	AD	AE	AF	AG	AH
47	**Table 21. SME product results:**				
48	target coal in SME prod (ppm) =		240		
49	ppm coal in SME prod =		=AI45/AL67*1000000		
50	cal'd SME product TS+NaOH		=(AI48+AL65-AL62-AL64)/AL67		
51	WL-adj'd SME product TS		=(AV48+AY65-AY62-AY64)/AY67		
52	measured TS in SME (wt%) =		='Smith SB9 SRAT-SME Data'IF56		
53	target TS in final feed				
54					
55	**Table 22. Na Balance (if V37=1):**				
56	actual frit (lb/hr) =				=AF69
57	calc'd WL (%) =				=(AO40-AH56)/AO40*100
58	calc'd insol Na2O (lb/hr) =				=Y20
59	target frit Na2O (lb/hr) =				=(V43/(1-V44/100)-V46)*AE9/100
60	insol Na in sldg (%) =				=IF(AH58>0,(AH58-AH59)/(AH58-AH59+G20*G49*(1-I20)*V43/G48)*100,"n/a")
61	Required CO3 (ppm) =				=T33/G43*1000/P96*12.011
62					
63	**Table 23. Frit Balance (if V37=1):**				
64		target	actual		% Diff
65	B2O3	=(V$43-V$46)*AE6/100	=AO30		=(AF65-AE65)/AE65*100
66	Li2O	=(V$43-V$46)*AE7/100	=AO31		=(AF66-AE66)/AE66*100
67	Na2O	=(V$43-V$46)*AE9/100	=AI20		=(AF67-AE67)/AE67*100
68	SiO2	=(V$43-V$46)*AE11/100	=Y19-Y7/L7*B7''Report Tables'IF35/'SB9-894B'IB19''SB9-894B'IF19		=(AF68-AE68)/AE68*100
69	total	=SUM(AE65:AE68)	=SUM(AF65:AF68)		=(AF69-AE69)/AE69*100

	AK	AL	AM	AN	AO	AP
76	**Table 24. SB9 Waste Loading Calculatons:**					
77	total glass (g) =					100
78	normalized Li2O b4 charge balance (g/100g glass) =					=G31/101.877*100
79	pre NaOH strike waste loading (wt%) =					=100-AP78/(AE7/100)
80	normalized Li2O after charge balance (g/100g glass) =					=G31/G40*100
81	pre NaOH strike waste loading 2 (wt%) =					=100-AP80/(AE7/100)
82	normalized Li2O after NaOH strike (g/100g glass) =					=AO31/AO40*AP77
83	post NaOH strike waste loading (wt%) =					=100-AP82/(AE7/100)
84	target waste loading (wt%) =					36
85	additional sludge required to meet target WL (fraction) =					=(AO40*(1-AP83/100)*AP84/100/(1-AP84/100)-AO40*AP83/100)/AO40/(AP83/100)
86	actual WL in adjusted glass (wt%) =					=100-BB31/BB40*100/(AE7/100)
87						
88	Adjust sludge flow to match target WL ? (If = 0, No)					1

	AH	AI	AJ	AK	AL
3	**Table 25. Melter Feed Flow @ 100% attainment**				
4	insoluble			soluble	
5	solids	lb/hr		solids	lb/hr
6					
7	Fe(OH)3	=Y7		Ca(COOH)2	=AB7
8	Al(OH)3	=Y8		Ca(C2H3O3)2	=AB8
9	MnO2	=Y9		Ca(NO3)2	=AB9
10	Ca(OH)2	=Y10		Fe(COOH)3	=AB10
11	Na2U2O7	=Y11		Fe(C2H3O3)3	=AB11
12	Mg(OH)2	=Y12		Fe(NO3)3	=AB12
13	HgO	=Y13		Al(COOH)3	=AB13
14	Ca3(PO4)2	=Y14		Al(C2H3O3)3	=AB14
15	Ni(OH)2	=Y15		Al(NO3)3	=AB15
16	Cr(OH)3	=Y16		CsCOOH	=AB16
17	Cu(OH)2	=Y17		CsC2H3O3	=AB17
18	TiO2	=Y18		CsNO3	=AB18
19	SiO2	=IF(V48=1,Y19+AF35/AF34*(AB66-Y44)*AE11/100,Y19+AF11)		Cu(COOH)2	=AB19
20	Na2O	=IF(V48=1,IF(AF25>7,Y20+AF35/AF34*(AB66-Y44)*AE9/100-AF14/P64/2*L20,Y20+AF35/AF34*(AB66-Y44)*AE9/100),IF(AF25>7,Y20+AF9-AF14/P64/2*L20,Y20+AF9))		Cu(C2H3O3)2	=AB20
21	ThO2	=Y21		Cu(NO3)2	=AB21
22	Zn(OH)2	=Y22		KCOOH	=AB22
23	PuO2	=Y23		KC2H3O3	=AB23
24	K2O	=Y24		KNO3	=AB24
25	RuO2	=Y25		Mg(COOH)2	=AB25
26	RhO2	=Y26		Mg(C2H3O3)2	=AB26
27	PdO	=Y27		Mg(NO3)2	=AB27
28	Cd(OH)2	=Y28		Mn(COOH)2	=AB28
29	Sr(OH)2	=Y29		Mn(C2H3O3)2	=AB29
30	B2O3	=IF(V48=1,Y30+AF35/AF34*(AB66-Y44)*AE6/100,Y30+AF6)		Mn(NO3)2	=AB30
31	Li2O	=IF(V48=1,Y31+AF35/AF34*(AB66-Y44)*AE7/100,Y31+AF7)		NH4COOH	=AB31
32	Cs2O	=Y32		NH4NO3	=AB32
33	BaSO4	=Y33		NaCl	=AB33
34	Sn(OH)2	=Y34		NaF	=AB34
35	PbSO4	=Y35		NaCOOH	=IF(AF25>7,AB35+AF14/P64*P35,AB35)
36	TcO2	=Y36		NaC2H3O3	=AB36
37	La(OH)3	=Y37		NaNO3	=AB37
38	ZrO2	=Y38		NaNO2	=AB38
39	CaCO3	=Y39		NaOH	=IF(V49=1,'Report Tables'!F224*(AI7/L7+AL10/P10+AL11/P11+AL12/P12)*B7/B20*(B20+15.9994+1.0079),0)
40	CaSO4	=Y40		Na3PO4	=AB40
41	CaC2O4	=Y41		Ni(COOH)2	=AB41
42	Na2C2O4	=Y42		Ni(C2H3O3)2	=AB42
43	AlOOH	=Y43		Ni(NO3)2	=AB43

	AH	AI	AJ	AK	AL
43	**Table 25. Melter Feed Flow @ 100% attainment**				
44	MgO	=IF(V48=1,AF35/AF34*(AB66-Y44)*AE8/100,AF8)		Pb(NO3)2	=AB44
45	Coal	=AF15		Pd(NO3)2	=AB45
46	antifoam	=IF(Q142=1,Y44,IF(Q142=0,Y44,IF(V37=1,Y44,Y44+AI7/L7*B7*Q125*(1-G132))))		Sr(COOH)2	=AB46
47	solvent-Isopar	0		Sr(C2H3O3)2	=AB47
48	total insoluble	=SUM(AI7:AI47)		Sr(NO3)2	=AB48
49				UO2(COOH)2	=AB49
50				UO2(C2H3O3)2	=AB50
51				UO2(NO3)2	=AB51
52				La(COOH)3	=AB52
53				La(C2H3O3)3	=AB53
54				La(NO3)3	=AB54
55				Zn(COOH)2	=AB55
56				Zn(C2H3O3)2	=AB56
57				Zn(NO3)2	=AB57
58				Na2CO3	=AB58
59				Na2C2O4	=AB59
60				Na2SO4	=AB60
61				H4SiO4	=AB61
62				HCOOH	=IF(AF25>7,AB62,AB62+AF14)
63				C2H4O3	=IF(V48=1,AB63+AF37/AF34*(AB66-Y44)*AF33/100,AB63)
64				HNO3	=IF(V48=1,AF36/AF34*(AB66-Y44)*AF32/100,0)
65				total soluble	=SUM(AL7:AL64)
66				H2O	=IF(V48=1,IF(AF25>7,AB65+AF14/P64/2*P66+AF38/AF34*(AB66-Y44)+AF36/AF34*(AB66-Y44)*(1-AF32/100)+AF37/AF34*(AB66-Y44)*(1-AF33/100)+AL68,AB65+AF38/AF34*(AB66-Y44)+AF36/AF34*(AB66-Y44)*(1-AF32/100)+AF37/AF34*(AB66-Y44)*(1-AF33/100)+AL68),IF(V49=1,AB65+AL39+AL68,IF(AF25>7,AB65+AF14/P64/2*P66+AL68,AB65+AL68)))
67				Total Slurry	=AI48+AL65+AL66

	AN	AO	AP	AQ	AR	AS
3	**Table 26. Confirm glass production**					
4	glass			glass		
5	oxides	lb/hr	lb mole/hr	oxides	mole %	wt%
6						
7	Fe2O3	=(AI7/$L7+AL11/$P11+AL10/$P10+AL12/$P12)/2*$F7*(1-$V44/100)	=AO7/$F7	Fe2O3	=AP7/$AP$40*100	=AO7/$AO$40*100
8	Al2O3	=(AI8/$L8+AI43/$L43+AL13/$P13+AL14/$P14+AL15/$P15)/2*$F8*(1-$V44/100)	=AO8/$F8	Al2O3	=AP8/$AP$40*100	=AO8/$AO$40*100
9	MnO	=(AI9/$L9+AL28/$P28+AL29/$P29+AL30/$P30)*$F9*(1-$V44/100)	=AO9/$F9	MnO	=AP9/$AP$40*100	=AO9/$AO$40*100
10	CaO	=(AI10/$L10+AI14/$L14*3+AI39/$L39+AI40/$L40+AI41/$L41+AL7/$P7+AL8/$P8+AL9/$P9)*$F10*(1-$V44/100)	=AO10/$F10	CaO	=AP10/$AP$40*100	=AO10/$AO$40*100
11	U3O8	=((AI11/$L11*2/3+(AL49/$P48+AL50/$P49+AL51/$P50)/3)*$F11)*(1-$V44/100)	=AO11/$F11	U3O8	=AP11/$AP$40*100	=AO11/$AO$40*100
12	MgO	=(AI12/$L12*$F12+AI44+(AL25/$P25+AL26/$P26+AL27/$P27)*$F12)*(1-$V44/100)	=AO12/$F12	MgO	=AP12/$AP$40*100	=AO12/$AO$40*100
13	HgO			HgO	=AP13/$AP$40*100	=AO13/$AO$40*100
14	P2O5	=(AI14/$L14+AL40/$P39/2)*$F14*(1-$V44/100)	=AO14/$F14	P2O5	=AP14/$AP$40*100	=AO14/$AO$40*100
15	NiO	=(AI15/$L15+AL41/$P40+AL42/$P41+AL43/$P42)*$F15*(1-$V44/100)	=AO15/$F15	NiO	=AP15/$AP$40*100	=AO15/$AO$40*100
16	Cr2O3	=AI16/$L16/2*$F16*(1-$V44/100)	=AO16/$F16	Cr2O3	=AP16/$AP$40*100	=AO16/$AO$40*100
17	CuO	=(AI17/$L17+AL19/$P19+AL20/$P20+AL21/$P21)*$F17*(1-$V44/100)	=AO17/$F17	CuO	=AP17/$AP$40*100	=AO17/$AO$40*100
18	TiO2	=AI18*(1-$V44/100)	=AO18/$F18	TiO2	=AP18/$AP$40*100	=AO18/$AO$40*100
19	SiO2	=(AI19+AI46/$G146*3*$L19+AL61/$P60*$L19)*(1-$V44/100)	=AO19/$F19	SiO2	=AP19/$AP$40*100	=AO19/$AO$40*100
20	Na2O	=(AI20+(AI11/$L11+(AL35/$P35+AL36/$P36+AL37/$P37+AL38/$P38)/2+AL39/($B20+15.9994+1.0079)/2+AL40/$P39*3/2+AL58/$P57+(AL59+AI42)/$P58+AL60/$P59)*$F20)*(1-$V44/100)	=AO20/$F20	Na2O	=AP20/$AP$40*100	=AO20/$AO$40*100
21	ThO2	=AI21/$L21*$F21*(1-$V44/100)	=AO21/$F21	ThO2	=AP21/$AP$40*100	=AO21/$AO$40*100
22	ZnO	=(AI22/$L22+AL55/$P54+AL56/$P55+AL57/$P56)*$F22*(1-$V44/100)	=AO22/$F22	ZnO	=AP22/$AP$40*100	=AO22/$AO$40*100
23	PuO2	=AI23/$L23*$F23*(1-$V44/100)	=AO23/$F23	PuO2	=AP23/$AP$40*100	=AO23/$AO$40*100
24	K2O	=((AI24/$L24+(AL22/$P22+AL23/$P23+AL24/$P24)/2)*$F24)*(1-$V44/100)	=AO24/$F24	K2O	=AP24/$AP$40*100	=AO24/$AO$40*100
25	RuO2	=AI25*(1-$V44/100)	=AO25/$F25	RuO2	=AP25/$AP$40*100	=AO25/$AO$40*100
26	RhO2	=AI26*(1-$V44/100)	=AO26/$F26	RhO2	=AP26/$AP$40*100	=AO26/$AO$40*100
27	PdO	=(AI27+AL45/$P44*$F27)*(1-$V44/100)	=AO27/$F27	PdO	=AP27/$AP$40*100	=AO27/$AO$40*100
28	CdO	=AI28/$L28*$F28*(1-$V44/100)	=AO28/$F28	CdO	=AP28/$AP$40*100	=AO28/$AO$40*100
29	SrO	=(AI29/$L29+AL46/$P45+AL47/$P46+AL48/$P47)*$F29*(1-$V44/100)	=AO29/$F29	SrO	=AP29/$AP$40*100	=AO29/$AO$40*100
30	B2O3	=AI30*(1-$V44/100)	=AO30/$F30	B2O3	=AP30/$AP$40*100	=AO30/$AO$40*100
31	Li2O	=AI31*(1-$V44/100)	=AO31/$F31	Li2O	=AP31/$AP$40*100	=AO31/$AO$40*100
32	Cs2O	=(AI32+(AL16/$P16+AL17/$P17+AL18/$P18)/2*$F32)*(1-$V44/100)	=AO32/$F32	Cs2O	=AP32/$AP$40*100	=AO32/$AO$40*100
33	BaO	=AI33/$L33*$F33*(1-$V44/100)	=AO33/$F31	BaO	=AP33/$AP$40*100	=AO33/$AO$40*100
34	SnO	=AI34/$L34/2*$F34*(1-$V44/100)	=AO34/$F34	SnO	=AP34/$AP$40*100	=AO34/$AO$40*100
35	PbO	=(AI35/$L35+AL44/$P43)*$F35*(1-$V44/100)	=AO35/$F35	PbO	=AP35/$AP$40*100	=AO35/$AO$40*100
36	TcO2	=AI36*(1-$V44/100)	=AO36/$F36	TcO2	=AP36/$AP$40*100	=AO36/$AO$40*100
37	La2O3	=(AI37/$L37+AL52/$P51+AL53/$P52+AL54/$P53)/2*$F37*(1-$V44/100)	=AO37/$F37	La2O3	=AP37/$AP$40*100	=AO37/$AO$40*100
38	ZrO2	=AI38*(1-$V44/100)	=AO38/$F38	ZrO2	=AP38/$AP$40*100	=AO38/$AO$40*100
39	SO3	=(AI33/$L33+AI35/$L35+AI40/$L40+AL60/$P59)*$F39*(1-$V44/100)	=AO39/$F39	SO3	=AP39/$AP$40*100	=AO39/$AO$40*100
40	Total	=SUM(AO7:AO39)	=SUM(AP7:AP39)	Total	=SUM(AR7:AR39)	=SUM(AS7:AS39)
41	Δ from target	=IF($V49=1,0,(AO40-$V43)/$V43)				

	AU	AV	AW	AX	AY
3	**Table 27. WL-Adjusted Melter Feed Flow @ 100% attainment**				
4	insoluble			soluble	
5	solids	lb/hr		solids	lb/hr
6					
7	Fe(OH)3	=AI7*(1+AP$85)		Ca(COOH)2	=AL7*(1+AP$85)
8	Al(OH)3	=AI8*(1+AP$85)		Ca(C2H3O3)2	=AL8*(1+AP$85)
9	MnO2	=AI9*(1+AP$85)		Ca(NO3)2	=AL9*(1+AP$85)
10	Ca(OH)2	=AI10*(1+AP$85)		Fe(COOH)3	=AL10*(1+AP$85)
11	Na2U2O7	=AI11*(1+AP$85)		Fe(C2H3O3)3	=AL11*(1+AP$85)
12	Mg(OH)2	=AI12*(1+AP$85)		Fe(NO3)3	=AL12*(1+AP$85)
13	HgO	=AI13*(1+AP$85)		Al(COOH)3	=AL13*(1+AP$85)
14	Ca3(PO4)2	=AI14*(1+AP$85)		Al(C2H3O3)3	=AL14*(1+AP$85)
15	Ni(OH)2	=AI15*(1+AP$85)		Al(NO3)3	=AL15*(1+AP$85)
16	Cr(OH)3	=AI16*(1+AP$85)		CsCOOH	=AL16*(1+AP$85)
17	Cu(OH)2	=AI17*(1+AP$85)		CsC2H3O3	=AL17*(1+AP$85)
18	TiO2	=AI18*(1+AP$85)		CsNO3	=AL18*(1+AP$85)
19	SiO2	=IF(V48=1,(Y19+AF35/AF34*(AB66-Y44)*AE11/100-AV31/AE7*AE11)*(1+AP85)+AV31/AE7*AE11,(Y19+AF11-AV31/AE7*AE11)*(1+AP85)+AV31/AE7*AE11)		Cu(COOH)2	=AL19*(1+AP$85)
20	Na2O	=(AI20-AI31/AE7*AE9)*(1+AP$85)+AI31/AE7*AE9		Cu(C2H3O3)2	=AL20*(1+AP$85)
21	ThO2	=AI21*(1+AP$85)		Cu(NO3)2	=AL21*(1+AP$85)
22	Zn(OH)2	=AI22*(1+AP$85)		KCOOH	=AL22*(1+AP$85)
23	PuO2	=AI23*(1+AP$85)		KC2H3O3	=AL23*(1+AP$85)
24	K2O	=AI24*(1+AP$85)		KNO3	=AL24*(1+AP$85)
25	RuO2	=AI25*(1+AP$85)		Mg(COOH)2	=AL25*(1+AP$85)
26	RhO2	=AI26*(1+AP$85)		Mg(C2H3O3)2	=AL26*(1+AP$85)
27	PdO	=AI27*(1+AP$85)		Mg(NO3)2	=AL27*(1+AP$85)
28	Cd(OH)2	=AI28*(1+AP$85)		Mn(COOH)2	=AL28*(1+AP$85)
29	Sr(OH)2	=AI29*(1+AP$85)		Mn(C2H3O3)2	=AL29*(1+AP$85)
30	B2O3	=AI30		Mn(NO3)2	=AL30*(1+AP$85)
31	Li2O	=AI31		NH4COOH	=AL31*(1+AP$85)
32	Cs2O	=AI32*(1+AP$85)		NH4NO3	=AL32*(1+AP$85)
33	BaSO4	=AI33*(1+AP$85)		NaCl	=AL33*(1+AP$85)
34	Sn(OH)2	=AI34*(1+AP$85)		NaF	=AL34*(1+AP$85)
35	PbSO4	=AI35*(1+AP$85)		NaCOOH	=AL35*(1+AP$85)
36	TcO2	=AI36*(1+AP$85)		NaC2H3O3	=AL36*(1+AP$85)
37	La(OH)3	=AI37*(1+AP$85)		NaNO3	=AL37*(1+AP$85)
38	ZrO2	=AI38*(1+AP$85)		NaNO2	=AL38*(1+AP$85)
39	CaCO3	=AI39*(1+AP$85)		NaOH	=AL39*(1+AP$85)
40	CaSO4	=AI40*(1+AP$85)		Na3PO4	=AL40*(1+AP$85)
41	CaC2O4	=AI41*(1+AP$85)		Ni(COOH)2	=AL41*(1+AP$85)
42	Na2C2O4	=AI42*(1+AP$85)		Ni(C2H3O3)2	=AL42*(1+AP$85)
43	AlOOH	=AI43*(1+AP$85)		Ni(NO3)2	=AL43*(1+AP$85)
44	MgO	=AI44*(1+AP$85)		Pb(NO3)2	=AL44*(1+AP$85)
45	Coal	=AI45		Pd(NO3)2	=AL45*(1+AP$85)
46	antifoam	=AI46		Sr(COOH)2	=AL46*(1+AP$85)
47	solvent-Isopar	=AI47		Sr(C2H3O3)2	=AL47*(1+AP$85)
48	total insoluble	=SUM(AV7:AV47)		Sr(NO3)2	=AL48*(1+AP$85)

	AU	AV	AW	AX	AY
48	**Table 27. WL-Adjusted Melter Feed Flow @ 100% attainment (Continued)**				
49				UO2(COOH)2	=AL49*(1+AP$85)
50				UO2(C2H3O3)2	=AL50*(1+AP$85)
51				UO2(NO3)2	=AL51*(1+AP$85)
52				La(COOH)3	=AL52*(1+AP$85)
53				La(C2H3O3)3	=AL53*(1+AP$85)
54				La(NO3)3	=AL54*(1+AP$85)
55				Zn(COOH)2	=AL55*(1+AP$85)
56				Zn(C2H3O3)2	=AL56*(1+AP$85)
57				Zn(NO3)2	=AL57*(1+AP$85)
58				Na2CO3	=AL58*(1+AP$85)
59				Na2C2O4	=AL59*(1+AP$85)
60				Na2SO4	=AL60*(1+AP$85)
61				H4SiO4	=AL61*(1+AP$85)
62				HCOOH	=AL62
63				C2H4O3	=AL63
64				HNO3	=AL64
65				total soluble	=SUM(AY7:AY64)
66				H2O	=AL66
67				Total Slurry	=AV48+AY65+AY66

	BA	BB	BC
3	**Table 29. Confirm glass production**		
4	glass		
5	oxides	lb/hr	lb mole/hr
6			
7	Fe2O3	=(AV7/$L7+AY11/$P11+AY10/$P10+AY12/$P12)/2*$F7*(1-$V44/100)	=BB7/$F7
8	Al2O3	=(AV8/$L8+AV43/$L43+AY13/$P13+AY14/$P14+AY15/$P15)/2*$F8*(1-$V44/100)	=BB8/$F8
9	MnO	=(AV9/$L9+AY28/$P28+AY29/$P29+AY30/$P30)*$F9*(1-$V44/100)	=BB9/$F9
10	CaO	=(AV10/$L10+AV14/$L14*3+AV39/$L39+AV40/$L40+AV41/$L41+AY7/$P7+AY8/$P8+AY9/$P9)*$F10*(1-$V44/100)	=BB10/$F10
11	U3O8	=((AV11/$L11*2/3+(AY49/$P48+AY50/$P49+AY51/$P50)/3)*$F11)*(1-$V44/100)	=BB11/$F11
12	MgO	=(AV12/$L12*$F12+AV44+(AY25/$P25+AY26/$P26+AY27/$P27)*$F12)*(1-$V44/100)	=BB12/$F12
13	HgO		
14	P2O5	=(AV14/$L14+AY40/$P39/2)*$F14*(1-$V44/100)	=BB14/$F14
15	NiO	=(AV15/$L15+AY41/$P40+AY42/$P41+AY43/$P42)*$F15*(1-$V44/100)	=BB15/$F15
16	Cr2O3	=AV16/$L16/2*$F16*(1-$V44/100)	=BB16/$F16
17	CuO	=(AV17/$L17+AY19/$P19+AY20/$P20+AY21/$P21)*$F17*(1-$V44/100)	=BB17/$F17
18	TiO2	=AV18*(1-$V44/100)	=BB18/$F18
19	SiO2	=(AV19+AV46/$G146*3*$L19+AY61/$P60*$L19)*(1-$V44/100)	=BB19/$F19
20	Na2O	=(AV20+(AV11/$L11+(AY35/$P35+AY36/$P36+AY37/$P37+AY38/$P38)/2+AY39/($B20+15.9994+1.0079)/2+AY40/$P39*3/2+AY58/$P57+(AY59+AV42)/$P58+AY60/$P59)*$F20)*(1-$V44/100)	=BB20/$F20
21	ThO2	=AV21/$L21*$F21*(1-$V44/100)	=BB21/$F21
22	ZnO	=(AV22/$L22+AY55/$P54+AY56/$P55+AY57/$P56)*$F22*(1-$V44/100)	=BB22/$F22
23	PuO2	=AV23/$L23*$F23*(1-$V44/100)	=BB23/$F23
24	K2O	=((AV24/$L24+(AY22/$P22+AY23/$P23+AY24/$P24)/2)*$F24)*(1-$V44/100)	=BB24/$F24
25	RuO2	=AV25*(1-$V44/100)	=BB25/$F25
26	RhO2	=AV26*(1-$V44/100)	=BB26/$F26
27	PdO	=(AV27+AY45/$P44*$F27)*(1-$V44/100)	=BB27/$F27
28	CdO	=AV28/$L28*$F28*(1-$V44/100)	=BB28/$F28
29	SrO	=(AV29/$L29+AY46/$P45+AY47/$P46+AY48/$P47)*$F29*(1-$V44/100)	=BB29/$F29
30	B2O3	=AV30*(1-$V44/100)	=BB30/$F30
31	Li2O	=AV31*(1-$V44/100)	=BB31/$F31
32	Cs2O	=(AV32+(AY16/$P16+AY17/$P17+AY18/$P18)/2*$F32)*(1-$V44/100)	=BB32/$F32
33	BaO	=AV33/$L33*$F33*(1-$V44/100)	=BB33/$F31
34	SnO	=AV34/$L34/2*$F34*(1-$V44/100)	=BB34/$F34
35	PbO	=(AV35/$L35+AY44/$P43)*$F35*(1-$V44/100)	=BB35/$F35
36	TcO2	=AV36*(1-$V44/100)	=BB36/$F36
37	La2O3	=(AV37/$L37+AY52/$P51+AY53/$P52+AY54/$P53)/2*$F37*(1-$V44/100)	=BB37/$F37
38	ZrO2	=AV38*(1-$V44/100)	=BB38/$F38
39	SO3	=(AV33/$L33+AV35/$L35+AV40/$L40+AY60/$P59)*$F39*(1-$V44/100)	=BB39/$F39
40	Total	=SUM(BB7:BB39)	=SUM(BC7:BC39)
41	Δ from target	=IF($V49=1,0,(BB40-$V43)/$V43)	

	BE	BF	BG	BH	BI
3	**Table 30. SB9 Baseline Melter Feed Component Flows at**				**=BH1**
4	insoluble			soluble	
5	solids	lb/hr		solids	lb/hr
6					
7	Fe(OH)3	=AI7*BH$1/ccinput_SB9-BaseID$7		Ca(COOH)2	=AL7*BH$1/ccinput_SB9SMESID$7
8	Al(OH)3	=AI8*BH$1/ccinput_SB9SMESID$7		Ca(C2H3O3)2	=AL8*BH$1/ccinput_SB9SMESID$7
9	MnO2	=AI9*BH$1/ccinput_SB9SMESID$7		Ca(NO3)2	=AL9*BH$1/ccinput_SB9SMESID$7
10	Ca(OH)2	=AI10*BH$1/ccinput_SB9SMESID$7		Fe(COOH)3	=AL10*BH$1/ccinput_SB9SMESID$7
11	Na2U2O7	=AI11*BH$1/ccinput_SB9SMESID$7		Fe(C2H3O3)3	=AL11*BH$1/ccinput_SB9SMESID$7
12	Mg(OH)2	=AI12*BH$1/ccinput_SB9SMESID$7		Fe(NO3)3	=AL12*BH$1/ccinput_SB9SMESID$7
13	HgO	=AI13*BH$1/ccinput_SB9SMESID$7		Al(COOH)3	=AL13*BH$1/ccinput_SB9SMESID$7
14	Ca3(PO4)2	=AI14*BH$1/ccinput_SB9SMESID$7		Al(C2H3O3)3	=AL14*BH$1/ccinput_SB9SMESID$7
15	Ni(OH)2	=AI15*BH$1/ccinput_SB9SMESID$7		Al(NO3)3	=AL15*BH$1/ccinput_SB9SMESID$7
16	Cr(OH)3	=AI16*BH$1/ccinput_SB9SMESID$7		CsCOOH	=AL16*BH$1/ccinput_SB9SMESID$7
17	Cu(OH)2	=AI17*BH$1/ccinput_SB9SMESID$7		CsC2H3O3	=AL17*BH$1/ccinput_SB9SMESID$7
18	TiO2	=AI18*BH$1/ccinput_SB9SMESID$7		CsNO3	=AL18*BH$1/ccinput_SB9SMESID$7
19	SiO2	=AI19*BH$1/ccinput_SB9SMESID$7		Cu(COOH)2	=AL19*BH$1/ccinput_SB9SMESID$7
20	Na2O	=AI20*BH$1/ccinput_SB9SMESID$7		Cu(C2H3O3)2	=AL20*BH$1/ccinput_SB9SMESID$7
21	ThO2	=AI21*BH$1/ccinput_SB9SMESID$7		Cu(NO3)2	=AL21*BH$1/ccinput_SB9SMESID$7
22	Zn(OH)2	=AI22*BH$1/ccinput_SB9SMESID$7		KCOOH	=AL22*BH$1/ccinput_SB9SMESID$7
23	PuO2	=AI23*BH$1/ccinput_SB9SMESID$7		KC2H3O3	=AL23*BH$1/ccinput_SB9SMESID$7
24	K2O	=AI24*BH$1/ccinput_SB9SMESID$7		KNO3	=AL24*BH$1/ccinput_SB9SMESID$7
25	RuO2	=AI25*BH$1/ccinput_SB9SMESID$7		Mg(COOH)2	=AL25*BH$1/ccinput_SB9SMESID$7
26	RhO2	=AI26*BH$1/ccinput_SB9SMESID$7		Mg(C2H3O3)2	=AL26*BH$1/ccinput_SB9SMESID$7
27	PdO	=AI27*BH$1/ccinput_SB9SMESID$7		Mg(NO3)2	=AL27*BH$1/ccinput_SB9SMESID$7
28	Cd(OH)2	=AI28*BH$1/ccinput_SB9SMESID$7		Mn(COOH)2	=AL28*BH$1/ccinput_SB9SMESID$7
29	Sr(OH)2	=AI29*BH$1/ccinput_SB9SMESID$7		Mn(C2H3O3)2	=AL29*BH$1/ccinput_SB9SMESID$7
30	B2O3	=AI30*BH$1/ccinput_SB9SMESID$7		Mn(NO3)2	=AL30*BH$1/ccinput_SB9SMESID$7
31	Li2O	=AI31*BH$1/ccinput_SB9SMESID$7		NH4COOH	=AL31*BH$1/ccinput_SB9SMESID$7
32	Cs2O	=AI32*BH$1/ccinput_SB9SMESID$7		NH4NO3	=AL32*BH$1/ccinput_SB9SMESID$7
33	BaSO4	=AI33*BH$1/ccinput_SB9SMESID$7		NaCl	=AL33*BH$1/ccinput_SB9SMESID$7
34	Sn(OH)2	=AI34*BH$1/ccinput_SB9SMESID$7		NaF	=AL34*BH$1/ccinput_SB9SMESID$7
35	PbSO4	=AI35*BH$1/ccinput_SB9SMESID$7		NaCOOH	=AL35*BH$1/ccinput_SB9SMESID$7
36	TcO2	=AI36*BH$1/ccinput_SB9SMESID$7		NaC2H3O3	=AL36*BH$1/ccinput_SB9SMESID$7
37	La(OH)3	=AI37*BH$1/ccinput_SB9SMESID$7		NaNO3	=AL37*BH$1/ccinput_SB9SMESID$7
38	ZrO2	=AI38*BH$1/ccinput_SB9SMESID$7		NaNO2	=AL38*BH$1/ccinput_SB9SMESID$7
39	CaCO3	=AI39*BH$1/ccinput_SB9SMESID$7		NaOH	=AL39*BH$1/ccinput_SB9SMESID$7
40	CaSO4	=AI40*BH$1/ccinput_SB9SMESID$7		Na3PO4	=AL40*BH$1/ccinput_SB9SMESID$7
41	CaC2O4	=AI41*BH$1/ccinput_SB9SMESID$7		Ni(COOH)2	=AL41*BH$1/ccinput_SB9SMESID$7
42	Na2C2O4	=AI42*BH$1/ccinput_SB9SMESID$7		Ni(C2H3O3)2	=AL42*BH$1/ccinput_SB9SMESID$7
43	AlOOH	=AI43*BH$1/ccinput_SB9SMESID$7		Ni(NO3)2	=AL43*BH$1/ccinput_SB9SMESID$7
44	MgO	=AI44*BH$1/ccinput_SB9SMESID$7		Pb(NO3)2	=AL44*BH$1/ccinput_SB9SMESID$7
45	Coal	=AI45*BH$1/ccinput_SB9SMESID$7		Pd(NO3)2	=AL45*BH$1/ccinput_SB9SMESID$7
46	antifoam	=AI46*BH$1/ccinput_SB9SMESID$7		Sr(COOH)2	=AL46*BH$1/ccinput_SB9SMESID$7
47	Total_1	=SUM(BF7:BF46)		Sr(C2H3O3)2	=AL47*BH$1/ccinput_SB9SMESID$7

	BF	BG	BH	BI
47	**Table 30. SB9 Baseline Melter Feed Component Flows at**			
48			Sr(NO3)2	=AL48*BH$1/ccinput_SB9SMESID$7
49			UO2(COOH)2	=AL49*BH$1/ccinput_SB9SMESID$7
50			UO2(C2H3O3)2	=AL50*BH$1/ccinput_SB9SMESID$7
51			UO2(NO3)2	=AL51*BH$1/ccinput_SB9SMESID$7
52			La(COOH)3	=AL52*BH$1/ccinput_SB9SMESID$7
53			La(C2H3O3)3	=AL53*BH$1/ccinput_SB9SMESID$7
54			La(NO3)3	=AL54*BH$1/ccinput_SB9SMESID$7
55			Zn(COOH)2	=AL55*BH$1/ccinput_SB9SMESID$7
56			Zn(C2H3O3)2	=AL56*BH$1/ccinput_SB9SMESID$7
57			Zn(NO3)2	=AL57*BH$1/ccinput_SB9SMESID$7
58			Na2CO3	=AL58*BH$1/ccinput_SB9SMESID$7
59			Na2C2O4	=AL59*BH$1/ccinput_SB9SMESID$7
60			Na2SO4	=AL60*BH$1/ccinput_SB9SMESID$7
61			H4SiO4	=AL61*BH$1/ccinput_SB9SMESID$7
62			HCOOH	=AL62*BH$1/ccinput_SB9SMESID$7
63			C2H4O3	=AL63*BH$1/ccinput_SB9SMESID$7
64			HNO3	=AL64*BH$1/ccinput_SB9SMESID$7
65			total soluble	=SUM(BI7:BI64)
66			H2O	=AL66*BH$1/ccinput_SB9SMESID$7
67			Total Slurry	=BF47+BI65+BI66

11.0 Appendix D

**Printout of Formulas for
Developing Cold Cap Model Input Vector**

	A	B	C	D	E
3	**Table 0. Melt Rate Case:**			**='SB9-17'!M2**	actual data
4	instantaneous feed rate (lb/hr) =			=IF('SB9-17'!AP88=0,'SB9-17'!AL67,'SB9-17'!AY67)	
5	total solids (wt%) =			=IF('SB9-17'!AP88=0,('SB9-17'!AL67-'SB9-17'!AL66-'SB9-17'!AL62-'SB9-17'!AL63-'SB9-17'!AL64)/'SB9-17'!AL67,('SB9-17'!AY67-'SB9-17'!AY66-'SB9-17'!AY62-'SB9-17'!AY63-'SB9-17'!AY64)/'SB9-17'!AY67)	n/a
6	estimated density of SME product =			=0.00011*(D5*100)^2+0.0032*(D5*100)+1	n/a
7	volumetric feed rate (gpm) =			=IF(E6="n/a",D4*453.6/3.7854/1000/D6/60,D4*453.6/3.7854/1000/E6/60)	
8	calc'd % calcination SME product =			=IF('SB9-17'!AP88=0,'SB9-17'!AO40/('SB9-17'!AL67-'SB9-17'!AL66-'SB9-17'!AL63-'SB9-17'!AL62-'SB9-17'!AL64),'SB9-17'!BB40/('SB9-17'!AY67-'SB9-17'!AY66-'SB9-17'!AY63-'SB9-17'!AY62-'SB9-17'!AY64))	n/a
9	average glass prod rate (lb/hr) =			=IF('SB9-17'!AP88=0,'SB9-17'!AO40,'SB9-17'!BB40)	
10	calcine gases (lb/hr) =			=D4*D5*(1-D8)	=D10/D7*1.5

	A	B	C
11	**Table 1. Formates/Nitrates in Melter Feed**		
12	Component	MW	lb/hr
13			
14	Ca(COOH)2	='SB9-17'!P7	=IF('SB9-17'!AP$88=0,'SB9-17'!AL7,'SB9-17'!AY7)
15	Ca(C2H3O3)2	='SB9-17'!P8	=IF('SB9-17'!AP$88=0,'SB9-17'!AL8,'SB9-17'!AY8)
16	Ca(NO3)2	='SB9-17'!P9	=IF('SB9-17'!AP$88=0,'SB9-17'!AL9,'SB9-17'!AY9)
17	Fe(COOH)3	='SB9-17'!P10	=IF('SB9-17'!AP$88=0,'SB9-17'!AL10,'SB9-17'!AY10)
18	Fe(C2H3O3)3	='SB9-17'!P11	=IF('SB9-17'!AP$88=0,'SB9-17'!AL11,'SB9-17'!AY11)
19	Fe(NO3)3	='SB9-17'!P12	=IF('SB9-17'!AP$88=0,'SB9-17'!AL12,'SB9-17'!AY12)
20	Al(COOH)3	='SB9-17'!P13	=IF('SB9-17'!AP$88=0,'SB9-17'!AL13,'SB9-17'!AY13)
21	Al(C2H3O3)3	='SB9-17'!P14	=IF('SB9-17'!AP$88=0,'SB9-17'!AL14,'SB9-17'!AY14)
22	Al(NO3)3	='SB9-17'!P15	=IF('SB9-17'!AP$88=0,'SB9-17'!AL15,'SB9-17'!AY15)
23	CsCOOH	='SB9-17'!P16	=IF('SB9-17'!AP$88=0,'SB9-17'!AL16,'SB9-17'!AY16)
24	CsC2H3O3	='SB9-17'!P17	=IF('SB9-17'!AP$88=0,'SB9-17'!AL17,'SB9-17'!AY17)
25	CsNO3	='SB9-17'!P18	=IF('SB9-17'!AP$88=0,'SB9-17'!AL18,'SB9-17'!AY18)
26	Cu(COOH)2	='SB9-17'!P19	=IF('SB9-17'!AP$88=0,'SB9-17'!AL19,'SB9-17'!AY19)
27	Cu(C2H3O3)2	='SB9-17'!P20	=IF('SB9-17'!AP$88=0,'SB9-17'!AL20,'SB9-17'!AY20)
28	Cu(NO3)2	='SB9-17'!P21	=IF('SB9-17'!AP$88=0,'SB9-17'!AL21,'SB9-17'!AY21)
29	KCOOH	='SB9-17'!P22	=IF('SB9-17'!AP$88=0,'SB9-17'!AL22,'SB9-17'!AY22)
30	KC2H3O3	='SB9-17'!P23	=IF('SB9-17'!AP$88=0,'SB9-17'!AL23,'SB9-17'!AY23)
31	KNO3	='SB9-17'!P24	=IF('SB9-17'!AP$88=0,'SB9-17'!AL24,'SB9-17'!AY24)
32	Mg(COOH)2	='SB9-17'!P25	=IF('SB9-17'!AP$88=0,'SB9-17'!AL25,'SB9-17'!AY25)
33	Mg(C2H3O3)2	='SB9-17'!P26	=IF('SB9-17'!AP$88=0,'SB9-17'!AL26,'SB9-17'!AY26)
34	Mg(NO3)2	='SB9-17'!P27	=IF('SB9-17'!AP$88=0,'SB9-17'!AL27,'SB9-17'!AY27)
35	Mn(COOH)2	='SB9-17'!P28	=IF('SB9-17'!AP$88=0,'SB9-17'!AL28,'SB9-17'!AY28)
36	Mn(C2H3O3)2	='SB9-17'!P29	=IF('SB9-17'!AP$88=0,'SB9-17'!AL29,'SB9-17'!AY29)
37	Mn(NO3)2	='SB9-17'!P30	=IF('SB9-17'!AP$88=0,'SB9-17'!AL30,'SB9-17'!AY30)
38	NH4COOH	='SB9-17'!P31	=IF('SB9-17'!AP$88=0,'SB9-17'!AL31,'SB9-17'!AY31)
39	NH4NO3	='SB9-17'!P32	=IF('SB9-17'!AP$88=0,'SB9-17'!AL32,'SB9-17'!AY32)
40	NaCOOH	='SB9-17'!P35	=IF('SB9-17'!AP$88=0,'SB9-17'!AL35,'SB9-17'!AY35)
41	NaC2H3O3	='SB9-17'!P36	=IF('SB9-17'!AP$88=0,'SB9-17'!AL36,'SB9-17'!AY36)
42	NaNO3	='SB9-17'!P37	=IF('SB9-17'!AP$88=0,'SB9-17'!AL37,'SB9-17'!AY37)
43	NaNO2	='SB9-17'!P38	=IF('SB9-17'!AP$88=0,'SB9-17'!AL38,'SB9-17'!AY38)
44	Ni(COOH)2	='SB9-17'!P40	=IF('SB9-17'!AP$88=0,'SB9-17'!AL41,'SB9-17'!AY41)
45	Ni(C2H3O3)2	='SB9-17'!P41	=IF('SB9-17'!AP$88=0,'SB9-17'!AL42,'SB9-17'!AY42)
46	Ni(NO3)2	='SB9-17'!P42	=IF('SB9-17'!AP$88=0,'SB9-17'!AL43,'SB9-17'!AY43)
47	Pb(NO3)2	='SB9-17'!P43	=IF('SB9-17'!AP$88=0,'SB9-17'!AL44,'SB9-17'!AY44)
48	Pd(NO3)2	='SB9-17'!P44	=IF('SB9-17'!AP$88=0,'SB9-17'!AL45,'SB9-17'!AY45)
49	Sr(COOH)2	='SB9-17'!P45	=IF('SB9-17'!AP$88=0,'SB9-17'!AL46,'SB9-17'!AY46)
50	Sr(C2H3O3)2	='SB9-17'!P46	=IF('SB9-17'!AP$88=0,'SB9-17'!AL47,'SB9-17'!AY47)
51	Sr(NO3)2	='SB9-17'!P47	=IF('SB9-17'!AP$88=0,'SB9-17'!AL48,'SB9-17'!AY48)
52	UO2(COOH)2	='SB9-17'!P48	=IF('SB9-17'!AP$88=0,'SB9-17'!AL49,'SB9-17'!AY49)
53	UO2(C2H3O3)2	='SB9-17'!P49	=IF('SB9-17'!AP$88=0,'SB9-17'!AL50,'SB9-17'!AY50)
54	UO2(NO3)2	='SB9-17'!P50	=IF('SB9-17'!AP$88=0,'SB9-17'!AL51,'SB9-17'!AY51)
55	La(COOH)3	='SB9-17'!P51	=IF('SB9-17'!AP$88=0,'SB9-17'!AL52,'SB9-17'!AY52)
56	La(C2H3O3)3	='SB9-17'!P52	=IF('SB9-17'!AP$88=0,'SB9-17'!AL53,'SB9-17'!AY53)
57	La(NO3)3	='SB9-17'!P53	=IF('SB9-17'!AP$88=0,'SB9-17'!AL54,'SB9-17'!AY54)
58	Zn(COOH)2	='SB9-17'!P54	=IF('SB9-17'!AP$88=0,'SB9-17'!AL55,'SB9-17'!AY55)
59	Zn(C2H3O3)2	='SB9-17'!P55	=IF('SB9-17'!AP$88=0,'SB9-17'!AL56,'SB9-17'!AY56)
60	Zn(NO3)2	='SB9-17'!P56	=IF('SB9-17'!AP$88=0,'SB9-17'!AL57,'SB9-17'!AY57)
61	Total (lb/hr)		=SUM(C14:C60)
62	**anions (ppm) inc. free acids**		
63	Tom White's IC data (ppm)		
64	D (%)		
65	F+2G-N, M	=(D61/'SB9-17'!P89+2*G61/'SB9-17'!P90-E61/'SB9-17'!P87)*453.6/(D7*3.7854*60)	

	D	E	F	G
11	**Table 1. Formates/Nitrates in Melter Feed (Continued)**			
12	COOH-, pph	NO3-/NO2-, pph		C2H3O3-, pph
13				
14	=C14/B14*2*J$6			
15				=C15/B15*2*J$7
16		=C16/B16*2*J$4		
17	=C17/B17*3*J$6			
18				=C18/B18*3*J$7
19		=C19/B19*3*J$4		
20	=C20/B20*3*J$6			
21				=C21/B21*3*J$7
22		=C22/B22*3*J$4		
23	=C23/B23*J$6			
24				=C24/B24*J$7
25		=C25/B25*J$4		
26	=C26/B26*2*J$6			
27				=C27/B27*2*J$7
28		=C28/B28*2*J$4		
29	=C29/B29*J$6			
30				=C30/B30*J$7
31		=C31/B31*J$4		
32	=C32/B32*2*J$6			
33				=C33/B33*2*J$7
34		=C34/B34*2*J$4		
35	=C35/B35*2*J$6			
36				=C36/B36*2*J$7
37		=C37/B37*2*J$4		
38	=C38/B38*J$6			
39		=C39/B39*J$4		
40	=C40/B40*J$6			
41				=C41/B41*J$7
42		=C42/B42*J$4		
43		=C43/B43*J$5		
44	=C44/B44*2*J$6			
45				=C45/B45*2*J$7
46		=C46/B46*2*J$4		
47		=C47/B47*2*J$4		
48		=C48/B48*2*J$4		
49	=C49/B49*2*J$6			
50				=C50/B50*2*J$7
51		=C51/B51*2*J$4		
52	=C52/B52*2*J$6			
53				=C53/B53*2*J$7
54		=C54/B54*2*J$4		
55	=C55/B55*3*J$6			
56				=C56/B56*3*J$7
57		=C57/B57*3*J$4		
58	=C58/B58*2*J$6			
59				=C59/B59*2*J$7
60		=C60/B60*2*J$4		
61	=SUM(D14:D60)	=SUM(E14:E60)		=SUM(G14:G60)
62	=(D61+C108/B108*J6)/I102*1000000	=(E61+C109/B109*J4)/I102*1000000		=(G61+C101/B101*J7)/I102*1000000
63	n/a	n/a		n/a
64	=IF(D63="n/a","n/a",(D62-D63)/D63)	=IF(E63="n/a","n/a",(E62-E63)/E63)		=IF(G63="n/a","n/a",(G62-G63)/G63)
65	F+2G-3N, M	=(D61/'SB9-17'!P89+2*G61/'SB9-17'!P90-3*E61/'SB9-17'!P87)*453.6/(D7*3.7854*60)		

	I	J	K	L	M	N	O
11	**Table 2. Species produced from Formate/Nitrate/Glycolate Decomposition**						
12	Oxides	MW		gmole/hr	lb/hr		
13							
14	CaO	56.0774		=(C14/B14+C15/B15+C16/B16)*453.6	=L14*J14/453.6		
15							
16							
17	Fe2O3	159.6922		=(C17/B17+C18/B18+C19/B19)/2*453.6	=L17*J17/453.6		
18							
19							
20	Al2O3	101.9612		=(C20/B20+C21/B21+C22/B22)/2*453.6	=L20*J20/453.6		
21							
22							
23	Cs2O	281.8094		=(C23/B23+C24/B24+C25/B25)/2*453.6	=L23*J23/453.6		
24							
25							
26	CuO	79.5454		=(C26/B26+C27/B27+C28/B28)*453.6	=L26*J26/453.6		
27							
28							
29	K2O	94.196		=(C29/B29+C30/B30+C31/B31)/2*453.6	=L29*J29/453.6		
30							

	P	Q	R	S
11	**Table 2. Species produced from Formate/Nitrate/Glycolate Decomposition (Continued)**			
12	Gases	MW	gmole/hr	lb/hr
13				
14	CO	28.0107	=(C14/B14+C15/B15*3+C17/B17/2*3+C18/B18/2*9+C20/B20/2*3+C21/B21/2*9+C23/B23/2+C24/B24/2*3+C26/B26+C27/B27*3+C29/B29/2+C30/B30/2*3+C32/B32+C33/B33*3+C35/B35+C36/B36*3+C40/B40/2+C41/B41/2*3+C44/B44+C45/B45*3+C49/B49+C50/B50*3+C52/B52+C53/B53/3*8+C55/B55/2*3+C56/B56/2*9+C58/B58+C59/B59*3)*453.6	=R14*Q14/453.6
15	CO2	44.0107	=(C14/B14+C15/B15+C17/B17/2*3+C18/B18/2*3+C20/B20/2*3+C21/B21/2*3+C23/B23/2+C24/B24/2+C26/B26+C27/B27+C29/B29/2+C30/B30/2+C32/B32+C33/B33+C35/B35+C36/B36+C38/B38+C40/B40/2+C41/B41/2+C44/B44+C45/B45+C49/B49+C50/B50+C52/B52+C53/B53/3*4+C55/B55/2*3+C56/B56/2*3+C58/B58+C59/B59)*453.6	=R15*Q15/453.6
16	H2	2.0158	=(C14/B14+C15/B15*3+C17/B17/2*3+C18/B18/2*9+C20/B20/2*3+C21/B21/2*9+C23/B23/2+C24/B24/2*3+C26/B26+C27/B27*3+C29/B29/2+C30/B30/2*3+C32/B32+C33/B33*3+C35/B35+C36/B36*3+C38/B38+C40/B40/2+C41/B41/2*3+C44/B44+C45/B45*3+C49/B49+C50/B50*3+C52/B52/3*2+C53/B53/3*9+C55/B55/2*3+C56/B56/2*9+C58/B58+C59/B59*3)*453.6	=R16*Q16/453.6
17	N2O5	=14.00674*2+15.9994*5	=(C16/B16+C19/B19/2*3+C22/B22/2*3+C25/B25/2+C28/B28+C31/B31/2+C34/B34+C37/B37+C39/B39/2+C42/B42/2+C46/B46+C47/B47+C48/B48+C51/B51+C54/B54+C57/B57/2*3+C60/B60)*453.6	=R17*Q17/453.6
18	NH3	=14.00674+1.0079*3	=(C38/B38+C39/B39)*453.6	=R18*Q18/453.6
19	H2O	18.0158	=(C39/B39/2+C52/B52/3)*453.6	=R19*Q19/453.6
20	O2	31.9988	=C54/B54/3*0.5*453.6	=R20*Q20/453.6
21	NO	30.00674	=C43/B43/2*453.6	=R21*Q21/453.6
22	NO2	46.00674	=C43/B43/2*453.6	=R22*Q22/453.6
23	Total		=SUM(R14:R22)	=SUM(S14:S22)
24				
25	oxides from nitrate/nitrite =			=C16/B16*J14+C19/B19/2*J17+C22/B22+C25/B25/2*J23+C28/B28*J26+C31/B31+C34/B34*J32+C37/B37*J35+(C42/B42+43)/2*J38+C46/B46*J41+C47/B47*J44+C8*J45+C51/B51*J46+C54/B54/3*J49+C52*J52+C60/B60*J55
26	oxides from formate =			=C14/B14*J14+C17/B17/2*J17+C20/B20+C23/B23/2*J23+C26/B26*J26+C29/B29+C32/B32*J32+C35/B35*J35+C40/B40/2C44/B44*J41+C49/B49*J46+C52/B52/3*55/B55/2*J52+C58/B58*J55
27	oxides from glycolate =			=C15/B15*J14+C18/B18/2*J17+C21/B21+C24/B24/2*J23+C27/B27*J26+C30/B30+C33/B33*J32+C36/B36*J35+C41/B41/2C45/B45*J41+C50/B50*J46+C53/B53/3*56/B56/2*J52+C59/B59*J55
28	total oxides =			=S25+S26+S27
29	total NO3/NO2 salts =			=C16+C19+C22+C25+C28+C31+C34+C9+C42+C43+C46+C47+C48+C51+C54+
30	total COOH salts =			=C14+C17+C20+C23+C26+C29+C32+C8+C40+C44+C49+C52+C55+C58

	I	J	K	L	M	N	O
30	**Table 2. Species produced from Formate/Nitrate/Glycolate Decomposition (Continued)**						
31							
32	MgO	40.3044		=(C32/B32+C33/B33+C34/B34)*453.6	=L32*J32/453.6		
33							
34							
35	MnO	70.9374		=(C35/B35+C36/B36+C37/B37)*453.6	=L35*J35/453.6		
36							
37							
38	Na2O	61.979		=(C40/B40+C41/B41+C42/B42+C43/B43)/2*453.6	=L38*J38/453.6		
39							
40							
41	NiO	74.6928		=(C44/B44+C45/B45+C46/B46)*453.6	=L41*J41/453.6		
42							
43							
44	PbO	223.1994		=C47/B47*453.6	=L44*J44/453.6		
45	PdO	122.4194		=C48/B48*453.6	=L45*J45/453.6		
46	SrO	103.6194		=(C49/B49+C50/B50+C51/B51)*453.6	=L46*J46/453.6		
47							
48							
49	U3O8	842.0852		=(C52/B52+C53/B53+C54/B54)/3*453.6	=L49*J49/453.6		
50							
51							
52	La2O3	325.8092		=(C55/B55+C56/B56+C57/B57)/2*453.6	=L52*J52/453.6		
53							
54							
55	ZnO	81.3894		=(C58/B58+C59/B59+C60/B60)*453.6	=L55*J55/453.6		
56	Total			=SUM(L14:L50)	=SUM(M14:M55)		
57	Total_1 (Oxide+Gas) =				=M56+S23		
58	Diff from COOH/NO3 input				=(M57-C61)/C61		

	P	Q	R	S
30	**Table 2. Species produced from Formate/Nitrate/Glycolate Decomposition (Continued)**			
31	total CH2OHCOO salts =			=C15+C18+C21+C24+C27+C30+C33+C 1+C45+C50+C53+C56+C59
32	total NO3/NO2/COOH salts =			=S29+S30+S31
33	wt% oxide in nitrate =			=S25/S28
34	wt% oxide in formate =			=S26/S28
35	wt% oxide in glycolate =			=S27/S28
36	% CO from glycolate decomposition =			=(C15/B15*3+C18/B18/2*9+C21/B21/2*9 B24/2*3+C27/B27*3+C30/B30/2*3+C33/B C36/B36*3+C41/B41/2*3+C45/B45*3+C5 3+C53/B53/3*8+C56/B56/2*9+C59/B59*3 6/R14
37	% CO2 from glycolate decomposition =			=(C15/B15+C18/B18/2*3+C21/B21/2*3+(4/2+C27/B27+C30/B30/2+C33/B33+C36/ 41/B41/2+C45/B45+C50/B50+C53/B53/3 6/B56/2*3+C59/B59)*453.6/R15
38	% H2 from glycolate decomposition =			=(C15/B15*3+C18/B18/2*9+C21/B21/2*9 B24/2*3+C27/B27*3+C30/B30/2*3+C33/B C36/B36*3+C41/B41/2*3+C45/B45*3+C5 3+C53/B53/3*9+C56/B56/2*9+C59/B59*3 6/R16
39				
40	2NaCH2OHCOO = Na2O + CO2 + 3CO + 3H2			
41	Ca(CH2OHCOO)2 = CaO + CO2 + 3CO + 3H2			
42	2Fe(CH2OHCOO)3 = Fe2O3 + 3 CO2 + 9CO + 9H2			
43	2NaCOOH = CO + CO2 + H2 + Na2O			
44	Ca(COOH)2 = CaO + CO + CO2 + H2			
45	2 La(COOH)3 = La2O3 + 3CO + 3CO2 + 3H2			
46	Ca3(PO4)3 = 3CaO + P2O5			
47	2Na3PO4 = 3Na2O + P2O5			
48	3Na2U2O7 = 2U3O8 + 3Na2O + O2			
49	3 UO2(COOH)2 = U3O8 + 3CO + 3CO2 + 2H2 + H2O			
50	3 UO2(C2H3O3)2 = U3O8 + 8CO + 4CO2 + 9H2			
51	3UO2(NO3)2 = U3O8 + 3N2O5 + 1/2 O2			
52	NH4COOH = NH3 + CO2 + H2			
53	2NH4NO3 = 2NH3 + N2O5 + H2O			
54	2Fe(NO3)3 = Fe2O3 + 3N2O5			
55	2 NaNO2 = Na2O + NO + NO2			
56	N2O5 = NO + NO2 + O2			
57	C2H4O3 = 2CO + H2 + H2O			
58	HNO3 = NO + NO2 + O2 + H2O			

	A	B	C	D
86	**Table 3A. Other Nonorganic Melter Feeds**			
87		MW	lb/hr	gmole
88				
89	Al(OH)3	='SB9-17'!L8	=IF('SB9-17'!AP$88=0,'SB9-17'!AI8,'SB9-17'!AV8)	=C89/B89*453.6
90	AlOOH	='SB9-17'!L43	=IF('SB9-17'!AP$88=0,'SB9-17'!AI43,'SB9-17'!AV43)	=C90/B90*453.6
91	B2O3	='SB9-17'!F30	=IF('SB9-17'!AP$88=0,'SB9-17'!AI30,'SB9-17'!AV30)	=C91/B91*453.6
92	Ba(OH)2	='SB9-17'!B33+(15.9994+1.0079)*2		=C92/B92*453.6
93	BaSO4	='SB9-17'!L33	=IF('SB9-17'!AP$88=0,'SB9-17'!AI33,'SB9-17'!AV33)	=C93/B93*453.6
94	Ca(OH)2	='SB9-17'!L10	=IF('SB9-17'!AP$88=0,'SB9-17'!AI10,'SB9-17'!AV10)	=C94/B94*453.6
95	Ca3(PO4)2	='SB9-17'!L14	=IF('SB9-17'!AP$88=0,'SB9-17'!AI14,'SB9-17'!AV14)	=C95/B95*453.6
96	CaC2O4	='SB9-17'!L41	=IF('SB9-17'!AP$88=0,'SB9-17'!AI41,'SB9-17'!AV41)	=C96/B96*453.6
97	CaF2	='SB9-17'!B10+18.9984*2		=C97/B97*453.6
98	CaCO3	='SB9-17'!L39	=IF('SB9-17'!AP$88=0,'SB9-17'!AI39,'SB9-17'!AV39)	=C98/B98*453.6
99	CaSO4	='SB9-17'!L40	=IF('SB9-17'!AP$88=0,'SB9-17'!AI40,'SB9-17'!AV40)	=C99/B99*453.6
100	Cd(OH)2	='SB9-17'!L28	=IF('SB9-17'!AP$88=0,'SB9-17'!AI28,'SB9-17'!AV28)	=C100/B100*453.6
101	CH2OHCOOH	='SB9-17'!P65	=IF('SB9-17'!AP$88=0,'SB9-17'!AL63,'SB9-17'!AY63)	=C101/B101*453.6
102	coal	12.011	=IF('SB9-17'!AP$88=0,'SB9-17'!AI45,'SB9-17'!AV45)	=C102/B102*453.6
103	Cr(OH)3	='SB9-17'!L16	=IF('SB9-17'!AP$88=0,'SB9-17'!AI16,'SB9-17'!AV16)	=C103/B103*453.6
104	Cs2O	='SB9-17'!F32	=IF('SB9-17'!AP$88=0,'SB9-17'!AI32,'SB9-17'!AV32)	=C104/B104*453.6
105	Cu(OH)2	='SB9-17'!L17	=IF('SB9-17'!AP$88=0,'SB9-17'!AI17,'SB9-17'!AV17)	=C105/B105*453.6
106	Fe(OH)3	='SB9-17'!L7	=IF('SB9-17'!AP$88=0,'SB9-17'!AI7,'SB9-17'!AV7)	=C106/B106*453.6
107	Sn(OH)2	='SB9-17'!L34	=IF('SB9-17'!AP$88=0,'SB9-17'!AI34,'SB9-17'!AV34)	=C107/B107*453.6
108	HCOOH	='SB9-17'!P64	=IF('SB9-17'!AP$88=0,'SB9-17'!AL62,'SB9-17'!AY62)	=C108/B108*453.6
109	HNO3	=1.0079+J4	=IF('SB9-17'!AP$88=0,'SB9-17'!AL64,'SB9-17'!AY64)	=C109/B109*453.6
110	H3BO3	='SB9-17'!B30+(15.9994+1.0079)*3		=C110/B110*453.6
111	HgO	='SB9-17'!L13	=IF('SB9-17'!AP$88=0,'SB9-17'!AI13,'SB9-17'!AV13)	=C111/B111*453.6
112	solvent-Isopar	='SB9-17'!G245	='SB9-17'!G232	=C112/B112*453.6
113	K2O	='SB9-17'!F24	=IF('SB9-17'!AP$88=0,'SB9-17'!AI24,'SB9-17'!AV24)	=C113/B113*453.6
114	La(OH)3	='SB9-17'!L37	=IF('SB9-17'!AP$88=0,'SB9-17'!AI37,'SB9-17'!AV37)	=C114/B114*453.6
115	Li2O	='SB9-17'!F31	=IF('SB9-17'!AP$88=0,'SB9-17'!AI31,'SB9-17'!AV31)	=C115/B115*453.6
116	MgO	='SB9-17'!F12	=IF('SB9-17'!AP$88=0,'SB9-17'!AI44,'SB9-17'!AV44)	=C116/B116*453.6
117	Mg(OH)2	='SB9-17'!L12	=IF('SB9-17'!AP$88=0,'SB9-17'!AI12,'SB9-17'!AV12)	=C117/B117*453.6

	G	H	I	J
67	**Table 3B. Nonorganic Melter Feeds**			
68	Species	MW	lb/hr	gmole/hr
69				
70	MnO2	='SB9-17'!B9+15.9994*2	=IF('SB9-17'!AP$88=0,'SB9-17'!AI9,'SB9-17'!AV9)	=I70/H70*453.6
71	MoO2	=95.94+15.9994*2		=I71/H71*453.6
72	NH4OH	=14.007+1.0079*5+15.9994		=I72/H72*453.6
73	Na2O	='SB9-17'!F20	=IF('SB9-17'!AP$88=0,'SB9-17'!AI20,'SB9-17'!AV20)	=I73/H73*453.6
74	NaCl	='SB9-17'!P33	=IF('SB9-17'!AP$88=0,'SB9-17'!AL33,'SB9-17'!AY33)	=I74/H74*453.6
75	NaF	='SB9-17'!P34	=IF('SB9-17'!AP$88=0,'SB9-17'!AL34,'SB9-17'!AY34)	=I75/H75*453.6
76	Na2CO3	='SB9-17'!P57	=IF('SB9-17'!AP$88=0,'SB9-17'!AL58,'SB9-17'!AY58)	=I76/H76*453.6
77	Na2C2O4	='SB9-17'!P58	=IF('SB9-17'!AP$88=0,'SB9-17'!AL59,'SB9-17'!AY59)	=I77/H77*453.6
78	NaOH	=22.9898+15.9994+1.0079	=IF('SB9-17'!AP$88=0,'SB9-17'!AL39,'SB9-17'!AY39)	=I78/H78*453.6
79	Na2SO4	='SB9-17'!P59	=IF('SB9-17'!AP$88=0,'SB9-17'!AL60,'SB9-17'!AY60)	=I79/H79*453.6
80	Na3PO4	='SB9-17'!P39	=IF('SB9-17'!AP$88=0,'SB9-17'!AL40,'SB9-17'!AY40)	=I80/H80*453.6
81	Na2U2O7	='SB9-17'!L11	=IF('SB9-17'!AP$88=0,'SB9-17'!AI11,'SB9-17'!AV11)	=I81/H81*453.6
82	Ni(OH)2	='SB9-17'!L15	=IF('SB9-17'!AP$88=0,'SB9-17'!AI15,'SB9-17'!AV15)	=I82/H82*453.6
83	PbCO3	='SB9-17'!B35+12.011+15.9994*3		=I83/H83*453.6
84	PbSO4	='SB9-17'!L35	=IF('SB9-17'!AP$88=0,'SB9-17'!AI35,'SB9-17'!AV35)	=I84/H84*453.6
85	PuO2	='SB9-17'!F23	=IF('SB9-17'!AP$88=0,'SB9-17'!AI25,'SB9-17'!AS25)	=I85/H85*453.6
86	PdO	='SB9-17'!F27	=IF('SB9-17'!AP$88=0,'SB9-17'!AI27,'SB9-17'!AV27)	
87	RhO2	='SB9-17'!F26	=IF('SB9-17'!AP$88=0,'SB9-17'!AI26,'SB9-17'!AV26)	=I87/H87*453.6
88	RuO2	='SB9-17'!F25	=IF('SB9-17'!AP$88=0,'SB9-17'!AI25,'SB9-17'!AV25)	=I88/H88*453.6
89	SiO2	='SB9-17'!F19	=IF('SB9-17'!AP$88=0,'SB9-17'!AI19,'SB9-17'!AV19)	=I89/H89*453.6
90	H4SiO4	='SB9-17'!P60	=IF('SB9-17'!AP$88=0,'SB9-17'!AL61,'SB9-17'!AY61)	=I90/H90*453.6
91	Sr(OH)2	='SB9-17'!B29+(15.9994+1.0079)*2	=IF('SB9-17'!AP$88=0,'SB9-17'!AI29,'SB9-17'!AV29)	=I91/H91*453.6
92	TcO2	='SB9-17'!F36	=IF('SB9-17'!AP$88=0,'SB9-17'!AI36,'SB9-17'!AV36)	=I92/H92*453.6
93	ThO2	='SB9-17'!F21	=IF('SB9-17'!AP$88=0,'SB9-17'!AI21,'SB9-17'!AV21)	=I93/H93*453.6
94	TiO2	='SB9-17'!F18	=IF('SB9-17'!AP$88=0,'SB9-17'!AI18,'SB9-17'!AV18)	=I94/H94*453.6
95	Zeolite		=IF('SB9-17'!AP$88=0,'SB9-17'!AI34,'SB9-17'!AV34)	
96	Zn(OH)2	='SB9-17'!L22	=IF('SB9-17'!AP$88=0,'SB9-17'!AI22,'SB9-17'!AV22)	=I96/H96*453.6
97	ZrO2	='SB9-17'!F38	=IF('SB9-17'!AP$88=0,'SB9-17'!AI38,'SB9-17'!AV38)	=I97/H97*453.6
98	antifoam	=IF('SB9-17'!Q151=0,'SB9-17'!G136,'SB9-17'!I13	=IF('SB9-17'!AP$88=0,'SB9-17'!AI46,'SB9-17'!AV46)	=I98/H98*453.6
99	H2O	=1.0079*2+15.9994	=IF('SB9-17'!AP$88=0,'SB9-17'!AL66,'SB9-17'!AY66)	=I99/H99*453.6
100				
101	Total_3 =		=SUM(C89:C117)+SUM(I70:I99)	
102	total feed		=C61+C83+I101	
103	total feed exc. MCU/ARP		=I102-C112	
104	% trimethylsiloxane volatilization =			0

	G	H	I	J
105	**Table 4. Carbon Feeds**			
106			lb/hr	ppm
107	Formate		=D61*12.0107/'SB9-17'!P89	=I107/$I$102*1000000
108	glycolate		=G61/'SB9-17'!P90*12.011*2	=I108/$I$102*1000000
109	Aromatic		=C70*0.93+C71*0.94+C72*0.85+C73*0.591+C74*0.847 +C75*0.773+C76*0.6942+C77*0.6722+C78*0.585+C79* 0.77+C80*0.923+C81*0.6+C82*0.375	=I109/$I$102*1000000
110	coal		=C102	=I110/$I$102*1000000
111	oxalate		=(C96/B96+I77/H77)*12.011*2	=I111/$I$102*1000000
112	free formic		=C108/B108*12.011	=I112/$I$102*1000000
113	free glycolic		=C101/B101*12.011*2	=I113/$I$102*1000000
114	strip effluent		='SB9-17'!G255	=I114/$I$102*1000000
115	antifoam		='SB9-17'!G137	=I115/$I$102*1000000
116	TOC		=SUM(I107:I115)	=SUM(J107:J115)
117	TOC-free formic		=I116-I112-I113	=J116-J112
118	measured TOC (SB9 simulant SME)			='Report Tables'!C199
119	Δ TOC			=IF(J118="n/a","n/a",(J116-J118)/J118)
120	measured TOC-antifoam from IC =			='remed 100%-125%GN SME'!M55
121	antifoam from calc'd TOC-IC =			=J116-J120
122	carbonate		=I76/H76*12.011	=I122/$I$102*1000000
123	measured carbonate			='C:\DWPF\Alt reductant flowsheet\2014 CEF test\model eval glycolic FS\[SB6-CEF-FN analytical IC.xlsx]PSAL FN2'!E76

	L	M	N	O
67	**Table 5. CC Model Input for:**			**='SB9-17'!M2**
68	Species	Stage 1	Stage 2	Stage 3
69		gmole/hr	gmole/hr	gmole/hr
70				
71	Al2O3	=0	=D89/2+D90/2	0
72	B2O3	=D91+D73/2+D110/2	=0	0
73	CaO		=D94+D96+L14+3*D95+D98	0
74	CuO	=L26+D105	0	0
75	Fe2O3	=D106/2	=0	0
76	K2O	=L29	=D113	0
77	Li2O	=0	=D115	0
78	MgO	0	0	=L32+D117+D116
79	MnO2	=0	=J70	0
80	MnO	=L35	=0	0
81	Na2O	=L38+J78/2	=J73+J76+J80*1.5+J77+J81	0
82	NiO	=L41+J82	0	0
83	La2O3	=L52+D114/2	0	0
84	SiO2	=J89+J90+3*(1-J104)*J98*M127/100	=3*(1-J104)*J98*N127/100	=3*(1-J104)*J98*O127/100
85	CaSO4	=0	0	=D99
86	Na2SO4	=0	0	=J79
87	U3O8	=L49	=J81/3*2	0
88	coal	=D102*M126/100+D112*'SB9-17'!G267	=D102*N126/100	=D102*O126/100
89	CF4	=D112*'SB9-17'!G265		
90	CCl4	=D112*'SB9-17'!G266		
91	H2O	=IF(D144<0,IF('SB9-17'!Q151>0,R19+D89/2*3+D90/2+D92+D94+D100+D103/2*3+D105+D106/2*3+D107+D110/2*3+D114/2*3+D117+J72+J78/2+J82+J90*2+J91+J96+J98*(1-J104)*M127/100*2-J98*J104+(D109+D144)/2*(1-C139)*M125/100,R19+D89/2*3+D90/2+D92+D94+D100+D103/2*3+D105+D106/2*3+D107+D110/2*3+D114/2*3+D117+J72+J78/2+J82+J90*2+J91+J96+J98*(1-J104)*M127/100*4-J98*J104+(D109+D144)/2*(1-C139)*M125/100),IF('SB9-17'!Q151>0,R19+D89/2*3+D90/2+D92+D94+D100+D103/2*3+D105+D106/2*3+D107+D110/2*3+D114/2*3+D117+J72+J78/2+J82+J90*2+J91+J96+J98*(1-J104)*M127/100*2-J98*J104+D101*(1-D146)*M129/100+(D109+D145)/2*(1-C139)*M125/100,R19+D89/2*3+D90/2+D92+D94+D100+D103/2*3+D105+D106/2*3+D107+D110/2*3+D114/2*3+D117+J72+J78/2+J82+J90*2+J91+J96+J98*(1-J104)*M127/100*4-J98*J104+D101*(1-D146)*M129/100+(D109+D145)/2*(1-C139)*M125/100))	=IF(D144<0,IF('SB9-17'!Q151>0,J98*(1-J104)*N127/100*2+(D109+D144)/2*(1-C139)*N125/100,J98*(1-J104)*N127/100*4+(D109+D144)/2*(1-C139)*N125/100),IF('SB9-17'!Q151>0,J98*(1-J104)*N127/100*2+D101*(1-D146)*N129/100+(D109+D145)/2*(1-C139)*N125/100,J98*(1-J104)*N127/100*4+D101*(1-D146)*N129/100+(D109+D145)/2*(1-C139)*N125/100))	=IF(D144<0,IF('SB9-17'!Q151>0,(D109+D144)/2*(1-C139)*O125/100+J98*(1-J104)*O127/100*2,(D109+D144)/2*(1-C139)*O125/100+J98*(1-J104)*O127/100*4),IF('SB9-17'!Q151>0,D101*(1-D146)*O129/100+(D109+D145)/2*(1-C139)*O125/100+J98*(1-J104)*O127/100*2,D101*(1-D146)*O129/100+(D109+D145)/2*(1-C139)*O125/100+J98*(1-J104)*O127/100*4))

	L	M	N	O
91	**Table 5. CC Model Input for: (Continued)**			
92	CO	=IF(D144<0,IF('SB9-17'!Q151>0,J98*(1-J104)*M127/100*(11+'SB9-17'!I141)+D112*'SB9-17'!G264+(R14*S36-D145/2*3)*M128/100,J98*(1-J104)*M127/100*(8+'SB9-17'!G141)+D112*'SB9-17'!G264+(R14*S36-D145/2*3)*M128/100),IF('SB9-17'!Q151>0,J98*(1-J104)*M127/100*(11+'SB9-17'!I141)+D112*'SB9-17'!G264+(R14*S36+D145/2*3)*M128/100+D101*2*(1-D146)*M129/100,J98*(1-J104)*M127/100*(8+'SB9-17'!G141)+D112*'SB9-17'!G264+(R14*S36+D145/2*3)*M128/100+D101*2*(1-D146)*M129/100))	=IF(D144<0,IF('SB9-17'!Q151>0,D96+J77+R14*(1-S36)+(R14*S36-D145/2*3)*N128/100+J98*(1-J104)*N127/100*(11+'SB9-17'!I141),D96+J77+R14*(1-S36)+(R14*S36-D145/2*3)*N128/100+J98*(1-J104)*N127/100*(8+'SB9-17'!G141)),IF('SB9-17'!Q151>0,D96+J77+R14*(1-S36)+(R14*S36+D145/2*3)*N128/100+J98*(1-J104)*N127/100*(11+'SB9-17'!I141)+D101*2*(1-D146)*N129/100,D96+J77+R14*(1-S36)+(R14*S36+D145/2*3)*N128/100+J98*(1-J104)*N127/100*(8+'SB9-17'!G141)+D101*2*(1-D146)*N129/100))	=IF(D144<0,IF('SB9-17'!Q151>0,(R14*S36-D145/2*3)*O128/100+J98*(1-J104)*O127/100*(11+'SB9-17'!I141),(R14*S36-D145/2*3)*O128/100+J98*(1-J104)*O127/100*(8+'SB9-17'!G141)),IF('SB9-17'!Q151>0,(R14*S36+D145/2*3)*O128/100+D101*2*(1-D146)*O129/100+J98*(1-J104)*O127/100*(11+'SB9-17'!I141),(R14*S36+D145/2*3)*O128/100+D101*2*(1-D146)*O129/100+J98*(1-J104)*O127/100*(8+'SB9-17'!G141)))
93	CO2	=IF(D144<0,(R15*S37-D145/2)*M128/100,(R15*S37+D145/2)*M128/100)	=IF(D144<0,D96+D98+J76+J77+J83+R15*(1-S37)+(R15*S37-D145/2)*N128/100,D96+D98+J76+J77+J83+R15*(1-S37)+(R15*S37+D145/2)*N128/100)	=IF(D144<0,(R15*S37-D145/2)*O128/100,(R15*S37+D145/2)*O128/100)
94	H2	=IF(D144<0,IF('SB9-17'!Q151>0,R16*(1-S38)+(R16*S38-D145/2*3)*M128/100+J98*(1-J104)*M127/100*13,R16*(1-S38)+(R16*S38-D145/2*3)*M128/100+J98*(1-J104)*M127/100*8),IF('SB9-17'!Q151>0,R16*(1-S38)+(R16*S38+D145/2*3)*M128/100+J98*(1-J104)*M127/100*13+D101*(1-D146)*M129/100,R16*(1-S38)+(R16*S38+D145/2*3)*M128/100+J98*(1-J104)*M127/100*8+D101*(1-D146)*M129/100))	=IF(D144<0,IF('SB9-17'!Q151>0,(R16*S38-D145/2*3)*N128/100+J98*(1-J104)*N127/100*13,(R16*S38-D145/2*3)*N128/100+J98*(1-J104)*N127/100*8),IF('SB9-17'!Q151>0,(R16*S38+D145/2*3)*N128/100+J98*(1-J104)*N127/100*13+D101*(1-D146)*N129/100,(R16*S38+D145/2*3)*N128/100+J98*(1-	=IF(D144<0,IF('SB9-17'!Q151>0,(R16*S38-D145/2*3)*O128/100+J98*(1-J104)*O127/100*13,(R16*S38-D145/2*3)*O128/100+J98*(1-J104)*O127/100*8),IF('SB9-17'!Q151>0,(R16*S38+D145/2*3)*O128/100+D101*(1-D146)*O129/100+J98*(1-J104)*O127/100*13,(R16*S38+D145/2*3)*O128/100+D101*(1-
95	N2O5	0	0	0
96	N2	=D112*'SB9-17'!G268	=0	0
97	O2	=IF(D144<0,(R20+(R17+D145/2)*(1-C139))*M125/100-8*J98*(1-J104)*M127/100+(D109+D144)/2*(1-C139)*M125/100,(R20+(R17+D145/2)*(1-C139))*M125/100-8*J98*(1-J104)*M127/100+(D109+D145)/2*(1-C139)*M125/100)	=IF(D144<0,(R20+(R17+D145/2)*(1-C139))*N125/100+J81/3-8*J98*(1-J104)*N127/100+(D109+D144)/2*(1-C139)*N125/100,(R20+(R17+D145/2)*(1-C139))*N125/100+J81/3-8*J98*(1-J104)*N127/100+(D109+D145)/2*(1-C139)*N125/100)	=IF(D144<0,(R20+(R17+D145/2)*(1-C139))*O125/100+(D109+D144)/2*(1-C139)*O125/100-8*J98*(1-J104)*O127/100,(R20+(R17+D145/2)*(1-C139))*O125/100+(D109+D145)/2*(1-C139)*O125/100-8*J98*(1-J104)*O127/100)
98	NO	=IF(D144<0,(R21+(R17+D145/2)*(1-C139))*M125/100+(D109+D144)*(1-C139)/2*M125/100,(R21+(R17+D145/2)*(1-C139))*M125/100+(D109+D145)*(1-C139)/2*M125/100)	=IF(D144<0,(R21+(R17+D145/2)*(1-C139))*N125/100+(D109+D144)*(1-C139)/2*N125/100,(R21+(R17+D145/2)*(1-C139))*N125/100+(D109+D145)*(1-C139)/2*N125/100)	=IF(D144<0,(R21+(R17+D145/2)*(1-C139))*O125/100+(D109+D144)*(1-C139)/2*O125/100,(R21+(R17+D145/2)*(1-C139))*O125/100+(D109+D145)*(1-C139)/2*O125/100)
99	NO2	=IF(D144<0,(R22+(R17+D145/2)*(1-C139))*M125/100+(D109+D144)*(1-C139)/2*M125/100,(R22+(R17+D145/2)*(1-C139))*M125/100+(D109+D145)*(1-C139)/2*M125/100)	=IF(D144<0,(R22+(R17+D145/2)*(1-C139))*N125/100+(D109+D144)*(1-C139)/2*N125/100,(R22+(R17+D145/2)*(1-C139))*N125/100+(D109+D145)*(1-C139)/2*N125/100)	=IF(D144<0,(R22+(R17+D145/2)*(1-C139))*O125/100+(D109+D144)*(1-C139)/2*O125/100,(R22+(R17+D145/2)*(1-C139))*O125/100+(D109+D145)*(1-C139)/2*O125/100)
100	NH3	=R18+J72	=0	0
101	HCOOH	=D108		
102	C2H4O3	=D101*D146		
103	HNO3	=IF(D144<0,(D109+D144)*C139,(D109+D145)*C139		
104	CH4	=J98*'SB9-17'!I141+D112*'SB9-17'!G263		
105	(CH3)3SiOH	=J98*J104*2		
106	(CH3)2Si(OH)2	=J98*J104		
107	N2O5	=IF(D144<0,(R17+D144/2)*C139+(D109+D144)/2*C		

	R	S	T
67	**Table 6. Mass Balance: Required CC Input to make 228 lb/hr glass**		
68			=O67
69	**Species Included**	MW	ccinput (lb/hr)
70			
71	Al2O3	='SB9-17'!F8	=SUM(M71:O71)*S71/453.6
72	B2O3	=B91	=SUM(M72:O72)*S72/453.6
73	CaO	='SB9-17'!F10	=SUM(M73:O73)*S73/453.6
74	CuO	='SB9-17'!F17	=SUM(M74:O74)*S74/453.6
75	Fe2O3	='SB9-17'!F7	=SUM(M75:O75)*S75/453.6
76	K2O	='SB9-17'!F24	=SUM(M76:O76)*S76/453.6
77	Li2O	='SB9-17'!F31	=SUM(M77:O77)*S77/453.6
78	MgO	='SB9-17'!F12	=SUM(M78:O78)*S78/453.6
79	MnO2	=H70	=SUM(M79:O79)*S79/453.6
80	MnO	='SB9-17'!F9	=SUM(M80:O80)*S80/453.6
81	Na2O	='SB9-17'!F20	=SUM(M81:O81)*S81/453.6
82	NiO	='SB9-17'!F15	=SUM(M82:O82)*S82/453.6
83	SiO2	='SB9-17'!F19	=SUM(M84:O84)*S83/453.6
84	CaSO4	=B99	=SUM(M85:O85)*S84/453.6
85	Na2SO4	=H79	=SUM(M86:O86)*S85/453.6
86	coal	=B102	=SUM(M88:O88)*S86/453.6
87	H2O	=H99	=SUM(M91:O91)*S87/453.6
88	CO	='C:\DWPF\Alt reductant flowsheet\2014 CEF test\model eval glycolic FS\[SB6-CEF-FN analytical IC.xlsx]ccout_CEF-FNH'!B12	=SUM(M92:O92)*S88/453.6
89	CO2	='C:\DWPF\Alt reductant flowsheet\2014 CEF test\model eval glycolic FS\[SB6-CEF-FN analytical IC.xlsx]ccout_CEF-FNH'!B9	=SUM(M93:O93)*S89/453.6
90	H2	='C:\DWPF\Alt reductant flowsheet\2014 CEF test\model eval glycolic FS\[SB6-CEF-FN analytical IC.xlsx]ccout_CEF-FNH'!B10	=SUM(M94:O94)*S90/453.6
91	N2O5	=14.007*2+15.9994*5	=SUM(M95:O95)*S91/453.6
92	N2	='C:\DWPF\Alt reductant flowsheet\2014 CEF test\model eval glycolic FS\[SB6-CEF-FN analytical IC.xlsx]ccout_CEF-FNH'!B11	=SUM(M96:O96)*S92/453.6
93	O2	='C:\DWPF\Alt reductant flowsheet\2014 CEF test\model eval glycolic FS\[SB6-CEF-FN analytical IC.xlsx]ccout_CEF-FNH'!B13	=SUM(M97:O97)*S93/453.6
94	NO	='C:\DWPF\Alt reductant flowsheet\2014 CEF test\model eval glycolic FS\[SB6-CEF-FN analytical IC.xlsx]ccout_CEF-FNH'!B15	=SUM(M98:O98)*S94/453.6
95	NO2	='C:\DWPF\Alt reductant flowsheet\2014 CEF test\model eval glycolic FS\[SB6-CEF-FN analytical IC.xlsx]ccout_CEF-FNH'!B16	=SUM(M99:O99)*S95/453.6
96	NH3	='C:\DWPF\Alt reductant flowsheet\2014 CEF test\model eval glycolic FS\[SB6-CEF-FN analytical IC.xlsx]ccout_CEF-FNH'!B20	=SUM(M100:O100)*S96/453.6
97	HCOOH	='SB9-17'!P64	=SUM(M101:N101)*S97/453.6
98	C2H4O3	='SB9-17'!P65	=SUM(M102:O102)*S98/453.6
99	HNO3	=B109	=SUM(M103:N103)*S99/453.6
100	CH4	=12.011+1.0079*4	=SUM(M104:N104)*S100/453.6

	R	S	T
100	**Table 6. Mass Balance: Required CC Input to make 228 lb/hr glass (Continued)**		
101	(CH3)3SiOH	=(12.0107+1.0079*3)*3+28.0855+15.9994+1.0079	=SUM(M105:N105)*S101/453.6
102	(CH3)2Si(OH)2	=(12.0107+1.0079*3)*2+28.0855+(15.9994+1.0079)*2	=SUM(M106:N106)*S102/453.6
103	N2O5	108.01048	=M107*S103/453.6
104	total CC model input		=SUM(T71:T103)-T97-T98-T99-T101-T102-T103
105	dried feed inc. free acids		=I102-I99
106	CC model input (% dry feed)		=T104/T105
107	total volatiles to vapor space exc. H2O		=T97+T98+T99+T101+T102+T103
108	total volatile+nonvolatile included (% dry feed)		=(T104+T107)/T105
109			
110	**Species Excluded**	MW	lb/hr
111	CCl4	=12.0107+4*35.4527	=SUM(M90:O90)*S111/453.6
112	CF4	=12.0107+4*18.9984	=SUM(M89:O89)*S112/453.6
113	NaCl	=H74	=I74
114	NaF	=H75	=I75
115	BaO	='SB9-17'!F33	=C92/B92*S115
116	La2O3	='SB9-17'!F37	=SUM(M83:O83)*S116/453.6
117	Cr2O3	='SB9-17'!F16	=C103/B103/2*S117
118	U3O8	='SB9-17'!F11	=SUM(M87:O87)*S118/453.6
119	ZnO	='SB9-17'!F22	=I96/H96*S119+M55
120	TiO2	='SB9-17'!F18	=I94
121	RuO2	='SB9-17'!F25	=I88
122	RhO2	='SB9-17'!F26	=I87
123	PdO	='SB9-17'!F27	=I86
124	CdO	='SB9-17'!F28	=C100/B100/2*S124
125	SnO	='SB9-17'!F34	=C107/B107*S125
126	Ba(OH)2	171.3416	=C92
127	BaSO4	='SB9-17'!L33	=C93
128	PbSO4	='SB9-17'!L35	='SB9-17'!AV35
129	P2O5	='SB9-17'!F14	=(I80/H80/2+C95/B95)*S129
130	TcO2	='SB9-17'!F36	=I92
131	ZrO2	='SB9-17'!F38	=I97
132	total excluded =		=SUM(T113:T131)
133	total excluded (% dry feed) =		=T132/T105
134	sum of mode input+excluded (% dry feed)		=(T104+T107+T132)/T105

	V	W	X	Y
67	**Table 7. CC Model Input at:**		**=dyninput!L103**	**GPM**
68	Species	Stage 1	Stage 2	Stage 3
69		gmole/hr	gmole/hr	gmole/hr
70				
71	Al2O3	=M71*$X$67/$D$7	=N71*$X$67/$D$7	=O71*$X$67/$D$7
72	B2O3	=M72*$X$67/$D$7	=N72*$X$67/$D$7	=O72*$X$67/$D$7
73	CaO	=M73*$X$67/$D$7	=N73*$X$67/$D$7	=O73*$X$67/$D$7
74	CuO	=M74*$X$67/$D$7	=N74*$X$67/$D$7	=O74*$X$67/$D$7
75	Fe2O3	=M75*$X$67/$D$7	=N75*$X$67/$D$7	=O75*$X$67/$D$7
76	K2O	=M76*$X$67/$D$7	=N76*$X$67/$D$7	=O76*$X$67/$D$7
77	Li2O	=M77*$X$67/$D$7	=N77*$X$67/$D$7	=O77*$X$67/$D$7
78	MgO	=M78*$X$67/$D$7	=N78*$X$67/$D$7	=O78*$X$67/$D$7
79	MnO2	=M79*$X$67/$D$7	=N79*$X$67/$D$7	=O79*$X$67/$D$7
80	MnO	=M80*$X$67/$D$7	=N80*$X$67/$D$7	=O80*$X$67/$D$7
81	Na2O	=M81*$X$67/$D$7	=N81*$X$67/$D$7	=O81*$X$67/$D$7
82	NiO	=M82*$X$67/$D$7	=N82*$X$67/$D$7	=O82*$X$67/$D$7
83	La2O3	=M83*$X$67/$D$7	=N83*$X$67/$D$7	=O83*$X$67/$D$7
84	SiO2	=M84*$X$67/$D$7	=N84*$X$67/$D$7	=O84*$X$67/$D$7
85	CaSO4	=M85*$X$67/$D$7	=N85*$X$67/$D$7	=O85*$X$67/$D$7
86	Na2SO4	=M86*$X$67/$D$7	=N86*$X$67/$D$7	=O86*$X$67/$D$7
87	U3O8	=M87*$X$67/$D$7	=N87*$X$67/$D$7	=O87*$X$67/$D$7
88	coal	=M88*$X$67/$D$7	=N88*$X$67/$D$7	=O88*$X$67/$D$7
89	CF4	=M89*$X$67/$D$7	=N89*$X$67/$D$7	=O89*$X$67/$D$7
90	CCl4	=M90*$X$67/$D$7	=N90*$X$67/$D$7	=O90*$X$67/$D$7
91	H2O	=M91*$X$67/$D$7	=N91*$X$67/$D$7	=O91*$X$67/$D$7
92	CO	=M92*$X$67/$D$7	=N92*$X$67/$D$7	=O92*$X$67/$D$7
93	CO2	=M93*$X$67/$D$7	=N93*$X$67/$D$7	=O93*$X$67/$D$7
94	H2	=M94*$X$67/$D$7	=N94*$X$67/$D$7	=O94*$X$67/$D$7
95	N2O5	=M95*$X$67/$D$7	=N95*$X$67/$D$7	=O95*$X$67/$D$7
96	N2	=M96*$X$67/$D$7	=N96*$X$67/$D$7	=O96*$X$67/$D$7
97	O2	=M97*$X$67/$D$7	=N97*$X$67/$D$7	=O97*$X$67/$D$7
98	NO	=M98*$X$67/$D$7	=N98*$X$67/$D$7	=O98*$X$67/$D$7
99	NO2	=M99*$X$67/$D$7	=N99*$X$67/$D$7	=O99*$X$67/$D$7
100	NH3	=M100*$X$67/$D$7	=N100*$X$67/$D$7	=O100*$X$67/$D$7
101	HCOOH	=M101*$X$67/$D$7	=N101*$X$67/$D$7	=O101*$X$67/$D$7
102	C2H4O3	=M102*$X$67/$D$7	=N102*$X$67/$D$7	=O102*$X$67/$D$7
103	HNO3	=M103*$X$67/$D$7	=N103*$X$67/$D$7	=O103*$X$67/$D$7
104	CH4	=M104*$X$67/$D$7	=N104*$X$67/$D$7	=O104*$X$67/$D$7
105	(CH3)3SiOH	=M105*$X$67/$D$7	=N105*$X$67/$D$7	=O105*$X$67/$D$7
106	(CH3)2Si(OH)2	=M106*$X$67/$D$7	=N106*$X$67/$D$7	=O106*$X$67/$D$7
107	N2O5	=M107*$X$67/$D$7	=N107*$X$67/$D$7	=O107*$X$67/$D$7

Distribution:

T. B. Brown, 773-A
M. E. Cercy, 773-42A
D. A. Crowley, 773-43A
A. P. Fellinger. 773-42A
S. D. Fink, 773-A
C. C. Herman, 773-A
D. T. Hobbs, 773-A
E. N. Hoffman, 999-W
J. E. Hyatt, 773-A
K. M. Kostelnik, 773-42A
B. B. Looney, 773-42A
C. J. Martino, 999-W
D. A. McGuire, 773-42A
T. O. Oliver, 773-42A
F. M. Pennebaker, 773-42A
G. N. Smoland, 773-42A
M. E. Stone, 999-W
W. R. Wilmarth, 773-A
Records Administration (EDWS)

H. P. Boyd, 704-27S
J. M. Bricker, 704-S
J. S. Contardi, 704-56H
T. L. Fellinger, 766-H
E. J. Freed, 704-S
J. M. Gillam, 766-H
B. A. Hamm, 766-H
E. W. Holtzscheiter, 766-H
J. F. Iaukea, 704-27S
V. Jain, 766-H
J. W. Ray, 704-27S
P. J. Ryan, 704-26S
M. A. Rios-Armstrong, 766-H
H. B. Shah, 766-H
D. C. Sherburne, 249-8H
C. Sudduth, 707-7E

P. R. Jackson, DOE-SR, 703-46A
J. A. Crenshaw, 703-46A